AD_____

Award Number: DAMD17-99-1-9002

TITLE: Characterization of Putative Homeostatic Molecules in Prostate Development and Androgen-Independent Prostate Cancer

PRINCIPAL INVESTIGATOR: Jer-Tsong Hsieh, Ph.D.

CONTRACTING ORGANIZATION: The University of Texas
Southwestern Medical Center at Dallas
Dallas, Texas 75390-9105

REPORT DATE: August 2002

TYPE OF REPORT: Annual

PREPARED FOR: U.S. Army Medical Research and Materiel Command
Fort Detrick, Maryland 21702-5012

DISTRIBUTION STATEMENT: Approved for Public Release;
Distribution Unlimited

The views, opinions and/or findings contained in this report are those of the author(s) and should not be construed as an official Department of the Army position, policy or decision unless so designated by other documentation.

REPORT DOCUMENTATION PAGE

Form Approved
OMB No. 074-0188

Public reporting burden for this collection of information is estimated to average 1 hour per response, including the time for reviewing instructions, searching existing data sources, gathering and maintaining the data needed, and completing and reviewing this collection of information. Send comments regarding this burden estimate or any other aspect of this collection of information, including suggestions for reducing this burden to Washington Headquarters Services, Directorate for Information Operations and Reports, 1215 Jefferson Davis Highway, Suite 1204, Arlington, VA 22202-4302, and to the Office of Management and Budget, Paperwork Reduction Project (0704-0188), Washington, DC 20503

1. AGENCY USE ONLY (Leave blank)	2. REPORT DATE	3. REPORT TYPE AND DATES COVERED
	August 2002	Annual (15 Jul 01 - 14 Jul 02)

4. TITLE AND SUBTITLE
Characterization of Putative Homeostatic Molecules in Prostate Development and Androgen-Independent Prostate Cancer

5. FUNDING NUMBERS
DAMD17-99-1-9002

6. AUTHOR(S)
Jer-Tsong Hsieh, Ph.D.

7. PERFORMING ORGANIZATION NAME(S) AND ADDRESS(ES)
The University of Texas
Southwestern Medical Center at Dallas
Dallas, Texas 75390-9105

E-Mail:JT.Hsieh@UTSouthwestern.edu

8. PERFORMING ORGANIZATION REPORT NUMBER

9. SPONSORING / MONITORING AGENCY NAME(S) AND ADDRESS(ES)
U.S. Army Medical Research and Materiel Command
Fort Detrick, Maryland 21702-5012

10. SPONSORING / MONITORING AGENCY REPORT NUMBER

20030226 085

11. SUPPLEMENTARY NOTES

12a. DISTRIBUTION / AVAILABILITY STATEMENT
Approved for Public Release; Distribution Unlimited

12b. DISTRIBUTION CODE

13. Abstract ***(Maximum 200 Words)*** *(abstract should contain no proprietary or confidential information)*
The mortality associated with prostate cancer (PCa) is mostly due to the recurrent of an androgen-independent (AI) PCa. It is believed that AIPCa may derive from stem (or basal) cell population of prostate gland with a malignant phenotype. However, the characterization of stem cell in prostate gland is still lacking. Therefore, the main goal of this project is to define the phenotype of stem cell in normal prostate gland and the molecule(s) involved in maintaining its normal phenotype. In this grant, we are proposing to isolate different basal cell population of prostatic epithelia from normal prostate gland and document the molecular markers during the differentiation lineage of these cells. Currently, we have isolated several clones derived from basal cell population of prostate gland with various differentiation potentials. Using a three-dimension cell culture system, we were able to observe their different cell polarization abilities. On the other hand, we have delineated the biologic function and gene regulation two unique molecules (i.e., DOC-2 and DIP1/2) isolated from normal basal cell of prostatic epithelium in AIPCa. The outcome of these results could have a significant impact on understanding the biology of AIPCa and developing new target for PCa therapy.

14. SUBJECT TERMS	15. NUMBER OF PAGES
stem cell, androgen-independent growth, tumor suppressor, adaptor protein, cell adhesion molecule, prostate cancer	46
	16. PRICE CODE

17. SECURITY CLASSIFICATION OF REPORT	18. SECURITY CLASSIFICATION OF THIS PAGE	19. SECURITY CLASSIFICATION OF ABSTRACT	20. LIMITATION OF ABSTRACT
Unclassified	Unclassified	Unclassified	Unlimited

Table of Contents

INTRODUCTION

Androgen-independent (AI) basal epithelial cell in prostate, a progenitor for luminal epithelial cells (1-4), are considered as the stem cell because it is responsible for maintaining homeostasis of normal prostate. Many studies also indicate that AI prostate cancer (PCa) exhibits several marker proteins as seen in basal cells (5-6), suggesting that these two cell population may have some functional relationship. Nevertheless, the AIPCa acquires a malignant phenotype because the homeostatic control is impaired in this cell. To delineate the biology of these basal cells, we proposed to isolate different population of prostatic epithelia based on these three markers and characterize the morphologic changes associated with these cells from *in vitro* and to determine the stem cell potential of each cell population from *in vivo*. The ultimate goal of this project is to document the cell lineage of prostate stem cell based on molecular markers. This information will help not only early diagnosis of AIPCa and also development of new intervention for prostate cancer.

RECENT PROGRESS

The study had progressed smoothly in the past year. Three manuscripts and one review manuscript have been published (Appendix 1-4). Overall, Task 1 is 75% completed; Task 2 will begin shortly. Detailed progress of these aims is outlined below.

Task 1. To isolate different population of prostatic epithelia based on these three markers and characterize the morphologic changes associated with these cells from *in vitro*

Although the origin of AIPCa is not well characterized, many data indicate that AIPCa possesses many similar characteristics as the basal cell population of the normal prostatic epithelia. Therefore, defining the factor that controls homeostasis in the basal cells of the prostate may lead to the discovery of the critical defect(s) associated with AI cancer.

To characterize the potential stem cell in prostate gland, we enriched basal cell population from the degenerated prostate induced androgen deprivation and then isolated different cell population based on C-CAM1 pattern (Table 1) using FACS analysis. So far, we were able to obtain three clones and we further characterized the phenotype of these cells as summarized in Table 1. We observed that each clone has very unique expression profile, suggesting that there is a heterogeneous population among basal cell population of prostate gland. To examine their differentiation ability, an *in vitro* three-dimension cell culture system was employed; this system is to plate cells on a polyester membrane of Transwell® (Costar, Cambridge, MA) and then to measure the level of transepithelial resistance (TER) as an indication of cell polarization (7). We observed that one of clones exhibits elevated TER in the presence of 20% serum (Fig. 1A). In contrast, cancer cells lose their polarized phenotype as well as tissue architecture (Fig. 1B). Using confocal microscope, we were able to confirm these cells form a tight junction (2) that is a continuous circumferential intercellular contact at the apical pole of lateral cell membrane. As shown in Fig. 1C, ZO-1 protein, a key component in tight junction, exhibited a distinct network structure of polarized NbE. This data indicate that this clone can undergo differentiation *in vitro*. We will begin *Task 2* to test whether this clone is able

to form glandular structure *in vivo* and delineate the molecule changes associated with this process.

Table 1 Profiling protein expression pattern of prostatic epithelia.

Clone	C-CAM1[a]	CK8/18[b]	CK5[b]	Bcl-2[b]	DOC-2[b]	DIP1/2[b]	AR[c]
NbE	100%[d]	100%	100%	100%	100%	100%	100%
VPE	50%	50%	10%	100%	100%	90%	20%
VPE-12	25%	5%	5%	75%	100%	80%	1%

a: C-CAM1 levels were determined by FACS analysis.
b: All the results were determined by western blot analyses.
c: Androgen receptor (AR) was determined by RT-PCR.
d: All the data was normalized using NbE cells as 100% for each marker.

Fig. 1 Characterization of cell polarization using prostatic epithelial cells. A, determination of TER in normal prostatic epithelial cells. B, determination of TER in normal prostatic epithelial cells vs. Dunning cancer cells (9). C, staining of ZO-1 protein in NbE cells.

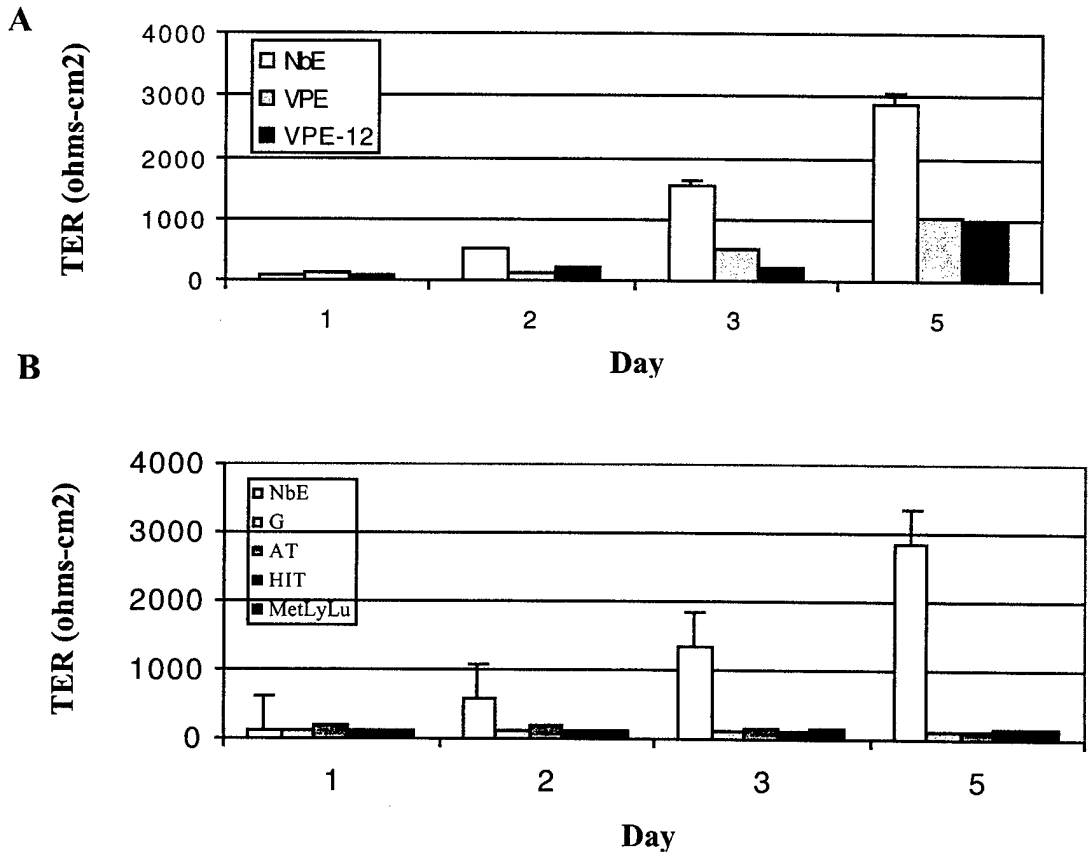

C

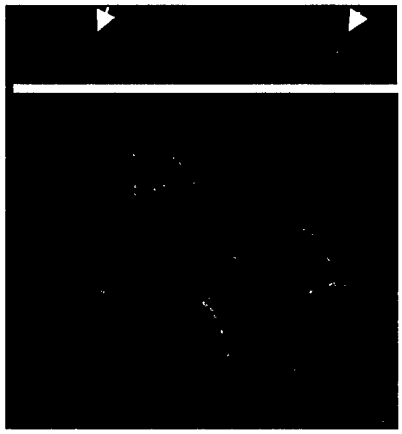

Using differential display RT-PCR (10), we have identified a novel gene-DOC-2 associated with basal cell. Our recent manuscripts (10-12) indicate that DOC-2 represents a critical regulatory element in controlling the signaling pathway(s) that leads to the growth/differentiation of prostatic epithelium. DOC-2 protein complex acts as the negative regulatory machinery operative in basal cell population of normal prostate. The altered expression of this complex leads to the uncontrolled growth of prostatic epithelium. From our publication (12), we demonstrate that protein kinase C (PKC) phosphorylates the S^{24} of the N-terminal of DOC-2/DAB2 critical for its inhibitory function on PKC-mediated gene transcription. In addition, the C-terminal of DOC-2 contains three proline–rich domains with specific interaction with several SH3-containing proteins (i.e., Grb2, Nck, Src, and PI3K). EGF and NT3 are able to enhance the binding between DOC-2 and Grb2 that interrupts the binding of SOS to Grb2 resulting in the suppression of MAP kinase activation (Appendix 1). It is likely that DOC-2 has a multiple inhibitory function on several signal pathways actively operated in prostatic epithelia.

We further searched the down stream effector(s) of DOC-2 using a yeast two-hybrid screening system. After ruling out potential false positive results, we identified a unique cDNA-DIP1/2 (DOC-2 interactive protein). To determine the regulation of the human DIP1/2 gene, we have screened a human BAC genomic library (RPCI-11) with a rat DIP1/2 cDNA probe. After two rounds of screening, we obtained two positive clones (298 A17and 419H3). DNA sequencing results revealed that the DIP1/2 gene contains at least 15 exons and 14 introns. The predicted amino acid sequences of human DIP1/2 share 98% homologue with rat DIP1/2. We were able to map the entire DIP1/2 gene and locate its chromosome position (9q33.1-33.3) where Ph chromosome translocation occurs in the Chronic Myeloid Leukemia patients. The entire length of the DIP1/2 gene is about 96 kb. All information regarding the exons and introns of DIP1/2 was summarized (Appendix 2). The DIP1/2 promoter does not contain any typical TATA-box—evidenced by the presence of various RNAs with differential transcription starting sites. Nevertheless, two potential promoter regions were mapped: one located at + 229 to +981 (1st intron) the other located at –359 to –141 (5'-upstream regulatory region). Moreover, we noticed that the both promoter activity in several AIPCa cell lines is significantly lower than that in normal prostatic epithelial cells (Appendix 2), indicating that transcriptional regulation of DIP1/2 gene underlined the decreased expression of DIP1/2 proteins in AIPCa cells.

In addition, we further characterized the functional role of DIP1/2 in normal basal cells but down regulated in AIPCa cell lines (Appendix 3). Sequencing data provides compelling evidence indicated the DIP1/2 belongs to a new member of RAS-GTPase activating protein family. Since RAS-mediated signal cascade is a major pathway for many exogenous stimuli, DIP1/2 appears to be a key regulator for RAS activity. Using specific reagents for DIP1/2 established in our laboratory, we demonstrated that DIP1/2 is down regulated in AIPCa cell lines. The presence of DIP1/2 protein was able to antagonize the signal transduction elicited by several exogenous stimuli. With respect to the rare frequency of *Ras* gene mutation found in human PCa patients and yet increased Ras protein is often found in AIPCa, these findings are significant (Appendix 3). Taken together, we believe that DOC-2 and DIP1/2 are part of the protein complex in controlling homeostasis of basal prostatic epithelium (Appendix 4).

KEY RESEARCH ACCOMPLISHMENT

- Isolate three different subpopulation of prostatic epithelium from degenerated prostate based on C-CAM1 expression and characterize each clone of epithelia using several different makers.
- Determine the differentiation potential (i.e., cell polarization) of these cells using a three-dimension cell culture system.
- Identify other molecules differentially expressing in polarized cell and non-polarized cell population.
- Characterize the homeostatic role of DOC-2 protein in the growth of prostatic epithelia.
- Identify the functional role of DIP1/2 protein in the growth/differentiation of PCa.
- Cloning of human DIP1/2 gene and demonstrate the differential transcription regulation of this gene in normal prostatic epithelia and PCa cells.

REPORTABLE OUTCOMES

FULL-LENGTH PAPER

1. Zhou, J., and Hsieh, J.T. (2001) The inhibitory role of DOC-2/DAB2 in growth factor receptors mediated signal cascade: DOC-2/DAB2-mediated inhibition of Erk phosphorylation via binding to Grb2. J. Biol. Chem., 278, 27793-27798.

2. Chen, H., Pong, R-C., Wang Z., and Hsieh, J.T. (2002) Differential regulation of the human DAB2IP gene in normal and malignant prostatic epithelia: cloning and characterization. Genomics, 79, 573-581.

3. Wang, Z., Tseng, C-P., Pong, R-C., Chen, H., McConnell, J.D., Navone, N., and Hsieh, J.T. (2002) A Novel RasGTPase activating protein that interacts with DOC-2/DAB2: A

downstream effector leading to the suppression of prostate cancer. J. Biol. Chem., 277, 12622-12631.

REVIEW PAPER

4. Zhou, J., Scholes, J., and Hsieh, J.T. (2001) Signal transduction targets in androgen independent prostate cancer. Cancer and Metastasis Review, 20: 351-362.

CONCLUSIONS

We hypothesize that the basal cells of the prostate gland, considered as a stem cell population, are responsible for maintaining homeostasis of the normal prostate. We have isolated several clones of basal cell from rat prostate and demonstrated that there are different cell populations based on several basal cell markers. These cells may represent a various cell lineage during cell differentiation. Nevertheless, one of cell clone can polarize using an *in vitro* culture system. We are currently dissecting the molecular changes associated with this process. The information obtained from this study will certainly help us to map out cell different of prostatic epithelium.

To understand the homeostatic control in prostatic epithelia, DOC-2 protein complex appears to be key homeostatic control machinery operative in basal cell population of normal prostate. The altered expression of this complex underlies the malignant phenotypic change of AIPCa cell. For the mechanism of action of DOC-2, PKC phosphorylates the S^{24} of the N-terminal of DOC-2 that enhances its binding to DIP1/2, a novel RAS GAP protein, which inhibits both PKC- and EGF-elicited MAP kinase pathways by inactivating RAS protein. With unique interaction with effector proteins (i.e., Grb2 and Src) containing SH3-domains, the C-terminal of DOC-2/DAB2 can inhibit EGF and NT3-induced signal pathways. Also, down regulation of these proteins are often seen in AIPCa cell lines. Thus, further analysis of this protein complex should provide more insight of the stem cell biology in prostate gland. Also, these new molecules could be useful in predicting the prognosis of AIPCa progression.

REFERENCES

1. English, H.F., *et al* (1987) Response of glandular versus basal rat ventral prostate. Prostate 11: 229-242.
2. Verhagan, A.P.M., *et al* (1988) Differential expression of keratins in the basal and luminal compartments of rat prostatic epithelium during degeneration and regeneration. Prostate 13: 25-38.
3. Sherwood, E.R., *et al* (1991) Differential expression of specific cytokeratin polypeptides in the basal and luminal epithelia of the human prostate. Prostate 18: 303-314.
4. Bruchovsky, N. *et al* (1990) The effects of androgen withdrawal on the stem cell composition of Shionogi carcinoma. Cancer Res., 50: 2275-2282.

5. Bonkohoff, H., and Remberger, K. (1996) Differentiation pathways and histogenetic aspects of normal and abnormal prostatic growth: A stem cell model. The Prostate 28: 98-106.
6. McDonnell, T.J., *et al* . (1992) Expression of the proto-oncogene bcl-2 in the prostate and its association with the emergence of androgen-independent prostate cancer. Cancer Res., 52: 6940-6944.
7. Cohen, C.J., *et al* (2001) Multiple regions within the Coxsackie and Adenovirus receptor cytoplasmic domain are required for basolateral sorting. J. Biol. Chem., 276: 25392-25398.
8. Anderson, J.M., and Van Itallie, C.M. (1995) Tight junctions and the molecular basis for regulation of paracellular permeability. A. J. Physiol. 269: G467-G475.
9. Isaacs, J.T., and Hukku, B. (1988) Nonrandom involvement of chromosome 4 in the progression of rat prostatic cancer. Prostate, 13: 165-188.
10. Tseng, C-P., *et al* (1998) Regulation of the DOC-2 gene during castration-induced rat ventral prostate degeneration and its growth inhibitory function in human prostatic carcinoma cells. Endocrinology, 139: 3542-3553.
11. Tseng, C-P., *et al* (1999) The role of DOC-2/DAB2 protein phosphorylation in the inhibition of AP-1 activity-an underlying mechanism of its tumor suppressive function. J. Biol. Chem., 274: 31981-31986.
12. Zhou, J., and Hsieh, J.T. (2001) The inhibitory role of DOC-2/DAB2 in growth factor receptors mediated signal cascade: DOC-2/DAB2-mediated inhibition of Erk phosphorylation via binding to Grb2. J. Biol. Chem., 278: 27793-27798.

THE JOURNAL OF BIOLOGICAL CHEMISTRY Vol. 276, No. 30, Issue of July 27, pp. 27793–27798, 2001
Printed in U.S.A.
© 2001 by The American Society for Biochemistry and Molecular Biology, Inc.

The Inhibitory Role of DOC-2/DAB2 in Growth Factor Receptor-mediated Signal Cascade

DOC-2/DAB2-MEDIATED INHIBITION OF ERK PHOSPHORYLATION VIA BINDING TO Grb2*

Received for publication, March 29, 2001, and in revised form, May 18, 2001
Published, JBC Papers in Press, May 22, 2001, DOI 10.1074/jbc.M102803200

Jian Zhou and Jer-Tsong Hsieh‡

From the Department of Urology, University of Texas Southwestern Medical Center, Dallas, Texas 75390-9110

DOC-2/DAB2 (differentially expressed in ovarian carcinoma-2/disabled 2) appears to be a potential tumor suppressor gene with a growth inhibitory effect on several cancer types. Previously, we have shown that DOC-2/DAB2 suppresses protein kinase C-induced AP-1 activation, which is modulated by serine 24 phosphorylation in the N terminus of DOC-2/DAB2. However, the functional impact of the C terminus of DOC-2/DAB2, containing three proline-rich domains, has not been explored. In this study, we examined this functional role in modulating signaling mediated by peptide growth factor receptor tyrosine kinase, particularly because it involves the interaction with Grb2. Using sequence-specific peptides, we found that the second proline-rich domain of DOC-2/DAB2 is the key binding site to Grb2 in the presence of growth factors. Such elevated binding interrupts the binding between SOS and Grb2, which consequently suppresses downstream ERK phosphorylation. Reduced ERK phosphorylation was restored when the binding between DOC-2/DAB2 and Grb2 was interrupted by a specific peptide or by increasing the expression of Grb2. Furthermore, the C terminus of the DOC-2/DAB2 construct can inhibit the AP-1 activity elicited by growth factors. We conclude that DOC-2/DAB2, a potent negative regulator, can suppress ERK activation by interrupting the binding between Grb2 and SOS that is elicited by peptide growth factors. This study further illustrates that DOC-2/DAB2 has multiple effects on the RAS-mediated signal cascades active in cancer cells.

DOC-2/DAB2 (differentially expressed in ovarian carcinoma-2/disabled 2) is a potential tumor suppressor associated with ovarian (1), choriocarcinoma (2), prostate (3), and mammary tumors (4). It is a novel phosphorprotein that contains several unique motifs such as the N-terminal disable-like domain and the C-terminal proline-rich SH3[1]-binding domain. The DOC-2/DAB2 gene was first cloned by a differential display polymerase chain reaction, which screened for gene(s) down-regulated in human ovarian cancer but not in their normal counterpart (5). Using the same technique, our laboratory cloned the rat homologue from a degenerated prostate gland. We demonstrated that DOC-2/DAB2 is: (*a*) associated with the basal cells of the prostate; (*b*) involved in the growth and differentiation of prostate epithelia, and (*c*) able to inhibit the growth of cell lines derived from human prostate cancer (3). Similarly, the inhibitory role of DOC-2/DAB2 has also been shown in cell lines of ovarian cancer and choriocarcinoma (1, 2, 6). Taken together, these data indicate that DOC-2/DAB2 is a potent growth inhibitor.

We examined the mechanism(s) of the DOC-2/DAB2-elicited growth inhibitory pathway in prostate cancer cell lines. We found that phosphorylation of DOC-2/DAB2 at the extreme N-terminal region by protein kinase C suppresses AP-1 activity. Specifically, the phosphorylation of serine 24 in the N terminus of DOC-2/DAB2 is the key amino acid residue modulating its inhibitory effect (7). Our recent study revealed that the N terminus of DOC-2/DAB2 interacts with a RAS GTPase-activating protein,[2] which suggests that DOC-2/DAB2 is involved in the RAS-mediated signal pathway.

The C terminus of DOC-2/DAB2, on the other hand, interacts with Grb2, which is an adapter protein critical in bridging signal transduction between the activated protein receptor tyrosine kinase (RPTK) and the RAS-mediated MAP kinase cascade (8, 9). The functional significance of the binding between DOC-2/DAB2 and Grb2 is undefined. Therefore, we investigated this relationship using two RPTK ligands: epidermal growth factor (EGF) and neurotrophin 3 (NT3).

We demonstrated in four different cell lines that RPTK activation increases the binding of DOC-2/DAB2 (particularly the C terminus) to Grb2. This binding further leads to a decrease in the activation of the downstream effector, ERK phosphorylation, and AP-1-mediated gene transcription. Our data illustrate the underlying mechanism of the C terminus of DOC-2/DAB2 in modulating RPTK activation.

EXPERIMENTAL PROCEDURES

Cell Lines, Synthetic Peptides, and Plasmid Constructs—A rat pheochromocytoma cell line (PC12) was grown in Dulbecco's modified Eagle's medium (Life Technologies, Inc.) supplemented with 10% heat-inactivated horse serum (Life Technologies, Inc.), 5% heat-inactivated fetal bovine serum, 100 units/ml penicillin, and 100 units/ml streptomycin. C4-2, NbE, and COS cells were maintained in T medium supplemented with 5% fetal bovine serum (3). Four peptides were synthesized corresponding to the protein sequence of DOC-2/DAB2: PPQ (amino acids 619–627); PPK (amino acids 714–722); PPL (amino acids 663–671); and LLL (amino acids 663–671, the substitution of proline with leucine). All DOC-2/DAB2 cDNA expression constructs,

* This work was supported in part by National Institutes of Health Grant CA 59939, by United States Army Grant PC970259, and by funds from the Gillson Longenbaugh Foundation. The costs of publication of this article were defrayed in part by the payment of page charges. This article must therefore be hereby marked "*advertisement*" in accordance with 18 U.S.C. Section 1734 solely to indicate this fact.

‡ To whom correspondence should be addressed: University of Texas Southwestern Medical Center, Dept. of Urology, 5323 Harry Hines Blvd., Dallas, TX 75390-9110. Tel.: 214-648-3988; Fax: 214-648-8786; E-mail: JT.Hsieh@UTSouthwestern.edu.

[1] The abbreviations used: SH, Src homology; RPTK, receptor protein tyrosine kinase; EGF, epidermal growth factor; EGFR, epidermal growth factor receptor; NT3, neurotrophin 3; ERK, extracellular signal-related protein kinase; MAP, mitogen-activated protein; Grb2, growth receptor binding protein 2.

[2] Z. Wang, C.-P. Tseng, R. C. Pong, H. Chen, J. D. McConnell, and J.-T. Hsieh, manuscript submitted.

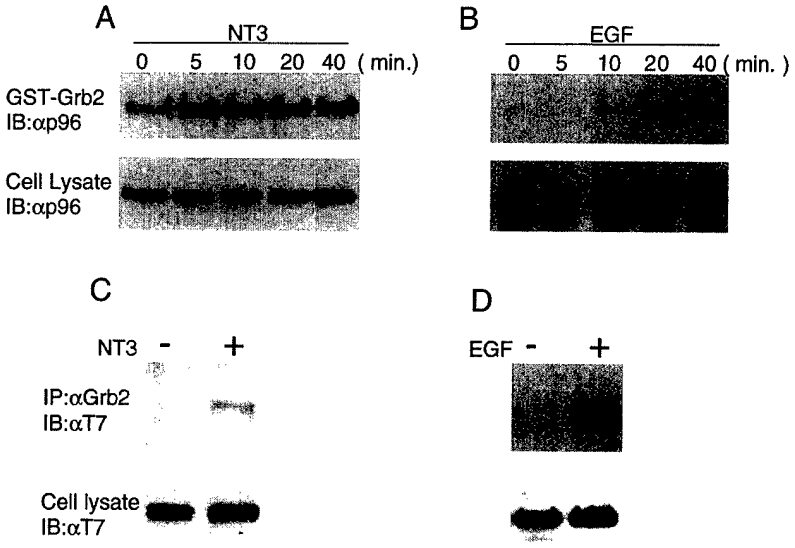

FIG. 1. **The effects of growth factor on the interaction between DOC-2/DAB2 and Grb2.** PC12 (*A*), C4-2 (*B*), and COS (*C* and *D*) cells (6×10^5/60-mm dish) were transfected with 0.6 μg of trkC and 2.4 μg (T7-p82) (*A* and *C*) or 3 μg of p82 (*B* and *D*) for 24 h. After incubating with NT3 (*A* and *C*) or EGF (*B* and *D*), cells were harvested at the indicated time. An aliquot of cell lysate was subjected to a Grb2 binding assay (*A* and *B*) or co-immunoprecipitation (*C* and *D*). In the *upper panels*, the precipitate was probed with anti-DOC-2/DAB2 antibody, αp96 (*A* and *B*) or the anti-T7 tag antibody, αT7 (*C* and *D*). In the *lower panels*, an aliquot of cell lysate was analyzed using Western blot detected by either αp96 (*A* and *B*) or αT7 (*C* and *D*). *IB*, immunoblot.

such as pCI-neo-T7-p82 (T7-p82) and pCI-neo-T7-ΔN (T7-ΔN), have been described (7).

Transfection of Plasmid Vector and Oligopeptide—The indicated number of cells was plated at 37 °C 24 h prior to LipofectAMINE transfection (Life Technologies, Inc.). In each experiment, the control plasmid (pCI-neo) was supplemented to reach an equal amount of total DNA. For the NT3 induction experiment, the trkC expression vector (10), pAC-CMV-trkC, was co-transfected with the DOC-2/DAB2 cDNA construct. 24 h after transfection, cells were switched to a low serum condition (1% heat-inactivated horse serum for PC12 cells; 0.5% fetal bovine serum for COS and C4-2 cells) for another 24 h prior to being treated with growth factors.

For peptide transfection, cells were plated in a 24-well plate with serum-free medium for 24 h. Chariot™ reagent (Active Motif) was mixed with 100 ng of different oligopeptides according to the manufacturer's protocol. 1 h after transfection, cells were treated with growth factors, and cell lysate was prepared at the indicated time.

In Vitro GST-Grb2 Binding Assay—After transfection, cells were exposed to 50 ng/ml of EGF or recombinant NT3 (Upstate Biotechnology). The cells were collected in 0.5 ml of lysis buffer (50 mM Tris-HCl, pH 7.5, 150 mM NaCl, 5 mM EDTA supplemented with 1% of Triton X-100, and a mixture of protease inhibitors) at the indicated time. After a low speed spin, 0.4 ml of supernatant was separately incubated overnight at 4 °C with either 60 μl of GST-Grb2-glutathione Sepharose or GST-glutathione Sepharose. After centrifugation, the pellet was washed twice with the lysis buffer, dissolved in the sample buffer, and then subjected to Western blot analysis probed with either monoclonal antibody against DOC-2/DAB2 (αp96) (Transduction Laboratories) or against the T7 tag (αT7) (Novagen).

Co-immunoprecipitation Assay—The cells were co-transfected with both DOC-2/DAB2 expression vectors and 0.6 μg of Grb2 expression vector (pHM6-Grb2). Using the same treatment protocol, cells were collected in 0.5 ml of lysis buffer. After a low speed spin, 0.4 ml of supernatant was incubated overnight at 4 °C with 1 μg of monoclonal antibody against Grb2 (Transduction Laboratories) and 40 μl of protein G PLUS-agarose (Santa Cruz Biotechnology, Inc.). The pellet was washed twice with lysis buffer, dissolved in sample buffer, and subjected to Western blot analysis detected by the antibody against T7 tag (αT7).

ERK Phosphorylation Assay—Transfected cells were exposed to 50 ng/ml of EGF or NT3 for 10 min and were collected in 70 μl of phosphate-buffered saline (with 1% of Triton X-100 and a mixture of protease inhibitors). After a low speed spin, 20 μl of supernatant was subjected to Western blot analysis. The filter was probed with the antibody against phosphorylated ERK p44/42 (New England Biolab), and the same filter was stripped and reprobed with antibodies against either total ERK 1/2 (p44/42) or p42 (New England Biolab).

Luciferase Reporter Gene Assay—The AP-1-Luciferase reporter construct (−73/+63-Col-Luc) (7) and internal control β-gal vector (pCH110) were used with various DOC-2/DAB2 cDNA expression vectors. The cells were treated with or without 50 ng/ml of EGF or recombinant NT3 for 16 h. Both luciferase and β-galactosidase were assayed (7). The data from the reporter gene activity were normalized with β-galactosidase activity.

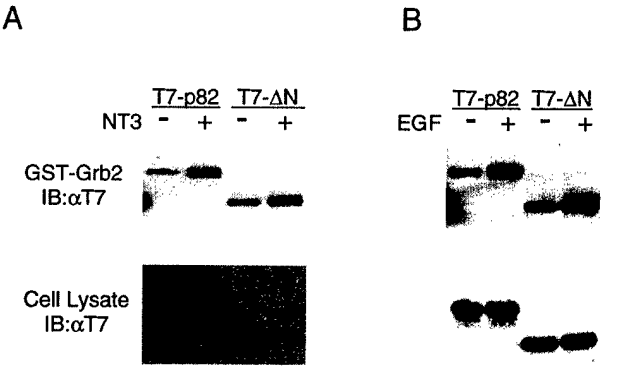

FIG. 2. **The interaction of the C terminus of DOC-2/DAB2 and Grb2.** *A*, COS cells (6×10^5/60-mm dish) were co-transfected with 0.6 μg of pAC-CMV-trkC and 2.4 μg of either DOC-2/DAB2 (T7-p82) or the C terminus of DOC-2/DAB2 (T7-ΔN) and then treated with NT3. *B*, COS cells (6×10^5/60-mm dish) were transfected with 3 μg of either T7-p82 or T7-ΔN and then treated with EGF. Cell lysates were prepared 10 min after treatment and subjected to a Grb2 binding assay. The precipitate (*upper panels*) or total cell lysate (*lower panels*) was detected by anti-T7 tag antibody (*αT7*). *IB*, immunoblot.

RESULTS

NT3 and EGF Increase the Binding of Grb2 to DOC-2/DAB2—In a previous study (7), we showed that the C terminus, but not the N terminus, of DOC-2/DAB2 binds to Grb2. In this study, we investigated the effect of growth factors on this binding. Because DOC-2/DAB2 is expressed in brain tissue (4) and prostate epithelia (3), we chose two RPTK systems: NT3/trkC cascade in PC12 cell and EGF/EGFR cascade in C4-2 cells.

PC12 cells were co-transfected with pAC-CMV-trkC and T7-p82 cDNAs and then treated with NT3 (50 ng/ml) for the indicated time. The cell lysate was prepared and subjected to Grb2-GST binding assay. As shown in the *upper panel* of Fig. 1*A*, a basal level interaction between DOC-2/DAB2 and Grb2 was detected in the PC12 cells; a similar result was shown previously (7). However, binding of DOC-2/DAB2 to Grb2 increased 5 min after treatment with NT3, and increased binding remained constant throughout the entire course of treatment. This indicates that trkC activation can immediately increase the interaction between DOC-2/DAB2 and Grb2. The same expression levels of DOC-2/DAB2 expression were detected in each lane (Fig. 1*A*, *lower panel*), and this rules out the possibility of a transfection artifact.

In the other RPTK signaling system (Fig. 1*B*, *upper panel*),

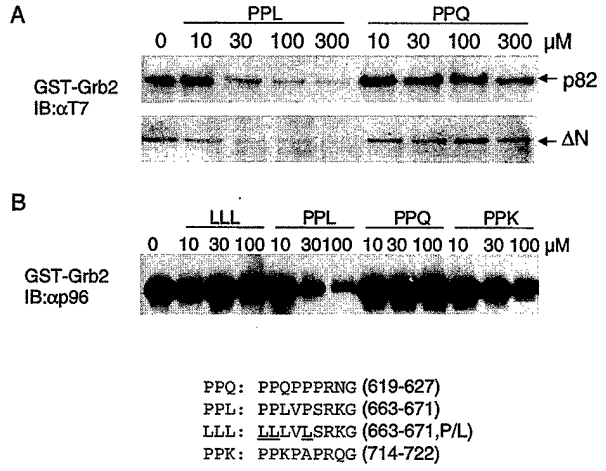

FIG. 3. **The specific interaction of the proline-rich domains in DOC-2/DAB2 and Grb2.** *A*, COS cells (6×10^5/100-mm dish) were transfected with either DOC-2/DAB2 (T7-p82) or the C terminus of DOC-2/DAB2 (T7-ΔN). The cell lysates were prepared 48 h after transfection and subjected to Grb2 binding assay in the presence of different concentrations of oligopeptides. *B*, cell lysate from 80% confluent NbE cells were prepared and subjected to Grb2 binding assay in presence of different concentrations of oligopeptides. The precipitate was detected by either anti-T7 (*αT7*) or anti-p96 (*αp96*) antibodies.

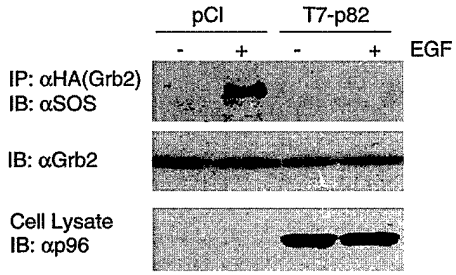

FIG. 4. **The interruption of SOS binding to Grb2 by DOC-2/DAB2.** COS cells (6×10^5/60-mm dish) were co-transfected with HA-Grb2 and either pCI-neo or DOC-2/DAB2 (T7-p82) and then treated with EGF (100 ng/ml) for 10 min. The cell lysates were prepared subjected to co-immunoprecipitation assay by anti-HA tag antibody (*αHA*). The precipitate was detected by anti-SOS antibody (*αSOS*) (*top panel*) and reprobed with anti-Grb2 antibody (*αGrb2*) (*middle panel*). Total cell lysate (*bottom panel*) was detected by anti-p96 antibody (*αp96*). *IB*, immunoblot.

increased binding of DOC-2/DAB2 to Grb2 occurred in a time-dependent manner in a prostatic epithelial cell line (C4-2) treated by EGF. Also, as shown in the *lower panel* of Fig. 1*B*, an equal amount of DOC-2/DAB2 protein expression was detected at each time point. There was difference in the Grb2 binding kinetics between NT3-treated PC12 cells and EGF-treated C4-2 cells. For example, EGF showed a slower rate of Grb2 binding than did NT3. Peak binding of Grb2 occurred 20 min after EGF treatment, compared with 5 min after NT3 treatment. Such difference may influence the effect of DOC-2/DAB2 on the downstream pathway mediated by these two growth factors.

In addition to data obtained from the *in vitro* binding assay, we used co-immunoprecipitation to examine the intracellular interaction between DOC-2/DAB2 and Grb2. As shown in Fig. 1 (*C* and *D*), the complex containing DOC-2/DAB2 significantly increased in the presence of either NT3 or EGF compared with the control. EGF also increased the intracellular interaction between the Grb2 and DOC-2/DAB2. Data from both Grb2 and co-immunoprecipitation assays indicate that the interaction between DOC-2/DAB2 and Grb2 was enhanced under the stimulation of peptide growth factors, which suggests that DOC-2/DAB2 may play a regulatory role in RPTK-mediated signaling.

Growth Factors Enhance the Binding of the C Terminus of DOC-2/DAB2 to Grb2—As we described, the C terminus but not the N terminus of DOC-2/DAB2 interacts with Grb2 (7). To determine whether growth factors increase the affinity of the C terminus of DOC-2/DAB2 to Grb2, we performed Grb2 binding assay using the N-terminal deletion mutant of DOC-2/DAB2 (T7-ΔN). We wanted to validate this interaction using different cell types. Therefore, COS cells were reconstituted with trkC in the presence of either T7-p82 or T7-ΔN construct. As expected, stimulation with NT3 significantly increased the binding of Grb2 to both DOC-2/DAB2 and the C terminus of DOC-2/DAB2 (Fig. 2*A*). This elevated binding was not caused by variable expressions of T7-p82 or T7-ΔN proteins because equal amounts of these proteins were detected. Similarly, Grb2 binding to DOC-2/DAB2 or to the C terminus of DOC-2/DAB2 also increased with EGF treatment (Fig. 2*B*). These data indicate that the binding domain of DOC-2/DAB2 to Grb2 is located in the C terminus of DOC-2/DAB2.

Binding of Grb2 Is Mediated by the Second Proline-rich Domain of DOC-2/DAB2—There are three proline-rich domains in DOC-2/DAB2 with the same consensus sequence as the SOS

FIG. 5. **The suppression of the growth factor-induced ERK phosphorylation mediated by sequestering Grb2 by DOC-2/DAB2 protein.** PC12 (*A* and *C*) and C4-2 (*B* and *D*) cells (8×10^4/12-well plate) were co-transfected with either the control plasmid pCI, full-length (T7-p82), or the C terminus of DOC-2/DAB2 (T7-ΔN) and pAC-CMV-trkC (*A* and *C*) or EGFR expression plasmid (*B* and *D*). In addition, pHM-Grb2 (C, D) was used for increasing Grb2 levels in cells. 24 h after transfection, cells were switched to a low serum medium for another 24 h. 50 ng/ml of NT3 (*A* and *C*) or EGF (*B* and *D*) were added for a 10-min incubation. An aliquot of cell lysate was analyzed by Western blot. In the *upper panels*, the filter was probed with an antibody against phosphorylated ERK p44/42 (αpERK), and in the *lower panels*, the same filter was reprobed with either ERK p42-specific antibody (*αERK2*) or ERK1/2-specific antibody (*αERK1/2*). *IB*, immunoblot.

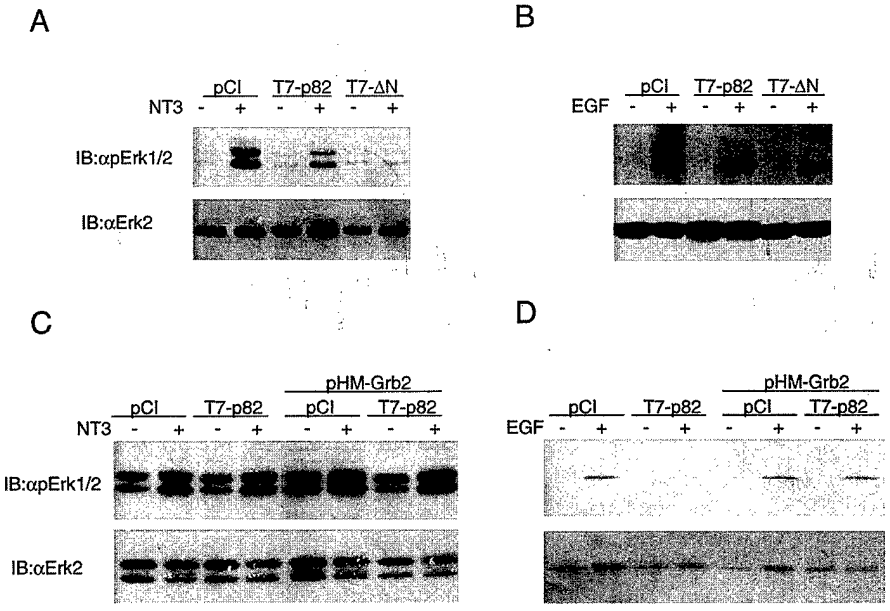

binding site to Grb2. Therefore, all three domains may be involved in Grb2 binding. To compare the binding affinity of these proline-rich sequences, four oligopeptides were synthesized according to the DOC-2/DAB2 protein sequence: PPQ (amino acids 619–627); PPL (amino acids 663–669); LLL (amino acids 663–669 with all proline residues substituted with leucine residues); and PPK (amino acids 714–722). Using the *in vitro* GST-Grb2 binding assay, the PPL peptide blocked the binding of either T7-p82 or T7-ΔN proteins to GST-Grb2, whereas the PPQ peptide had no effect (Fig. 3*A*). Moreover, we prepared cell lysates from NbE cells (a normal rat prostatic epithelial cell line with the endogenous expression of DOC-2/DAB2 proteins) to determine the *in vitro* binding of DOC-2/DAB2 proteins to Grb2. As shown in Fig. 3*B*, PPL effectively blocked the binding in a dose-dependent manner compared with the other two peptides (*i.e.* PPQ and PPK). The effective dose of PPL in COS and NbE cells was very similar, suggesting that the binding kinetics of these proteins remains consistent in different cell lines. The proline residues in this domain are critical for binding because the peptide with leucine substitution (*i.e.* LLL) cannot affect the binding between DOC-2/DAB2 and Grb2 (Fig. 3*B*). These data clearly indicate that the second proline-rich domain in the C terminus of DOC-2/DAB2 is the key interactive site with Grb2.

DOC-2/DAB2 interrupts the binding of Grb2 with SOS Interaction between the Grb2 protein, and the activated receptor can initiate translocation of a group of proteins, namely guanine nucleotide exchange factors (such as SOS), which modulate the GTPase activity of RAS. As shown in Fig. 4, stimulation with EGF increased the binding of Grb2 to SOS in COS cells with no detectable levels of DOC-2/DAB2. However, increased expression of p82 levels in COS cells diminished the binding of Grb2 to SOS, which indicates that DOC-2/DAB2 and SOS compete for the same SH3 site in Grb2.

Both Native DOC-2/DAB2 and the C Terminus of DOC-2/DAB2 Inhibit NT3- and EGF-induced ERK Activation—Grb2 is a key adapter protein for the growth factor-induced MAP kinase pathway (11). To understand the impact of the interaction between DOC-2/DAB2 and Grb2 on this pathway, we examined the phosphorylation status of ERK kinase in the presence of DOC-2/DAB2. Upon the treatment of growth factors, ERK phosphorylation reflected the activation of ERK kinase (12). ERK activation is transient. It peaks at 10 min and then returns to a basal level within 30 min. As shown in Fig. 5*A*, the basal level of phosphorylated ERK was very low in PC12 cells without NT3 treatment. The addition of DOC-2/DAB2 did not alter this level.

In contrast, increasing phosphorylation of ERK1 (44 kDa) and ERK2 (42 kDa) was detected in PC12 cells 10 min after NT3 treatment. Furthermore, NT3-induced phosphorylation of ERK1/2 decreased profoundly in the presence of either full-length DOC-2/DAB2 (T7-p82) or the C terminus of DOC-2/DAB2 (T7- ΔN). Such a change was not caused by the decrease of ERK1/2 protein levels (Fig. 5*A*, *middle* and *lower panel*).

Without EGF treatment, the basal level of ERK2 phosphorylation was lower in C4-2 cells than in PC12 cells (Fig. 5*B*). With EGF treatment, phosphorylation levels of ERK kinases, mainly ERK2 (42 kDa), were elevated. The presence of either T7-p82 or T7-ΔN dramatically suppressed EGF-induced ERK2 phosphorylation. However, the steady-state levels of the ERK2 protein remained the same. These data indicate that ERK2 phosphorylation was inhibited when DOC-2/DAB2 proteins decrease the availability of Grb2 to SOS.

Decreased ERK phosphorylation appears to be a potent downstream event that results from the binding between DOC-2/DAB2 and Grb2. We examined whether increased expression of Grb2 restores the ERK phosphorylation status in cells

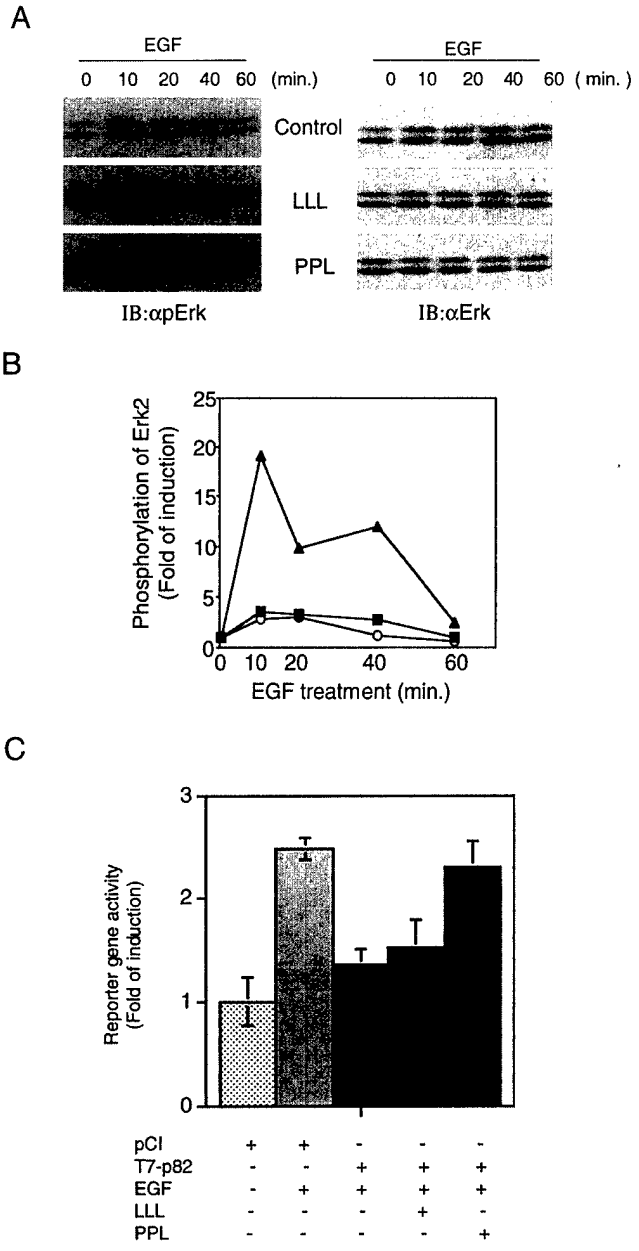

FIG. 6. **The effect of specific peptides derived from DOC-2/DAB2 on EGF-induced ERK phosphorylation.** NbE cells (1×10^4/24 well plate) grew in serum-free medium for 24 h and then were transfected with 100 ng of oligopeptides using Chariot™ reagent. 1 h after transfection, cells were treated with 50 ng of EGF. At the indicated time, cell lysate was prepared and analyzed by Western blot probed with αpERK antibody (*left panels*), and then the same filter was reprobed αERK 1/2 (*right panels*). The intensity of ERK2 signal was determined by densitometer (*A*). The fold of was calculated by normalizing the ratio between phosphorylated ERK2 and total ERK2 proteins induction from each time point with the time 0 (*B*). ○, control; ■, LLL; ▲, PPL. After 16 h of incubation with growth factors, cells were subjected to reporter gene assay (*C*) as described previously (6). *IB*, immunoblot.

treated with growth factors. As shown in Fig. 5 (*C* and *D*), in the absence of either NT3 or EGF, transfection of the Grb2 expression vector failed to induce ERK phosphorylation because Grb2 alone is not capable of activating the growth factor-induced downstream signal pathway (8). In contrast, in either EGF-treated C4-2 or NT3-treated PC12 cells, transfection of the Grb2 expression vector did restore the decreased ERK phosphorylation induced by T7-p82 proteins. This suggests that DOC-2/DAB2 binding to Grb2 is a key step in inactivating ERK phosphorylation.

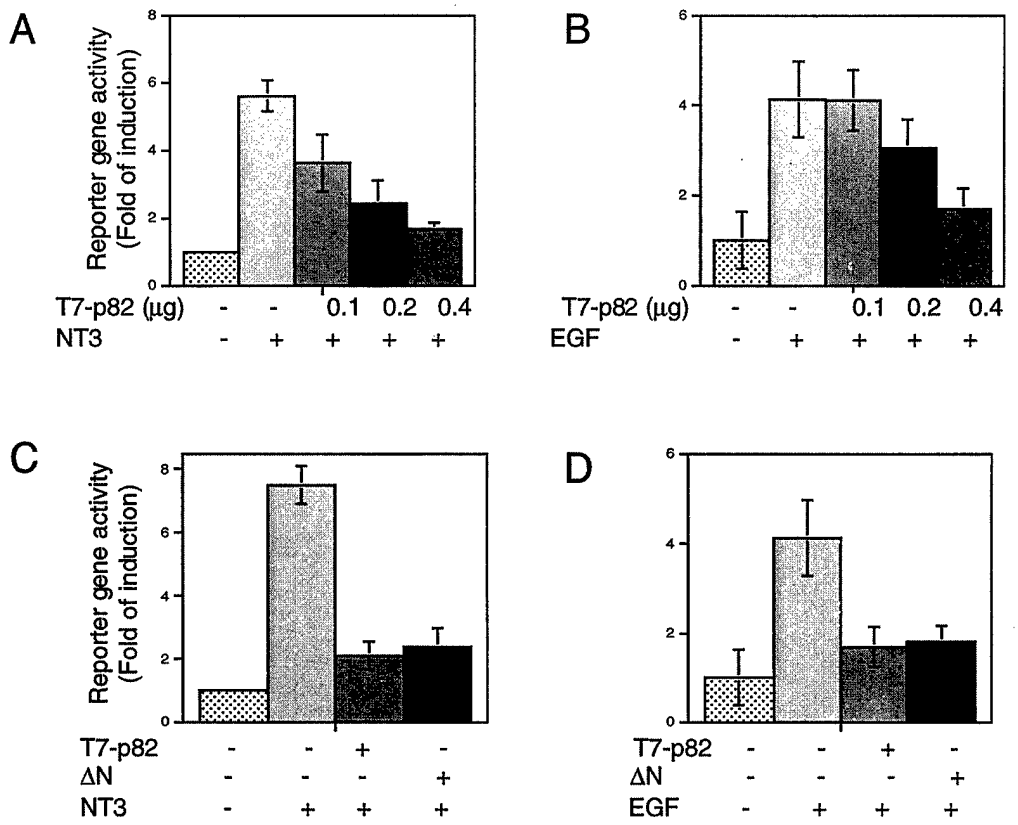

FIG. 7. **The effect of DOC-2/DAB2 and its C-terminal recombinant protein on the growth factor-induced AP-1 activation.** PC12 (*A* and *C*) and C4-2 (*B* and *D*) cells (2×10^5/6-well plate) were co-transfected with 0.2 μg of AP-1 luciferase reporter gene, 0.25 μg of pCH110 (β-gal), and the indicated amount of T7-p82 (*A* and *B*) or 0.4 μg of T7-p82 or T7-ΔN (*C* and *D*). For PC12 cells, 0.15 μg of trkC was included. The total amount of DNA (1 μg/transfection) was supplemented with pCI-neo. 24 h after transfection, cells were down-switched to a low serum for another 24 h. After 16 h of incubation with growth factors, cells were subjected to reporter gene assay. The data represent the means ± S.D. from three independent experiments.

Because the second proline-rich domain of DOC-2/DAB2 is a key binding site to Grb2, we investigated whether blocking this binding also affects the ERK phosphorylation status in cells stimulated with growth factors. To do this, NbE cells were transfected with either PPL or LLL peptide, and the ERK phosphorylation status in EGF-treated NbE cells was determined. As shown in Fig. 6 (*A* and *B*), minutes after EGF treatment, the ERK2 phosphorylation increased about 3–4-fold compared with basal level. PPL enhanced ERK2 phosphorylation about 20-fold. It peaked 10 min after EGF treatment, whereas LLL failed to have the same effect, indicating that PPL can specifically prevent the sequestering Grb2 by the second proline-rich domain of DOC-2/DAB2. These "free" Grb2 molecules amplify signal transduction via the downstream cascade, such as the activation of ERK kinase. Similarly, PPL but not LLL can also antagonize the inhibitory effect of DOC-2/DAB2 on EGF-induced gene transcription (Fig. 6*C*). The overall activity of the reporter gene in this experiment was lower than usual because cell death became more apparent when cells were incubated with both LipofectAMINE and Chariot™ transfection agents. Nevertheless, these data further indicate that one mechanism of DOC-2/DAB2 is to balance the growth factor-induced signal by modulating the availability of effector protein such as Grb2.

Native DOC-2/DAB2 and the C terminus of DOC-2/DAB2 Inhibit NT3- and EGF-induced AP-1 Activation—To determine whether the binding of DOC-2/DAB2 to Grb2 has any impact on RPTK-mediated gene activation, we chose the AP-1 reporter gene assay. AP-1 is activated in PC12 cells upon treatment with neurotrophin (13), and it is the downstream target of RPTK via Grb2 and ERK (14). Suppression on ERK activation indicates that RPTK-induced AP-1 activation may also be affected. As shown in Fig. 7*A*, NT3 induced activation of the AP-1 reporter gene in PC12 cells. In the presence of increasing amounts of T7-p82, the NT3-induced AP-1 activity was suppressed in a dose-dependent manner. In C4-2 cells, the EGF-induced AP-1 activation was also suppressed by T7-p82 in a dose-dependent manner (Fig. 7*B*).

From these results, we believe that the C-terminal recombinant protein has the same inhibitory effect on AP-1 as native DOC-2/DAB2. As depicted in Fig. 7 (*C* and *D*), both T7-p82 and T7-ΔN inhibited NT3- and EGF-induced AP-1 activity with similar magnitude. Thus, the C terminus of DOC-2/DAB2, which contains the Grb2-binding domain(s), is critical to modulate the RPTK-mediated gene expression that is mediated through ERK phosphorylation.

DISCUSSION

Grb2 is a potent adaptor protein. It contains both SH2 and SH3 domains in modulating RPTK-elicited signaling. The SH2 domain directly recognizes phosphotyrosine motifs and is thereby recruited to activated, phosphorylated RPTK. This interaction helps the recruitment of guanine nucleotide exchange factors (*i.e.* SOS) through the binding of the SH3 domain, which subsequently stimulates RAS-GTP binding. The RAS-mediated MAP kinase cascade, a key pathway controlling growth and differentiation, further leads to gene transcription by activating several transcription factors. We and others have shown that DOC-2/DAB2 can interact with Grb2 through its C terminus (7, 15). However, the functional role of this interaction has not been elucidated.

In this study, we manipulated PC12 cell lines without DOC-

2/DAB2 expression such as C4-2 and with different DOC-2/DAB2 cDNA constructs. We found that activation of RPTK by its own ligand also increases the binding of DOC-2/DAB2 to Grb2, which interrupts the binding of SOS to Grb2 (Figs. 1 and 4). We also demonstrated that the second proline-rich domain in the C terminus of DOC-2/DAB2 protein is the key site responsible for the Grb2 binding that prevents a sequential change in the downstream region of the RPTK-mediated pathway (Figs. 3 and 5), including suppressing ERK phosphorylation.

We used a cell line (NbE) that expresses endogenous DOC-2/DAB2 to demonstrate the interaction between endogenous DOC-2/DAB2 and Grb2 proteins. We showed that this interaction appears to be sequence-specific because only peptides with the same sequence as the second proline-rich domain of DOC-2/DAB2 can interrupt Grb2 binding, whereas substitution of key proline residues with leucine residues abolishes its inhibitory function (Fig. 3). Moreover, increasing Grb2 expression in C4-2 cells by using the transient transfection of the Grb2 expression vector alters the inhibitory effect of DOC-2/DAB2 (Fig. 5). We conclude that this inhibitory effect on the MAP kinase pathway results from sequestering Grb2 away from recruiting downstream signaling effectors such as SOS. Therefore, DOC-2/DAB2 represents a potent homeostatic factor that modulates many exogenous stimulus-mediated signal pathways.

To characterize the effect of DOC-2/DAB2 on the RPTK-mediated pathway, we studied two classic ligands in three different cell lines. NT3, which interacts with its receptor trkC, is an important neurotrophin for neuronal development and plasticity. Because other members of the disabled family (*i.e.* DAB1) have been associated with neuronal development (16, 17) and DOC-2/DAB2 is present in brain tissue, we employed PC12 cells (a well established cell model for studying neuronal differentiation) to examine the possible role of DOC-2/DAB2 in NT3-induced signaling. Our results (Figs. 1*A* and 3*A*) demonstrate that DOC-2/DAB2 can block the transient activation of ERK kinase that is considered a mitogenic signal (18) even though neurotrophins can induce a sustained activation of ERK kinase, which can last for several hours in PC12 cells and is related to neuronal differentiation (19). However, we failed to observe any inhibition of the second phase of ERK activation in the presence of DOC-2/DAB2 (data not shown). These results imply that DOC-2/DAB2 may modulate the mitogenic effect of NT3. This function differs from DAB1 protein in neuronal cells.

EGF, a potent mitogen for cell growth, elevation, and EGFR amplification and/or mutation is associated with the progression of many cancer types (20) including prostate cancer (21). Data from our laboratory and others indicate that DOC-2/DAB2 is a tumor suppressor, which is absent in many cancer types (1–6). In this study, we demonstrated that the C terminus of DOC-2/DAB2 may block EGFR-mediated signaling by sequestering Grb2 (Fig. 1) from the upstream of the cascade. This blocking essentially deactivates several key effectors such as ERK and AP-1 (Figs. 3 and 7). Several studies show that unregulated activation of ERK can cause cell transformation (22) and that AP-1 activation is crucial to angiogenesis and neoplastic invasion (23). Moreover, our recent publication indicates that the serine 24 phosphorylation of DOC-2/DAB2 inhibits protein kinase C-mediated gene activation (7). Taken together, we believe that DOC-2/DAB2 represents a unique negative regulator. Upon exogenous stimulus, it demonstrates multiple actions on signaling cascade.

The underlying mechanism regarding the increased affinity of DOC-2/DAB2 to Grb2 by growth factors is still unknown. Our data (Figs. 1 and 2) indicate that this is a rapid event and that the steady-state levels of DOC-2/DAB2 do not change. Therefore, post-translational modification, such as phosphorylation, is likely. Unlike with DAB1 (16), we did not detect any tyrosine phosphorylation in DOC-2/DAB2 (data not shown). Xie *et al.* (24) report that colony-stimulating factor-1 induces serine phosphorylation in DOC-2/DAB2, but they did not determine the key amino acid(s) responsible for this event. We demonstrated that the phorbol ester also induces serine phosphorylation in the N terminus but not in the C terminus of DOC-2/DAB2 (7). Therefore, post-translational modification of DOC-2/DAB2 may play a role in this event because there are several potential ERK phosphorylation sites in the C terminus of DOC2/DAB2 (24). Alternatively, however, we cannot rule out that the presence of other factor(s) may facilitate this interaction upon stimulation with growth factors. Therefore, more detailed study is warranted.

Acknowledgments—We thank Jessica Scholes for excellent technical assistance, Andrew Webb for editorial assistance, and Dr. Koeneman for reading this manuscript.

REFERENCES

1. Mok, S. C., Chan, W. Y., Wong, K. K., Cheung, K. K., Lau, C. C., Ng, S. W., Baldini, A., Colitti, C. V., Rock, C. O., and Berkowitz, R. S. (1998) *Oncogene* **16,** 2381–2387
2. Fulop, V., Colitti, C. V., Genest, D., Berkowitz, R. S., Yiu, G. K., Ng, S.-W., Szepesi, J., and Mok, S. C. (1998) *Oncogene* **17,** 419–424
3. Tseng, C.-P., Ely, B. D., Li, Y., Pong, R.-C., and Hsieh, J.-T. (1998) *Endocrinology* **139,** 3542–3553
4. Schwahn, D. J., and Medina, D. (1998) *Oncogene* **17,** 1171–1178
5. Mok, S. C., Wong, K.-K., Chan, R. K. W., Lau, C. C., Tsao, S.-W., Knapp, R. C., and Berkowitz, R. S. (1994) *Gynecol. Oncol.* **52,** 247–252
6. Fazili, Z., Sun, W., Mittelstaedt, S., Cohen, C., and Xu, X.-X. (1999) *Oncogene* **18,** 3104–3113
7. Tseng, C.-P., Ely, B. D., Pong, R.-C., Wang, Z., Zhou, J., and Hsieh, J.-T. (1999) *J. Biol. Chem.* **274,** 31981–31986
8. Lowenstein, E. J., Daly, R. J., Batzer, A. G., Li, W., Margolis, B., Lammers, R., Ullrich, A., Skolnik, E. Y., Bar-Sagi, D., and Schlessinger, J. (1992) *Cell* **70,** 432–442
9. Margolis, B. (1994) *Prog. Biophys. Mol. Biol.* **62,** 223–244
10. Tsoulfas, P., Soppet, D., Escandon, E., Tessarollo, L., Mendoza-Ramirez, J. l., Rosenthal, A., Nickolics, K., and Parada, L. F. (1993) *Neuron* **10,** 975–990
11. Cobb, M. H. (1999) *Prog. Biophys. Mol. Biol.* **71,** 479–500
12. Robbins, D. J., Cheng, M., Zhen, E., Vanderbilt, C. A., Feig, L. A., and Cobb, M. H. (1992) *Proc. Natl. Acad. Sci. U. S. A.* **89,** 6924–6928
13. Gutacker, C., Klock, G., Diel, P., and Koch-Brandt, C. (1999) *Biochem. J.* **339,** 759–766
14. Karin, M. (1995) *J. Biol. Chem.* **270,** 16483–16486
15. Xu, X.-X., Yi, T., Tang, B., and Lambeth, J. D. (1998) *Oncogene* **16,** 1561–1569
16. Howell, B. W., Gertler, F. B., and Cooper, J. A. (1997) *EMBO J.* **16,** 121–132
17. Howell, B. W., Hawkes, R., Soriano, P., and Cooper, J. A. (1997) *Nature* **389,** 733–737
18. Marshall, C. J. (1995) *Cell* **80,** 179–185
19. York, R. D., Yao, H., Dillon, T., Ellig, C. L., Eckert, S. P., McCleskey, E. W., and Stork, P. J. S. (1998) *Nature* **392,** 622–626
20. Khazaie, K., Schirrmacher, V., and Lichtner, R. B. (1993) *Cancer Metastasis Rev.* **12,** 255–274
21. Ware, J. L. (1998) *Cancer Metastasis Rev.* **17,** 443–447
22. Robinson, M. J., Stippec, S. A., Goldsmith, E., White, M. A., and Cobb, M. H. (1998) *Curr. Biol.* **8,** 1141–1150
23. McCarty, M. F. (1998) *Med. Hypotheses* **50,** 511–514
24. Xu, X.-X., Yang, W., Jackowski, S., and Rock, C. O. (1995) *J. Biol. Chem.* **270,** 14184–14191

THE JOURNAL OF BIOLOGICAL CHEMISTRY
Vol. 277, No. 15, Issue of April 12, pp. 12622–12631, 2002
Printed in U.S.A.
© 2002 by The American Society for Biochemistry and Molecular Biolog

The Mechanism of Growth-inhibitory Effect of DOC-2/DAB2 in Prostate Cancer

CHARACTERIZATION OF A NOVEL GTPase-ACTIVATING PROTEIN ASSOCIATED WITH N-TERMINAL DOMAIN OF DOC-2/DAB2*

Received for publication, November 2, 2001, and in revised form, January 15, 2002
Published, JBC Papers in Press, January 25, 2002, DOI 10.1074/jbc.M110568200

Zhi Wang‡, Ching-Ping Tseng§, Rey-Chen Pong‡, Hong Chen‡, John D. McConnell‡, Nora Navone¶, and Jer-Tsong Hsieh‖

From the ‡Department of Urology, University of Texas Southwestern Medical Center at Dallas, Dallas, Texas 75390-9110 and the ¶Department of GU Medical Oncology, University of Texas M.D. Anderson Cancer Center, Houston, Texas 77030

***DOC-2/DAB2* is a member of the disable gene family with tumor-inhibitory activity. Its down-regulation is associated with several neoplasms, and serine phosphorylation of its N terminus modulates DOC-2/DAB2's inhibitory effect on AP-1 transcriptional activity. We describe the cloning of *DIP1/2*, a novel gene that interacts with the N-terminal domain of DOC-2/DAB2. DIP1/2 is a novel GTPase-activating protein containing a Ras GTPase-activating protein homology domain (N terminus) and two other unique domains (*i.e.* 10 proline repeats and leucine zipper). Interaction between DOC-2/DAB2 and DIP1/2 is detected in normal tissues such as the brain and prostate. Altered expression of these two proteins is often detected in prostate cancer cells. Indeed, the presence of DIP1/2 effectively blocks mitogen-induced gene expression and inhibits the growth of prostate cancer. Thus, DOC-2/DAB2 and DIP1/2 appear to represent a unique negative regulatory complex that maintains cell homeostasis.**

DOC-2/DAB2 (differentially expressed in ovarian carcinoma 2/*disabled*-2) is identified in normal human ovarian epithelial cells but absent in ovarian cancer cell lines (1, 2). An absence of DOC-2/DAB2 expression is associated with malignant cells including mammary, prostate, and ovary (2–4). Increased expression of DOC-2/DAB2 inhibits the growth of several cancer cells (4, 5), which suggests that it functions as a tumor suppressor. DOC-2/DAB2 also appears to be a phosphoprotein, and its phosphorylation can be regulated by several stimuli (4, 6). We recently demonstrated that DOC-2/DAB2 expression is significantly increased in the enriched basal cell population with stem cell potential of the degenerated rat prostate (4), suggesting that DOC-2/DAB2 may play an important role in regulating the homeostasis of epithelial differentiation. Amino acid sequence analysis predicts that DOC-2/DAB2 is a potential signaling molecule. Its N terminus shares 54% homology with mouse DAB1 protein that can be phosphorylated by Src, and the disruption of the *DAB1* gene can cause developmental defects in central neurons (7, 8). In addition, we and others also show that the C terminus of DOC-2/DAB2 containing proline-rich domains can bind to Grb2 proteins (9, 10). Thus, it appears that DOC-2/DAB2 is involved in modulating the Ras signaling pathway.

To understand biochemical function of DOC-2/DAB2, we identified a key amino acid residue (Ser^{24}) in its N terminus. The phosphorylation of this residue by protein kinase C (PKC)[1] activator 12-*O*-tetradecanoylphorbol-13-acetate (TPA) can modulate its inhibitory activity on TPA-induced gene transcription (11). These data indicate that the DOC-2/DAB2 protein, particularly its N terminus, is a potent negative regulator for the PKC-elicited signal pathway. However, little is known about the downstream effector(s) mediated by DOC-2/DAB2.

In this study, we employed a yeast two-hybrid system to identify DIP1/2 as an immediate DOC-2/DAB2-interactive protein. DIP1/2, a novel Ras GTPase-activating protein (GAP), interacts with the N-terminal domain of DOC-2/DAB2. We cloned DIP1/2, characterized it as an immediate downstream effector of DOC-2/DAB2, and delineated its functional role in mitogen-induced gene expression and growth inhibition of prostate cancer.

EXPERIMENTAL PROCEDURES

Cell Cultures—Three human prostate cancer cell lines (TSU-Pr1, LNCaP, and C4-2) and COS cells were maintained in T medium supplemented with 5% fetal bovine serum (4). PrEC, a primary prostatic epithelial cell derived from a 17-year-old juvenile prostate, was maintained in a chemically defined medium purchased from Clonetics. PZ-HPV-7, a cell line derived from the peripheral zone of a normal prostate (12), was maintained in T medium containing 5% fetal bovine serum. $MDAPCa_{2a}$ and $MDAPCa_{2b}$ cell lines were derived from patients with bony metastasis (13). Three additional primary prostatic epithelial cells, derived from either cancer lesions (SWPC1, SWPC2) or adjacent normal tissue (SWNPC2), were obtained from patients with prostate cancer who had had radical prostatectomy. All these cells were maintained in the same medium as PrEC. Corresponding antibody staining indicated that all primary cells were cytokeratin-positive and vimentin-negative.

Yeast Two-hybrid Screening—Using primers 5′-GAATTCCCCGTC-ATGTCTAACGAA-3′ and 5′-GGATCCTAACTGAGGCTTTGGTCGAG-

* This work was supported by NIDDK, National Institutes of Health, Grant DK-47657, Department of Defense Grant PC970259 (to J. T. H.), and funding from Gillson Longenbaugh (to J. D. M.). The costs of publication of this article were defrayed in part by the payment of page charges. This article must therefore be hereby marked "*advertisement*" in accordance with 18 U.S.C. Section 1734 solely to indicate this fact.

The nucleotide sequence(s) reported in this paper has been submitted to the GenBank™/EBI Data Bank with accession number(s) AF236130.

§ Present address: School of Medical Technology, Chang Gung University, Tao-Yuan, Taiwan.

‖ To whom correspondence should be addressed: University of Texas Southwestern Medical Center, Dept. of Urology, 5323 Harry Hines Blvd., Dallas, TX 75390-9110. Tel.: 214-648-3988; Fax: 214-648-8786; E-mail: JT.Hsieh@UTSouthwestern.edu.

[1] The abbreviations used are: PKC, protein kinase C; TPA, 12-*O*-tetradecanoylphorbol-13-acetate; GAP, GTPase-activating protein; HA, hemagglutinin; PBS, phosphate-buffered saline; EGF, epidermal growth factor; FBS, fetal bovine serum; MEK, mitogen-activated protein kinase/extracellular signal-regulated kinase kinase; ERK, extracellular signal-regulated kinase; TRE, TPA response element; SRE, serum response element.

This paper is available on line at http://www.jbc.org

G-3′ and using DOC-2/DAB2 cDNA as a template we generated an 823-bp fragment corresponding to the 5′-end of the cDNA. The PCR-amplified fragment was sequenced before it was subcloned in-frame into pVJL11 vector as a bait construct. Equal amounts of constructed bait vector and pVP16 rat brain cDNA library vector were co-transformed into the yeast strain of L40, and the transformed yeasts were plated on SD-L-T-H (synthetic medium lacking amino acids of leucine, tryptophan, and histidine) plates with 5 mM 3-aminotrizol. Only those colonies that had β-galactosidase activities were further analyzed. Plasmids from those positive clones were rescued and transformed into *Escherichia coli* HB101 strain for further amplification.

Four rounds of phage library screening were performed with a rat brain λ ZAP phage library (Stratagene) to clone the full-length cDNA of DIP1/2. After DNA sequencing for each positive clone, the full-length cDNA of DIP1/2 was assembled with the appropriate restriction enzyme digestion.

Northern Blot—Total RNA from various organs of the male rat was isolated with RNAzol (TEL-TEST). Twenty micrograms of total RNA/lane were separated on 1% formaldehyde agarose gel, transformed onto Zeta-Probe membrane (Bio-Rad), and then hybridized with ^{32}P-labeled DIP1/2 or glyceraldehyde-3-phosphate dehydrogenase cDNA probe.

Generation of the Anti-DIP1/2 Polyclonal Antibody—A peptide sequence (CTNPTKLQITENGEFRNSSNC) corresponding to DIP1/2 amino acid residues 976–996, with an extra cysteine at the N terminus as a linker, was synthesized and used as the antigen to immunize rabbits for generating polyclonal antibody by Zymed Laboratories Inc. Laboratory. After 7 weeks, rabbits were sacrificed to collect antiserum after the fourth boosting injection of antigen. SulfoLink gel (Pierce) was coupled with the synthetic peptide and then blocked with 50 mM cysteine in 50 mM Tris, 5 mM EDTA, pH 8.5; it was then washed with 1 M NaCl. Antibodies against DIP1/2 were first purified by slowly passing the antiserum to the coupled SulfoLink gel. After washing with five column volumes of 1 M NaCl, they were eluted with elution buffer from the Sulfolink kit (Pierce). Purified antibodies were dialyzed overnight against 4 liters of deionized water at 4 °C.

Coimmunoprecipitation and Immunoblotting—COS cells were co-transfected with a series of T7-tagged DOC-2/DAB2 vectors (wild type (p82), slicing form (p59), N-terminal deletion mutant (ΔN), and C-terminal deletion mutant (ΔB)) and HA-tagged DIP1/2 vector. Cells were lysed with a buffer (50 mM Tris, pH 7.5, 1% Nonidet P-40, 1 mM EDTA) and a mixture of protease and phosphatase inhibitors (1 mM phenylmethylsulfonyl fluoride, 0.2 mM sodium orthovanadate, 0.1 mM sodium fluoride, 10 μg/ml aprotinin, 10 μg/ml leupeptin). The supernatant was collected and incubated overnight with either 60 μl of T7-antibody-conjugated agarose bead solution (50% actual volume) or 60 μl of protein A-agarose beads with 10 μg of HA-antibody at 4 °C. After incubation, pellets were washed eight times and subjected to a 10% SDS-PAGE and Western blot analysis.

Purification of the GST Fusion Protein and Ras GAP Activity Assays—The minimal GAP domain of DIP1/2 cDNA was amplified by PCR using primers 5′-GGGATCCCAGAACGCAACAGC-3′ and 5′-AGAATTCTTAGCTTGAGCTGCGGGCAGG-3′. The amplified fragment was subcloned in-frame into the pGEX-5X vector and transformed into the *E. coli* strain of BL21. The bacteria culture was induced with 2.5 mM isopropyl-1-thio-β-D-galactopyranoside at 37 °C for 4 h. The bacterial pellet was washed once with cold PBS. After spin, the pellet was resuspended in PBS and subjected, five times, to 30-s sonication. The GST-GAP fusion protein was purified according to the manufacturer's manual (Roche Molecular Biochemicals), and the purified protein was analyzed using 10% SDS-PAGE analysis and followed by GELCODE Blue staining (Pierce). Assay of Ras GAP activity *in vitro* was performed according to Kim *et al.* (14). To prepare GTP-bound Ras protein, 0.25 μM human recombinant Ha-Ras protein (Calbiochem) was incubated with 20 nM [γ-^{32}P]GTP (6000 Ci/mmol; PerkinElmer Life Sciences) in a buffer containing 20 mM HEPES (pH 7.3), 1 mM EDTA, 2 mM dithiothreitol, and 1 mg/ml bovine serum albumin for 5 min at room temperature. Up to 1 μg of either GST-GAP or GST protein alone was added into a buffer containing 20 mM HEPES, pH 7.3, 5 mM $MgCl_2$, and 1 mM dithiothreitol. The loaded Ras was then incubated with either GST-DIP1/2 or GST for the indicated time, and the reaction was stopped by adding 5 volumes of ice-cold 20 mM HEPES, pH 7.3, and 1 mM $MgCl_2$. The reaction mixture was then filtered through 0.45-μm HA membrane (Millipore Corp.). Filters were air-dried and then subjected to scintillation counting.

C4-2 cells were transfected with either HA-tagged Ras alone or HA-tagged Ras and DIP1/2. Two days after transfection, cells were treated overnight with T medium without serum, and 100 ng/ml EGF was added for 20 min. Then cells were lysed with lysis buffer (PBS with 5 mM $MgCl_2$ and 1% Triton X-100). The whole lysate was spun down, and the supernatants were added with 10 μl of Raf-conjugated agarose beads (Upstate Biotechnology, Inc., Lake Placid, NY). The mixtures were incubated at 4 °C for 30 min. Pellets were spun down and washed four times with the same lysis buffer, and 20 ml of 1× SDS-PAGE sample buffer was added to the pellets and incubated at 100 °C for 3 min. Treated samples were loaded on SDS-PAGE gel, and Ras-Raf binding was detected using Western blot.

Generation of pCI-DIP1/2 Mutants and pGEX-5X-DIP1/2 Constructs—To make mutants of DIP1/2 and the GST fusion DIP, the QuikChange™ site-directed mutagenesis kit was employed. Site-directed mutagenesis was performed by PCR according to the manufacturer (Stratagene). Oligonucleotide used for each mutant was 5′-GGACAATGAGCACCTCATCTTTCTGGAGAACACATTGGCCACCAAGG-3′. Briefly, after denaturing the wild type plasmids, the oligonucleotide primer was annealed with template DNA and then extended with *Pfu* Turbo DNA polymerase. After PCR, the methylated and nonmutated parental DNA template was digested with *Dpn*I. The XL-1 Blue cells were then transformed with *Dpn*I-treated DNA for selecting the mutated DNA. Mutants were verified by sequencing.

In Vitro Characterization of the Effect of DIP1/2 on Prostate Cancer—To determine the effect of DIP1/2 on prostate cancer cells, we studied 1) gene transcription using either serum response element (SRE) or TPA response element (TRE) reporter gene assays and 2) cell growth using both crystal violet and colony formation assays.

For reporter gene assay, C4-2 cells were transiently transfected with either SRE or TRE reporter plasmids in the combination of DIP1/2, ΔB, and ΔB-S24A expression vectors. Two days after transfection, T medium with 0.5% FBS was changed for another 24 h, and then either 50 ng/ml EGF or 100 ng/ml TPA was added to the cells for an additional 14 h. Luciferase activity assays were performed as described previously (11).

Using LipofectAMINE (Invitrogen), C4-2 cells (2×10^5) were transfected with 2 μg of pCI-DIP1/2 or 2 μg of pCI-neo (control). Two days after transfection, cells were selected with G418 (800 μg/ml), and an individual colony was cloned by ring isolation (4). The *in vitro* growth rate of each clone was determined by plating cells in a 24-well plate at a density of 5000 cells/well with T medium containing 2% TCM™ (Celox) and 0.5% FBS. At the indicated days, cell numbers were determined by crystal violet assay (15).

For the colony formation assay, C4-2 cells (3×10^4) were pleated on a 35-mm dish with T-medium containing 5% FBS and co-transfected with 0.2 μg of β-galactosidase expression vector with 0.8 μg of cDNAs as indicated. Twenty-four hours after transfection, cells were changed to T-medium containing 0.2% FBS. At the indicated time, cells were washed with cold PBS twice and fixed. The number of blue cells was counted by β-galactosidase staining according to Yeung *et al.* (16).

RESULTS

Identifying and Cloning DIP cDNA—DOC-2/DAB2's first 260 amino acids were used as a "bait" sequence in the yeast two-hybrid system to search for protein(s) that interacts with the N-terminal domain of DOC-2/DAB2 (17). Of 10,000 transformants screened, 36 positive clones were selected, and two positive clones (DIP1, DIP2) were further analyzed. These two clones shared overlapping sequence and were identical. However, since neither alone contained a full-length sequence, we designated the full-length sequence "DIP1/2."

To obtain the full-length cDNA of DIP1/2, a λ ZAP cDNA library from a rat brain was screened. Eleven clones spanned about 6.3 kb and represented two different sizes of DIP1/2 mRNA transcripts with different 5′ upstream sequences (Fig. 1*A*). The DIP1/2 was predicted to have an open reading frame of 996 amino acids and a calculated molecular mass of 110 kDa.

According to the deduced protein sequence, DIP1/2 appears to be a novel protein with several potential functional domains (Fig. 1*B*). Its key feature is the Ras GAP homology domain, which spans from residues 177 to 409 and is present in all members of the Ras GAP family (18). Also, DIP1/2 had a stretch of 10 proline repeats (residues 727–736) with the capacity to bind to proteins containing an Src homology 3 domain (19) and a leucine zipper dimerization domain (residues 842–861) for protein dimerization (20). The amino acid sequence alignment of DIP1/2's GAP domain with other Ras GAP pro-

FIG. 1. **Schematic display and amino acid sequence analysis of DIP1/2.** *A*, diagram of different 5′-untranslated sequences between two isoforms of DIP1/2 cDNAs. *PR*, proline-rich motif; *LZ*, leucine zipper domain. *B*, three distinct domains of DIP1/2 protein: GAP domain (*boldface type*), 10-proline repeats (*italic type*), and a leucine zipper domain (*underlined*). *C*, multiple sequence alignment of the GAP domain of DIP1/2 with GAP120, *Homo sapiens* neurofibromin (*hNF1*), synaptic Ras GAP (*SynGAP*), *Rattus norvegicus* Ras GAP (*rn-GAP*), and a novel human Ras GAP (*nGAP*). *Boldface letters* indicate the consensus amino acid residues within the Ras GAP domain.

teins (Fig. 1*C*), including $p120^{GAP}$, *Homo sapiens* neurofibromine (*hNF1*), *Rattus norvegicus* Ras GAP (*rnGAP*), a novel human Ras GAP (*nGAP*), and synaptic Ras GAP (*SynGAP*), shows that DIP1/2 contains all of the critical consensus amino acids for Ras GAP activity (21). This suggests that DIP1/2 can function as a Ras GAP.

Characterizing the DIP1/2 Expression Profile—Northern blot analysis indicated that steady-state levels of DIP1/2 mRNA (about 6.9 kb) are detected in brain, lung, thymus, bladder, and skeletal muscle tissue (Fig. 2*A*). In both brain and kidney, a different size of RNA transcript with 9.6 kb was found that may represent DIP1/2a with an additional 5′-upstream sequence. Nevertheless, steady-state levels of DIP1/2 mRNA were not detected in several urogenital organs including the ventral prostate, dorsal lateral prostate, seminal vesicle, and coagulating gland. However, detectable DIP1/2 mRNA levels (Fig. 2*A*) were detected in Noble rat prostate epithelia (*NbE*) and Sprague-Dawley rat prostate epithelia (*VPE*) from basal cells of the ventral prostate. Increased levels were not detected in stromal cells (*i.e.* NbF and VPF) from the same animals. This indicates that DIP1/2 preferentially expresses in the prostatic basal epithelial cells. Further Northern analysis (Fig. 2*B*) indicated that expression of DIP1/2 mRNA increased in degenerated prostates in a time-dependent manner, and the expression patterns of DIP1/2 and DOC-2/DAB2 mRNA concur. These findings suggest that both genes co-express in the enriched basal cell population during prostate degeneration (Fig. 2*B*).

A polyclonal antibody was raised against a synthetic peptide derived from the C terminus of DIP1/2. With this antibody, a major band of 110 kDa was detected from the *in vitro* tran-

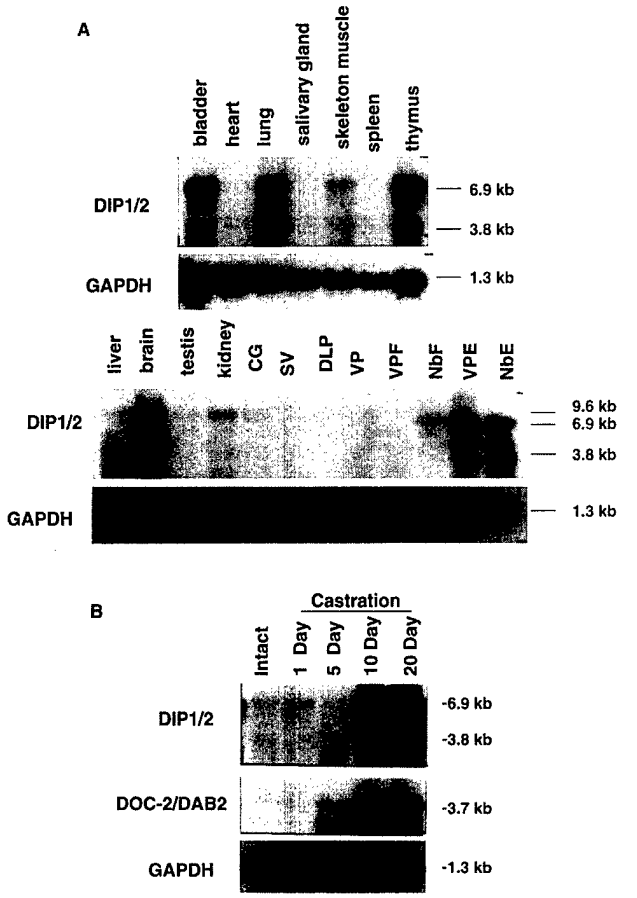

FIG. 2. **Profile of DIP1/2 mRNA expression in various rat organs and cell lines.** *A*, Northern blot analysis was performed to detect expression of DIP1/2 mRNA in different organs. *B*, increased expression of DIP1/2 and DOC-2/DAB2 mRNA in degenerated ventral prostate. Total cellular RNA (20 μg) from each organ or cell line were subjected to Northern analysis using ^{32}P-labeled DIP1/2 probe (1×10^6 cpm/ml). *NbE*, prostatic epithelia from Noble rat; *NbF*, prostatic fibroblasts from Noble rat; *VPE*, prostatic epithelia from Sprague-Dawley rat; *VPF*, prostatic fibroblasts from Sprague-Dawley rat; *VP*, ventral prostate; *DLP*, dorsolateral prostate; *SV*, seminal vesicle; *CG*, coagulating gland. The probe made from glyceraldehyde-3-phosphate dehydrogenase (*GAPDH*) cDNA was used as an internal control.

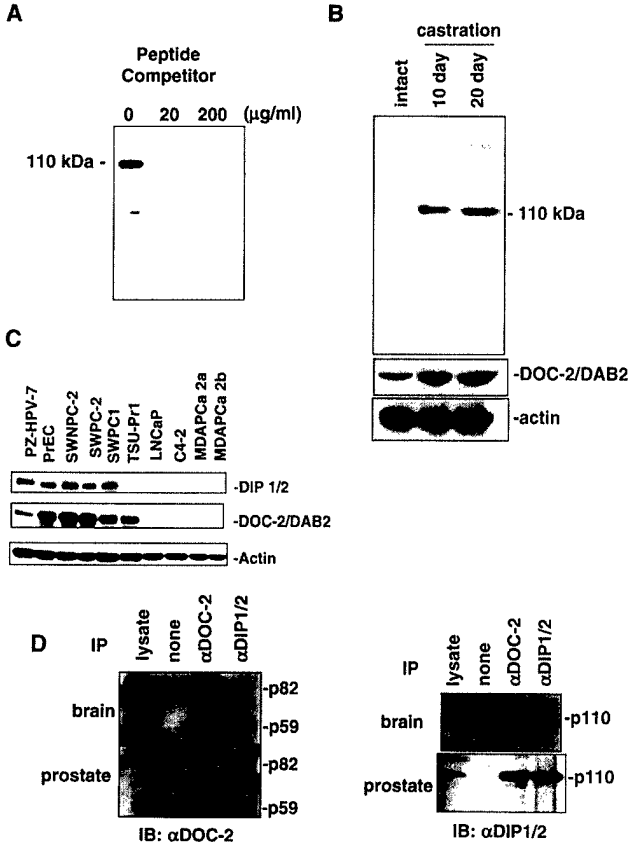

FIG. 3. **Characterization of anti-DIP1/2 polyclonal antibody and determination of DIP1/2 protein levels in rat organs and human prostate cell cultures.** *A, in vitro* translated DIP1/2 protein (5 μl) was subjected to Western blot analysis probed with anti-DIP1/2 polyclonal antibody with the indicated amount of synthetic peptide. *B*, 100 μg of protein were analyzed from degenerated ventral prostate harvested at the indicated time by Western blot with anti-DIP1/2 antibody, DOC-2/DAB2 monoclonal antibody, or anti-actin antibody. *C*, 60 μg of cell extract were subjected to Western blot analysis. PrEC, PZ-HPV-7, and SWNPC2 are normal primary prostatic epithelial cells; SWPC1 and SWPC2 are primary prostate cancer cells; TSU-Pr1, LNCaP, C4-2, MDAPCa$_{2a}$, and MDAPCa$_{2b}$ are metastatic prostate cancer cell lines. *D*, cell lysate from rat brain or prostate was incubated overnight with protein A-Sepharose beads alone or the beads plus either DOC-2/DAB2 antibody (Transduction Laboratories) or DIP1/2 antibody at 4 °C. The blots were probed with either p96 antibody or DIP1/2 antibody. *IP*, immunoprecipitation; *IB*, immunoblotting.

scription and translation of DIP1/2 cDNA (Fig. 3*A*). To further test the specificity of this antibody, serum was incubated with increasing concentrations of synthetic peptide of DIP1/2, ranging from 20 to 200 μg/ml, prior to probing with the blotted membrane. Results (Fig. 3*A*) indicated that the synthetic peptide effectively competes with the antibody in ability to bind to the DIP1/2 protein.

The increased protein expression of DIP1/2 was seen in degenerated prostate tissue (Fig. 3*B*), consistent with elevated DIP1/2 mRNA levels detected in degenerated prostate (Fig. 2*B*). Since they were parallel with DOC-2/DAB2 levels, these results (Fig. 3*B*) suggest that both DIP1/2 and DOC-2/DAB2 proteins coexist in degenerated prostate.

To further understand the profile of DIP1/2 and DOC-2/DAB2 expression in human prostate cancer, we screened a variety of prostate cancer cell lines. In Western blot analysis, only a 110-kDa protein band was detected in cell lysate of human prostate cells, indicating that the antibody also recognizes the homologue of human DIP1/2 (hDIP1/2). The sequence of hDIP1/2 is very similar to that of rDIP1/2.[2] As shown in Fig. 3*C*, we found that DIP1/2 and DOC-2/DAB2 proteins were present in both normal primary epithelial cells (PZ-HPV-7, PrEC, and SWNPC2) and primary tumors (SWPC1 and SWPC2). However, a significant decreased expression of DIP1/2 was detected in several metastatic cell lines such as TSU-Pr1, LNCaP, C4-2, MDAPCa$_{2a}$, and MDAPCa$_{2b}$, cancer cell lines. We believe this indicates that DIP1/2 is involved in the progression of prostate cancer.

Specific Interaction between DIP1/2 and DOC-2/DAB2—Because data from the yeast two-hybrid screening indicated that DIP1/2 and DOC-2/DAB2 directly interact, we further examined whether these two native proteins interact with each other using brain and prostate as tissue sources. Using antibodies against either DOC-2/DAB2 (transfection) or DIP1/2 in a co-immunoprecipitation experiment, we demonstrated that endogenous DIP1/2 and DOC-2/DAB2 proteins were present in the same immune complex (Fig. 3*D*). Noticeably, there were two sizes of DIP1/2 protein in the rat brain (molecular masses of 110 and 135 kDa, respectively) (Fig. 3*D*), and the predominant protein appears to be 135 kDa, which may correspond to the 9.6 kb of DIP1/2 mRNA detected in brain tissue (Fig. 2*A*).

To confirm whether DIP1/2 only interacts with the N-termi-

[2] Hong, C., Pong, R-C., Wang, Z., and Hsieh, J. T., *Genomics*, in press.

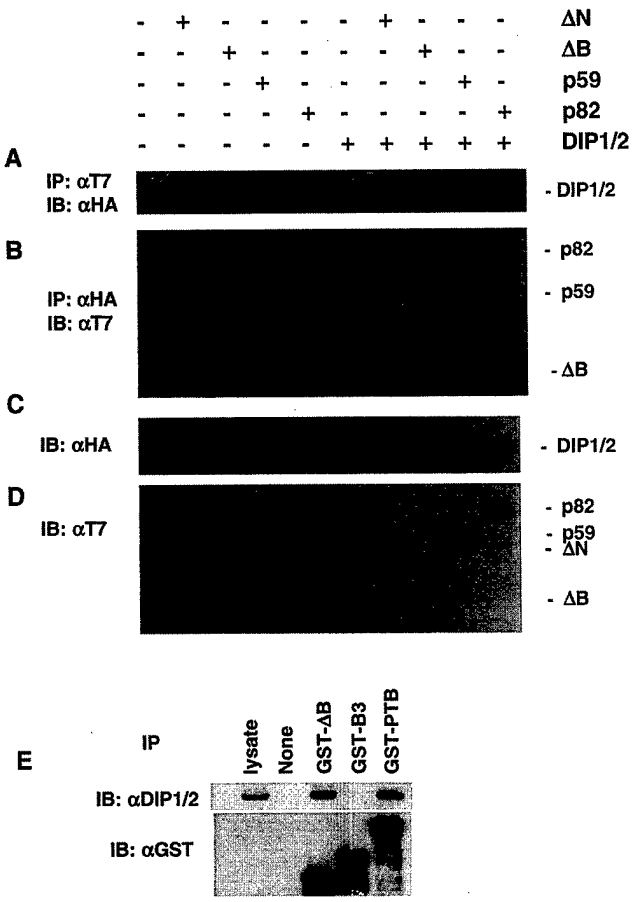

FIG. 4. **Direct interaction between DIP1/2 and DOC-2/DAB2 or DAB1.** COS cells were cotransfected with different T7-tagged DOC-2/DAB2 constructs and HA-tagged DIP1/2 constructs for 48 h. The supernatants were immunoprecipitated with either T7-antibody-conjugated agarose beads (*A*) or HA-antibody plus protein A/G-agarose beads (*B*). After centrifugation, pellets were subjected to immunoblotting analysis. The levels of protein expression from each transfection were determined by Western analysis (*C* and *D*). Cell lysate was prepared from COS cells transfected with each expression vector and subjected to pull-down by glutathione beads and then probed with DIP1/2 antibody (*E*). *IP*, immunoprecipitation; *IB*, immunoblotting.

nal domain of DOC-2/DAB2, we used a series of T7-tagged DOC-2/DAB2 wild type (p82), slicing form (p59), N-terminal deletion mutant (ΔN), and C-terminal deletion mutant (ΔB)) as described previously (11), and an HA-tagged DIP1/2 construct. Cells were co-transfected with both vectors for 24 h, and then cell lysates were immunoprecipitated with T7-antibody (for DOC-2/DAB2) and then probed with HA-antibody (for DIP1/2). The presence of DIP1/2 was only detected in the cells co-transfected with DIP1/2 and DOC-2/DAB2 containing the N terminus, such as p59, p82, and ΔB, but not in the cells co-transfected with DIP1/2 and the C terminus of DOC-2/DAB2 (ΔN) (Fig. 4*A*). Conversely, using HA-antibody for immunoprecipitation and then probing with T7-antibody, we demonstrated that DIP1/2 protein can be co-precipitated with p59, p82, and ΔB protein but not with ΔN protein (Fig. 4*B*). Furthermore, to rule out the possible experimental artifact that is due to differential protein expression in each transfection, levels of each recombinant protein were determined by Western analysis and appeared to be identical (Fig. 4, *C* and *D*). Taken together, these data indicate that DIP1/2 protein only interacts with the N-terminal, not the C-terminal, domain of DOC-2/DAB2 protein.

Since DAB1 and DOC-2/DAB2 share a high degree of homology at the PTB domain, we also examined whether mouse DAB1 can interact with DIP1/2. Two mouse DAB1 cDNA clones (PTB, B3) were used (22), and we found that DIP1/2 interacts with DAB-PTB (amino acids 29–197) but not DAB-B3 (amino acids 107–243), since DAB-B3 contains partial PTB sequences (22).

Function of DIP1/2 in Vitro and in Vivo—Due to the high sequence homology between DIP1/2 and other Ras GAPs, we thought it likely that DIP1/2 facilitates Ras GTPase activity. To test this, we prepared a GST-DIP1/2 fusion protein containing the minimal Ras GAP domain (23), and either this fusion protein or GST protein was incubated with human recombinant [γ-^{32}P]GTP-bound Ha-Ras protein. The increasing amounts of GST-DIP1/2 (ranging from 0.2 to 1 μg) stimulated Ras GTPase activity in a dose-dependent manner (Fig. 5*A*). Conversely, control GST protein (1 μg) had no effect on Ras GTPase activity.

To further compare the Ras GAP activity of DIP1/2 with a known Ras GAP protein (GAP120), we created a DIP1/2 cDNA construct (DIP1/2$_m$) as a control with a point mutation (R220L) that may disrupt GAP activity. As shown in Fig. 5*B*, the overall GAP activity between p120^{GAP} and DIP1/2 is very similar, and the DIP1/2$_m$ did not have any GAP activity toward Ha-Ras. These data clearly demonstrate that DIP1/2 can stimulate GTPase activity of Ha-Ras *in vitro*. To examine the specificity of DIP1/2 to other small G-proteins such as K-Ras, R-Ras, TC21, and Rap1A, we found that DIP1/2 has a similar GAP activity as p120^{GAP} by stimulating GTPase activity of K-Ras, R-Ras, and TC21 but not Rap1A (Fig. 5*C*). These data indicate that DIP1/2 is a typical Ras GAP.

Early study of Ras signal transduction indicates that Raf is an immediate downstream effector for Ras signaling (24). Because Raf binds tightly to the GTP-bound form of Ras but not to the GDP-bound form, such differential affinity can be used to determine the GTP-bound status of Ras. To analyze the GAP activity of DIP1/2 *in vivo*, C4-2 cells (25) were transfected with vectors expressing HA-tagged Ras, DIP1/2, or DIP1/2$_m$. After activating Ras using EGF, the GTP-bound form of Ras was precipitated with GST-RBD (GST-Raf containing Ras binding domain). Precipitated Ras was detected using the HA-antibody. As shown in Fig. 5*D*, in the presence of EGF, the amount of GTP-bound Ras increased over that of the control. Levels of the GTP-bound Ras significantly decreased in cells expressing DIP1/2; however, DIP1/2$_m$ failed to stimulate Ras GTPase in cells treated with EGF. The whole cell lysates were examined for expression of DIP1/2 and Ras proteins, and results demonstrated that expressions of DIP1/2 and Ras were identical between each transfection. These results indicate that DIP1/2 can function as a Ras GTPase-activating protein *in vivo*. Therefore, we conclude that DIP1/2 functions as a Ras GAP *in vivo* and *in vitro*.

Regulation of the Ras-Raf Signaling Pathway by DIP1/2—The Ras protein functions as an essential component in many intracellular signaling pathways responsible for differentiation, proliferation, and apoptosis (26). The Raf-MEK-ERK pathway is a key signal transduction pathway modulated by Ras protein (27). The downstream components of this pathway, including AP-1, which binds to TRE, and EIK-1, which binds to SRE, subsequently activate gene expression (28–30). Since PKC is able to activate the Raf/MEK/ERK axis (31, 32), we investigated the impact of DIP1/2 on this cascade. As shown in Fig. 6*A*, in the absence of EGF, increased expression of DIP1/2 could inhibit the basal levels of SRE reporter gene activity in prostate cancer cells.

The presence of EGF increased the reporter gene activity at least 5-fold. However, DIP1/2 could inhibit the reporter gene activity in a dose-dependent manner. Using the same reporter gene assay, we found that DIP1/2 or ΔB, a DOC-2/DAB2 cDNA

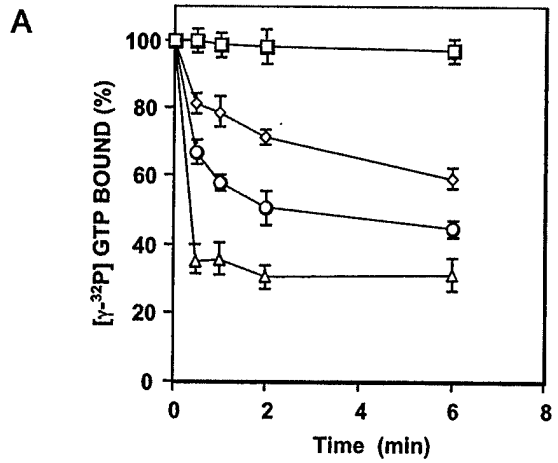

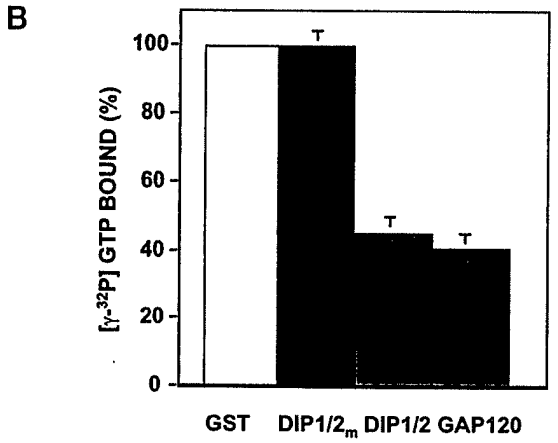

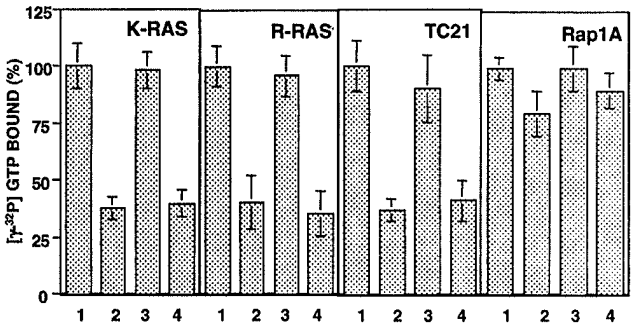

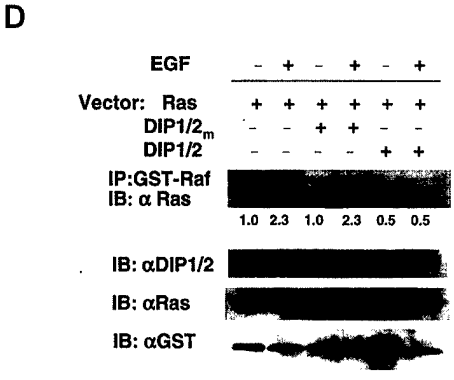

FIG. 5. ***In vitro* and *in vivo* Ras GAP activity assays.** *A*, kinetics of Ras GAP activity of DIP1/2 protein. One microgram of purified GST protein and different amounts of GST-DIP1/2 were incubated with [γ-^{32}P]GTP-bound Ha-Ras. At the indicated time, retention of the unhydrolyzed [γ-^{32}P]GTP was measured by a filter assay. GST, 1 μg (*d*); GST-DIP1/2, 0.2 μg (*h*), 0.4 μg (*b*), and 1.0 μg (*f*). Data represent the mean ± S.D. from three determinants. *B*, comparison of the *in vitro* GAP assay between DIP1/2 and p120^{GAP}. [γ-^{32}P]GTP-bound Ha-Ras was incubated separately with 1 μg of purified GST, GST-DIP1/2$_m$, GST-DIP1/2, and GST-p120^{GAP} protein at 25 °C for 10 min. The unhydrolyzed [γ-^{32}P]GTP was assayed by a filter assay. Data represent the mean ± S.D. from three determinants. *C*, determination of the specificity of DIP1/2 to other G-proteins. [γ-^{32}P]GTP-bound K-Ras, R-Ras, TC21, and Rap1A (36) were incubated separately with 1 μg of purified GST (*1*), GST-DIP1/2 (*2*), GST-DIP1/2$_m$ (*3*), and GST-p120^{GAP} (*4*) at 25 °C for 10 min. The unhydrolyzed [γ-^{32}P]GTP was assayed by a filter assay. Data represent the mean ± S.D. from three determinants. *D*, inhibition of Ras and Raf binding by DIP1/2. C4-2 cells transfected with both HA-tagged Ras and DIP1/2 vectors were treated with EGF (100 ng/ml) for 30 min. After incubating, cell supernatants were precipitated with GST-Raf-agarose beads, and the precipitates were subjected to immunoblotting. The levels of protein expression from each transfection were determined by Western analysis. Results were measured by densitometric scanning. *IP*, immunoprecipitation; *IB*, immunoblotting.

containing the N-terminal domain (11), alone can suppress SRE activity (Fig. 6*B*), but co-expression of ΔB and DIP1/2 had an additive effect on the inhibition of SRE activity in the presence of TPA. These data indicate that physical interaction between DIP1/2 and DOC-2/DAB2 has functional impact on Ras-mediated signal transduction.

Previously, we demonstrated that PKC-elicited DOC-2/DAB2 phosphorylation can block TPA-induced gene activity (11). Therefore, we investigated whether DIP1/2 is a mediator involved in this action. We employed the C4-2 cell line because both DOC-2/DAB2 and DIP1/2 are not detectable. Either a high concentration of ΔB or DIP1/2 alone was able to inhibit TPA-induced TRE reporter gene activity (Table I). At this concentration, we observed only an additive effect on inhibiting TRE reporter gene activity in the presence of ΔB and DIP1/2. When the concentration of ΔB or DIP1/2 decreased to 0.1 or 0.2 μg, respectively, we noticed that the inhibitory effect of each individual cDNA reduced significantly. Transfecting both cDNAs at this concentration, we observed a synergistic inhibitory effect on C4-2 cells. On the other hand, combing the ΔB-S24A mutant with DIP1/2 failed to have any synergistic effect; it appears that Ser^{24}, a PKC substrate, in DOC-2/DAB2 is the key amino acid to modulate this activity. Thus, the binding of DIP1/2 to ΔB can be enhanced by TPA, whereas ΔB-S24A cannot (Fig. 6*C*). Taken together, these data indicate that the interaction between DIP1/2 and the N-terminal domain of DOC-2/DAB2 has a significant functional impact on gene transcription.

Biological Effect of DIP1/2 on Prostate Cancer Cells—Because DIP1/2 appears to be a negative regulator for the Ras-mediated pathway, it may function as a growth inhibitor. To test this, C4-2 cells (a tumorigenic human prostate cancer cell line) were transfected with a DIP1/2 expression vector. Initially, we observed that there were fewer surviving clones in the DIP1/2-transfected plate than in plasmid control-transfected cells despite the same number of cells being used in transfection. After isolating two independent colonies (D1, D2), the protein levels of DIP1/2 in the D2 subline were higher than those in the D1 subline (Fig. 7*A*). Data from Fig. 7*B* indicated that expression of DIP1/2 significantly inhibited the *in vitro* cell growth compared with the plasmid control. This inhibitory effect of both D1 and D2 correlated with their DIP1/2 protein levels (Fig. 7*A*).

To rule out possible artifacts from stable transfection, we examined the growth suppression of DIP1/2 in C4-2 cells using transient transfection (16). As shown in Fig. 7*C*, the elevated DIP1/2 expression, determined by Western blot, inhibited the colony formation of C4-2 cells in a time-dependent manner.

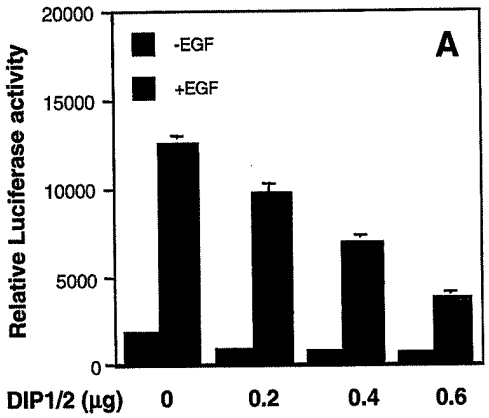

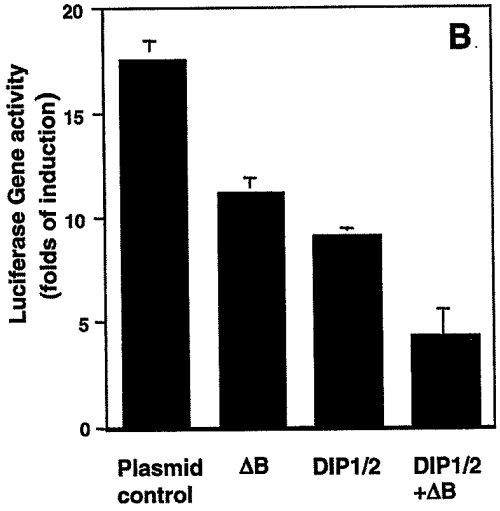

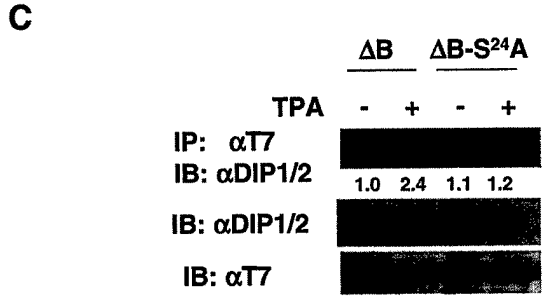

FIG. 6. **Interaction of DIP1/2 and DOC-2/DAB2 on SRE reporter gene activity.** *A*, C4-2 cells were co-transfected with SRE reporter gene (0.1 μg), β-galactosidase (*β-gal*, 0.1 μg), DIP1/2 (0–0.6 μg), and PCI-neo (0.8–0.2 μg) vectors and then treated with EGF (100 ng/ml) for 14 h. *B*, C4-2 cells were co-transfected with either ΔB (0.4 μg) or DIP1/2 (0.4 μg) in combination with SRE reporter gene and β-galactosidase vectors and treated with TPA (100 ng/ml) for 14 h. Cell lysates were determined by both luciferase and β-galactosidase activity assays. Reporter gene activity from each sample was normalized with β-galactosidase activity. Data represent means ± S.D. from three independent experiments. *C*, effect of TPA on interaction of DIP1/2 and DOC-2/DAB2. C4-2 cells were cotransfected with DIP1/2 in combination with either ΔB (0.4 μg) or ΔB-S24A (0.4 μg). Twenty-four hours after transfection, cells were treated with T-medium containing 0.1% FBS, and then 24 h later, cells were incubated with TPA (100 ng/ml) for 40 min. After incubation, cells were washed with PBS and lysed. Immunoprecipitation and Western blot were performed as described in the legend to Fig. 4. Results were measured by densitometrical scanning.

Conversely, increased DIP1/2_m expression did not effect colony formation of C4-2. These data indicate that DIP1/2's GAP activity modulates its growth-inhibitory effect. DIP1/2 alone appears to be a potent growth inhibitor for prostate cancer.

We also examined whether the growth suppression effect of

TABLE I
Effect of DIP1/2 and ΔB on TPA-induced gene activation in prostate cancer

	Relative luciferase activity[a]	
	Experiment I	Experiment II
	-fold	
PCI-neo	33.0 ± 0.2 (100%)	38.3 ± 0.7 (100%)
ΔB	13.7 ± 1.9 (42%)	37.0 ± 0.9 (97%)
ΔB-S24A	33.1 ± 0.3 (100%)	37.1 ± 1.9 (97%)
DIP1/2	12.4 ± 1.2 (38%)	23.8 ± 1.7 (62%)
ΔB + DIP1/2	6.3 ± 0.2 (20%)	7.3 ± 0.5 (19%)
ΔB-S24A + DIP1/2	11.4 ± 2.1 (35%)	24.4 ± 1.1 (64%)

[a] The relative luciferase gene activity is expressed as -fold induction compared with ethanol control. Both experiments I and II are typical representations from several experiments. In experiment I, 0.4 μg of each cDNA was used. In experiment II, ΔB or ΔB-S24A (0.1 μg) and DIP1/2 (0.2 μg) were used. The results were calculated as mean ± S.D. in triplicate.

C4-2 cells can be enhanced in the presence of both DIP1/2 and DOC-2/DAB2. In this experiment, we used half of the amount of DIP1/2 cDNA from the previous experiment (Fig. 7*C*) and only the N-terminal domain of DOC-2/DAB2 (*i.e.* ΔB), since we found some additional inhibitory activity associated with the C terminus (10). As shown in Fig. 7*D*, 0.1 μg of ΔB alone did not exhibit any growth-inhibitory effect, and DIP1/2 alone had a growth-inhibitory effect. However, we observed a synergistic effect of growth suppression of C4-2 cells transfected with both DIP1/2 and ΔB cDNAs compared with C4-2 cells transfected with either DIP1/2 or ΔB alone (Fig. 7*D*). In contrast, C4-2 cells transfected with both DIP1/2_m and ΔB did not exhibit enhanced growth suppression. These data indicated that the interaction between DIP1/2 and DOC-2/DAB2 is critical for the growth-inhibitory effect of DIP1/2 in prostate cancer cells.

DISCUSSION

The DIP1/2 expression profile in different organs appears to be diverse. Northern analysis (Fig. 2*A*) indicates a high level of DIP1/2 mRNA expression in brain, thymus, and bladder tissue and a low level in skeleton muscles, kidney, and liver tissue. But no expression can be detected in several urogenital organs, including the ventral prostate, dorsolateral prostate, seminal vesicle, and coagulating gland. This unique pattern of tissue distribution implies that DIP1/2 may have a specific physiological function in each organ. For example, DIP1/2 expression is detected in the enriched basal cell population of degenerated prostate and in prostatic epithelial cell lines (such as NbE and VPE) derived from the basal cell population (Fig. 2*A*), suggesting that DIP1/2 may be involved in prostate regeneration. This hypothesis can be supported by our results: 1) decrease or absence of either DIP1/2 or DOC-2/DAB2 is often detected in several metastatic human prostate cancer cell lines (Fig. 3*C*), and 2) DIP1/2 appears to be a potent growth inhibitor for human prostate cancer cells (Fig. 7). It is known that increased Ras activity is associated with high grade metastatic prostate cancer; however, *RAS* mutation is rarely detected (33, 34). Our results suggest an underlying mechanism with which to account for this phenomenon. In addition to DIP1/2, we found that altered expression of $p120^{GAP}$ is associated with prostate cancer cells (data not shown). Thus, our results indicate that altered Ras GAP expression plays a critical role in the progression of prostate cancer.

The phosphorylation of Ser^{24} in DOC-2/DAB2, which is involved in inhibiting TPA-induced AP-1 activity (11), provides evidence for the underlying functional mechanism of DOC-2/DAB2. In this study, our data indicate that DIP1/2 is an immediate downstream effector for DOC-2/DAB2 in both prostate and brain tissues (Fig. 3*D*), and the binding of DIP1/2 to DOC-

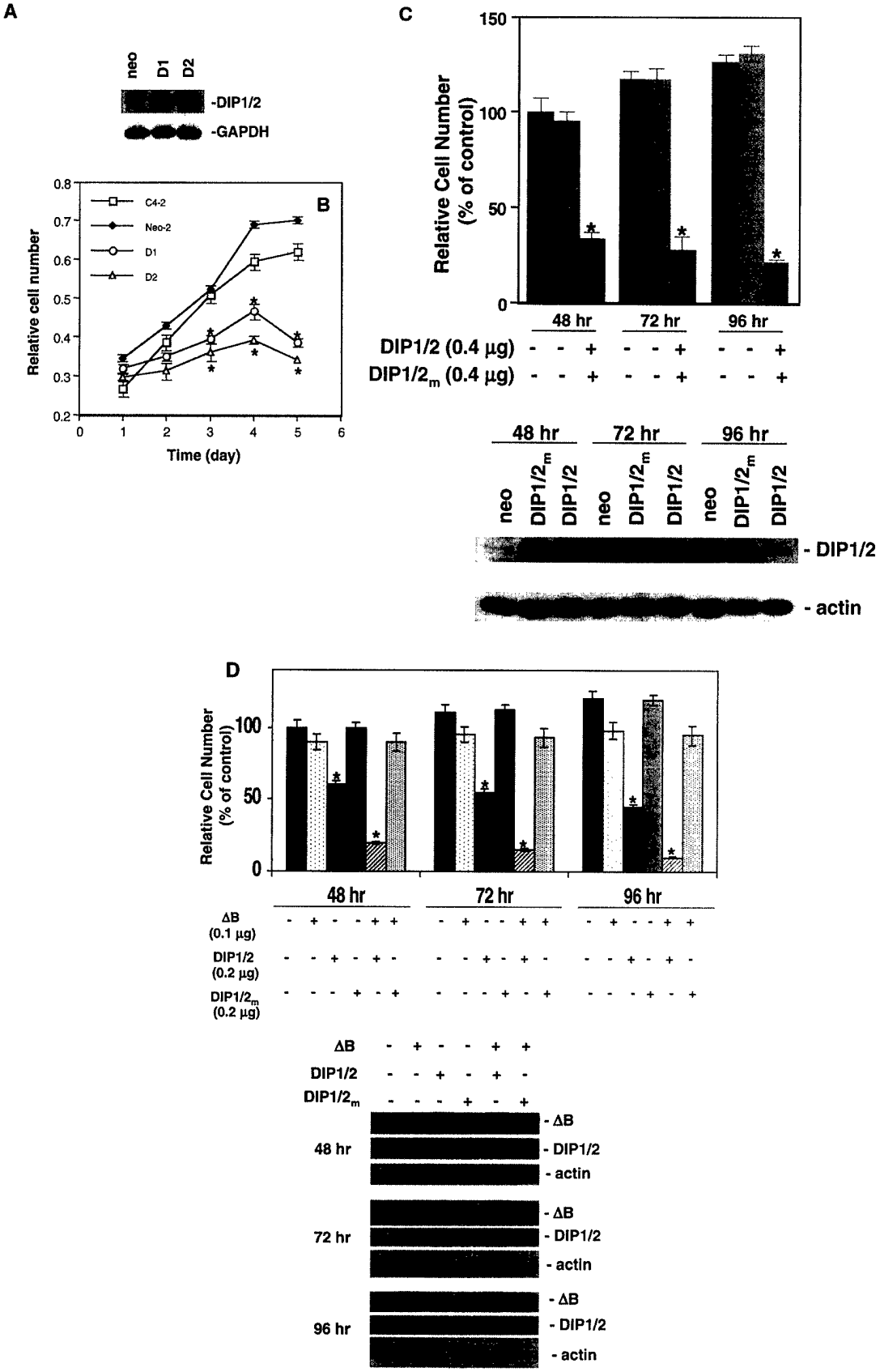

FIG. 7. **Growth-inhibitory effect of DIP1/2 on prostate cancer cells.** Cells were transfected with either pCI-neo or DIP1/2 expression vector. After G418 selecting, two independent clones were isolated and characterized. *A*, increased protein expression was detected by DIP1/2 antibody. *B*, the *in vitro* growth rate for each clone was determined by crystal violet assay. *C*, the colony formation of cells transfected with DIP1/2 cDNA. *D*, the colony formation of cells transfected with DIP1/2 cDNA and/or DOC-2/DAB2 cDNA. Data represent the mean ± S.D. from six determinants. *, significantly different from plasmid control ($p < 0.01$).

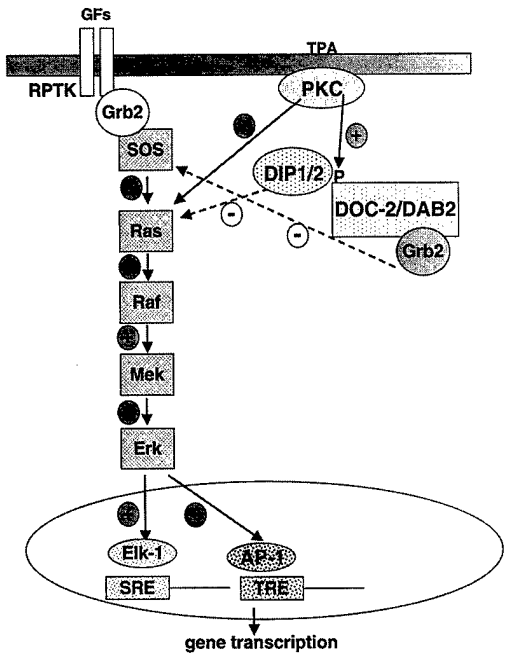

FIG. 8. **The mechanism of action of DOC-2/DAB2 and DIP1/2 complex in signal transduction pathway.** DOC-2/DAB2 and DIP1/2 complex represent a negative feedback machinery for several exogenous stimuli-elicited signal cascade. PKC can phosphorylate the N-terminal domain of DOC-2/DAB2 (serine 24) that recruits DIP1/2 to inactivate Ras protein. On the other hand, shortly after the treatment of peptide growth factors, the C terminus of DOC-2/DAB2 (proline-rich domain) competes with SOS for Grb 2 binding, which leads to the inactivation of the MAP pathway.

2/DAB2 can be enhanced when the Ser^{24} residue in DOC-2/DAB2 is phosphorylated (Fig. 6*C*). The most conserved region in DIP1/2 protein is the GAP domain, which has a high amino acid sequence homology (40–90%) compared with the GAP domains of other Ras GAPs, and DIP1/2's GAP domain contains all 31 consensus amino acids of other Ras GAPs. These consensus amino acid residues in the Ras GAP domain modulate Ras GTPase activity (13). For example, Arg^{789} of $p120^{GAP}$ participates in catalysis and simultaneously stabilizes Gln^{61} of Ras for optimal GTP hydrolysis (35). Our data (Fig. 5) indicate that DIP1/2 has Ras GAP activity *in vitro* and *in vivo*. Since Arg^{220} of DIP1/2 is equivalent to Arg^{789} of $p120^{GAP}$, once Arg^{220} was altered (R220L), the single amino acid mutant of DIP1/2 lost its Ras GAP activity *in vitro* and *in vivo* (Fig. 5, *B* and *D*). Similar to the GAP activity of $p120^{GAP}$ (36), DIP1/2 can stimulate the GTPase activity of several small G-protein of Ras family (Fig. 5*C*). In majority of PCa cell lines used in this study, we were able to detect the presence of R-Ras, K-Ras and Ha-Ras (data not shown). Therefore, we believe that loss of GAP protein in prostate cells may be an underlying mechanism leading to constitutive activation of Ras in these cells.

We demonstrate that co-expression of DIP1/2 and the N-terminal domain of DOC-2/DAB2 (*i.e.* ΔB) has an additive effect on suppressing either TPA-induced SRE or TRE reporter gene activity (Fig. 6*B* and Table I). Therefore, we believe that the *in vivo* interaction of DIP1/2 with the N-terminal domain of DOC-2/DAB2 acts as a feedback mechanism to modulate PKC-induced gene activation. It is known that the modulation of the Raf/MEK/ERK axis is also controlled by growth factors through their protein receptor tyrosine kinase, although our data indicate that DIP1/2 alone is also able to inhibit EGF-induced SRE reporter gene activity (Fig. 6*A*) and cell growth. However, the interaction between DIP1/2 and DOC-2/DAB2 certainly amplifies their individual inhibitory effect (Figs. 6*C* and 7*D* and Table I). Therefore, this protein complex containing both DOC-2/DAB2 and DIP1/2 represents a unique negative regulatory machinery to balance signals elicited by growth factors (such as EGF) or PKC activators (such as TPA).

In addition to the N-terminal domain of Ras GAP homology domain of DIP1/2, the proline-rich repeats and leucine zipper domains from its C terminus may contribute to DIP1/2 activity. Our preliminary data indicate that the proline-rich repeats (residues 727–736) in DIP1/2 interact with Grb2 (data not shown). Because Grb2 binds to SOS, a guanine nucleotide exchange factor critical for downstream signaling, the binding of DIP1/2 to Grb2 may interrupt Ras activation. It is also possible that DIP1/2 can interact with other proteins containing the Src homology 3 domain. On the other hand, the leucine zipper domain (residues 842–861) of DIP1/2 may form a homodimer or a heterodimer with other proteins. Although no direct evidence has been shown for DIP1/2 dimerization, we observed a self-dimerization of DIP1/2 using the yeast two-hybrid experiment, which suggests that the dimerization of DIP1/2 may affect its activity. More detailed studies are under way to examine this hypothesis.

In summary, both DIP1/2 and DOC-2/DAB2 form a unique protein complex (Fig. 8) with a negative regulatory activity that modulates the Ras-mediated signaling pathway. This complex is operative in basal cells of the prostate and may orchestrate the differentiation and proliferation potential of these cells during prostate regeneration. In contrast, altered expression of any component of this complex may result in abnormal growth and/or the acquired malignant phenotypes of prostate cancer and perhaps other types of cancer such as ovarian and breast cancer. Further dissection and functional examination of each component in this complex is warranted.

Acknowledgments—We thank Andrew Webb for editing the manuscript, Hana Sharif for valuable project assistance, Dr. Michael White for HA-tagged Ras expression vector, Dr. Jonathan Cooper for DAB1 cDNA constructs, and Dr. Matsuda for TC21, Rap1, and R-Ras cDNA constructs.

REFERENCES

1. Mok, S. C., Wong, K-K., Chan, R. K. W., Lau, C., Tsao, S-W., Knapp, R. C., and Berkowitz, R. S. (1994) *Gynecol. Oncol.* **52,** 247–252
2. Fuzili, Z., Sun, W., Mittellstaedt, S., Cohen, C., and Xu, X. X. (1999) Oncogene **18,** 3104–3113
3. Schwahn, D. J., and Medina, D. (1998) *Oncogene* **17,** 1173–1178
4. Tseng, C-P. Brent, D. E., Li, Y.-M., Pong, R.-C., and Hsieh, J.-T. (1998) *Endocrinology* **139,** 3542–3553
5. Fulop, V., Colitti, C. V., Genest, D., Berkowitz, R. S., Yiu, G. K., Ng, S-W., Szepesi, J., and Mok, S. C. (1998) *Oncogene* **17,** 419–424
6. Xu, X.-X., Yang, W., Jackowski, S., and Rock, C. O. (1995) *J. Biol. Chem.* **270,** 14184–14191
7. Howell, B. W., Hawkes, R., Soriano, P., and Cooper, J. A. (1997) *Nature* **389,** 733–737
8. Howell, B. W., Herrick T. M., Hildebrand, J. D., Zhang, Y., and Cooper, J. A. (1997) *Curr. Biol.* **10,** 877–885
9. Xu, X.-X., Yi, T., Tang, B., and Lambeth, J. D. (1998) *Oncogene* **16,** 1561–1569
10. Zhou, J., and Hsieh, J. T. (2001) *J. Biol. Chem.* **278,** 27793–27798
11. Tseng, C.-P., Ely, B. D., Pong, R.-C., Wang, Z., Zhou, J., and Hsieh, J.-T. (1999) *J. Biol. Chem.* **274,** 31981–31986
12. Weijerman, P. C., Konig, J. J., Wong, S. T., Niesters, H. G., and Peehl, D. M. (1994) *Cancer Res.* **54,** 5579–5583
13. Navone, N., Olive M., Ozen, M., Davis, R., Troncoso, P., Tu, S-M., Johnston, D., Pollack, A., Pathak, S., von Eschenbach, A. C., and Logothetis, C. J. (1997) *Clin. Cancer Res.* **3,** 2493–2500
14. Kim, J. H., Liao, D., Lau, L-F., and Huganir, R. (1998) *Neuron* **20,** 683–691
15. Gillies, R. J., Didier, N., and Denton, M. (1986) *Anal. Biochem.* **159,** 109–113
16. Yeung, K., Seitz, T., Li, S., Janosh, P., McFerran, B., Kaiser, C., Fee, F., Katsanakis, K. D., Rose, D. W., Mischak, H., Sedivy, J., and Kolch, W. (1999) *Nature* **401,** 173–177
17. Fields, S., and Song, O-K. (1989) *Nature* **340,** 245–246
18. Boguski, M. S., and McCormick, F. (1993) *Nature* **366,** 643–654
19. Feller, S. F., Ren, R., Hanafusa, H., and Baltimore, D. (1994) *Trends Biochem. Sci.* **19,** 453–458
20. Struhl, K. (1989) *Trends Biochem. Sci.* **14,** 137–140
21. Schheffzek, K., Lautwein, A., Ahmadian, M. R., and Wittinghofer, A. (1996) *Nature* **384,** 591–596
22. Howell, B. W., Gertler F. B., and Cooper J. A. (1997) *EMBO J.* **16,** 121–132
23. Gideon, P., John, J., Frech. M., Lautwein, A., Clark, R., Scheffler, J. E., and Wittinghofer, A. (1992) *Mol. Cell. Biol.* **12,** 2050–2056

24. Morrison, D., Kaplan, D. R., Rapp, U., and Roberts, T. M. (1998) *Proc. Natl. Acad. Sci. U. S. A.* **85,** 8855–8859
25. Wu, T. T., Sikes, R. A., Cui, O., Thalmann, G. N., Kao, C., Murphy, C. F., Yang, H., Zhau, H. E., Balian, G., and Chung, L. W. (1998) *Int. J. Cancer.* **77,** 877–894
26. McCormick, F. (1995) *Mol. Reprod. Dev.* **42,** 500–506
27. Porter, A. C., and Vaillancourt, R. R. (1998) *Oncogene* **17,** 1343–1352
28. Abate, C., and Curran, T. (1990) *Semin. Cancer Biol.* **1,** 19–26
29. Hakak, Y., and Martin, G. S. (1999) *Mol. Cell. Biol.* **19,** 6953–6962
30. Hata, A., Akita, Y., Suzuki, K., and Ohno, S. (1993) *J. Biol. Chem.* **268,** 9122–9129
31. Sozeri, O., Vollmer, K., Liyanage, M., Firth, D., Kour, G., Mark, G. E., and Stabel, S. (1992) *Oncogene* **7,** 2259–2262
32. Denhardt, D. T. (1996) *Biochem. J.* **318,** 729–747
33. Gumerlock, P. H., Poonamallee, U. R., Meyers, F. J., and deVere White, R. W. (1991) *Cancer Res.* **51,** 1632–1637
34. Pergolizzi, R. G., Kreis, W., Rottach, C., Susin, M., and Broome, J. D. (1993) *Cancer Invest.* **11,** 25–32
35. Wittinghofer, A. (1998) *J. Biol. Chem.* **379,** 933–937
36. Ohba, Y., Mochizuki, N., Yamashita, S., Chan, A. M., Schrader, J. W., Hatter, S., Nagashima, K., and Matsuda Michiyuki. (2000) *J. Biol. Chem.* **275,** 20020–20026

doi:10.1006/geno.2002.6739, available online at http://www.idealibrary.com on IDEAL

Article

Differential Regulation of the Human Gene *DAB2IP* in Normal and Malignant Prostatic Epithelia: Cloning and Characterization

Hong Chen, Rey-Chen Pong, Zhi Wang, and Jer-Tsong Hsieh*

Department of Urology, University of Texas Southwestern Medical Center, Dallas, Texas 75390-9110, USA

**To whom correspondence and reprint requests should be addressed. Fax: (214) 648-8786. E-mail: JT.Hsieh@UTSouthwestern.edu.*

Human *DAB2IP* (for DAB2 interaction protein) is a novel member of the RasGTPase-activating protein family. It interacts directly with DAB2, which suppresses growth of many cancer types. We demonstrated that DAB2IP is often downregulated in human prostate cancer cell lines. The predicted DAB2IP protein (967 amino acids) shares 94.2% homology with the rat DIP1/2 protein. We mapped the promoter of *DAB2IP* and studied its regulation in normal and malignant prostate cancer cells. This gene is located at 9q33.1–q33.3 and spans approximately 96 kb with 15 exons and 14 introns. The *DAB2IP* promoter does not contain any typical TATA box—evidenced by the presence of various RNAs with differential transcription starting sites. We further demonstrated that normal prostatic epithelial cells have elevated *DAB2IP* mRNA compared with cancer cells, which correlates with increased *DAB2IP* promoter activity. These data indicate that transcriptional regulation of *DAB2IP* is responsible for the downregulation of DAB2IP expression in prostate cancer cells.

Key Words: DAB2IP gene, prostate cancer, gene promoter, BAC clone, gene regulation

INTRODUCTION

We identified rat DIP1/2 (for DAB2 interaction protein) as a novel RasGTPase-activating protein using a yeast two-hybrid system (Z.W. *et al., J. Biol. Chem.*, in press). DIP1/2 interacts directly with the amino terminus of DAB2 (for disabled-2; also known as differentially expressed in ovarian carcinoma-2, DOC-2). DAB2 seems to be a tumor suppressor in several cancer types [1–4], whereas DIP1/2 acts as a downstream effector involved in the DAB2-elicited signal pathway. Together this complex blocks exogenous, stimuli-induced gene expression and results in the growth suppression of prostate cancer (Z.W. *et al., J. Biol. Chem.*, in press) [5].

DIP1/2 (996 amino acids) has a molecular mass of 110 kD containing several potential function domains: a RasGAP domain in the N terminus; proline repeats; and a leucine zipper domain in the carboxy terminus. Increased DIP1/2 expression in the rat prostate is found in the enriched basal cell population after castration-induced degeneration (Z.W. *et al., J. Biol. Chem.*, in press), which suggests that DIP1/2 may be associated with the differentiation of prostatic epithelium. However, the decreased or absent expression of human DAB2IP protein, a rat homolog, is often detected in several prostate cancer cell lines. The mechanism by which DAB2IP expression is regulated is largely unknown.

Because we found that the steady-state levels of *DAB2IP* mRNA were significantly lower in prostate cancer cell lines than in normal prostatic epithelia, we decided to explore the mechanism of *DAB2IP* regulation by cloning its 5′-regulatory sequence and entire genome sequence. The human genomic database indicates that *DAB2IP* locates at 9q33.1–q33.3 and seems to be a new gene. In this study, we further documented the structure of *DAB2IP* and investigated the differential promoter activity between normal and malignant prostate cancer cell lines. This study provides the first step toward understanding the regulation of *DAB2IP* in prostatic epithelia.

RESULTS

A High Sequence Homology between DAB2IP and DIP1/2 cDNA

To isolate human DAB2IP cDNA, we screened both PrEC and PZ-HPV-7 cells, and detected DAB2IP protein in both cells. Using RT-PCR we cloned the full-length DAB2IP cDNA sequence, which shares 94.2% homology with DIP1/2 (Fig. 1A). Analysis of the *DAB2IP* sequence (EMBL/GenBank acc.

Copyright © 2002 Elsevier Science (USA). All rights reserved.
0888-7543/02 $35.00

doi:10.1006/geno.2002.6739, available online at http://www.idealibrary.com on IDEAL

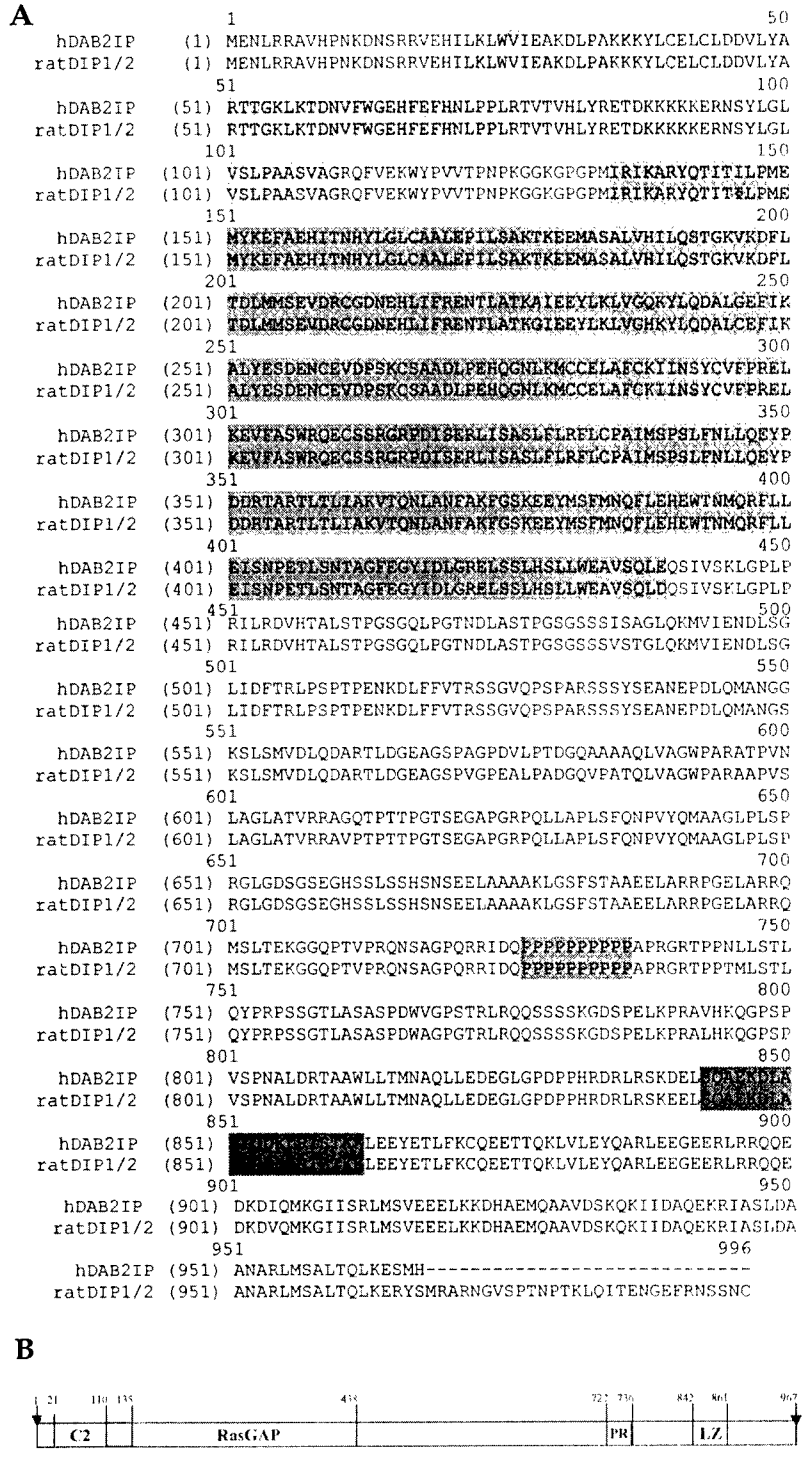

FIG. 1. The predicted functional domain of the DAB2IP protein. (A) Comparison of protein sequences between human and rat. Potential functional domains are boxed. Non-identical amino acids are in bold. (B) Schematic display of DAB2IP protein. C2 (amino acids 21–110), protein kinase C conserved region 2 domain, RasGAP (Ras GTPase-activator protein, amino acids 135–438), PR (proline-rich motif, amino acids 727–736), and LZ (leucine zipper domain, amino acids 842–861) are indicated.

no. AF367051) revealed an open reading frame encoding a 967-amino-acid protein with a predicted molecular weight of 110 kD. Using the program "Research for conserved domain" from the NCBI web site (http://www.ncbi.nih.gov/structure/cdd/wrpsb.cgi), we found that the deduced amino acid sequence of DAB2IP cDNA predicted that DAB2IP has four domains: C2 (protein kinase C conserved region2 (CalB), amino acids 21–110); RasGAP (GTPase-activator protein for Ras-like GTPase, amino acids 135–438); a proline-rich domain (amino acids 727–736); and a leucine zipper domain (amino acids 842–861; Fig. 1B). These data indicated that DAB2IP represents a new member of the RasGAP gene family.

Genomic Organization of *DAB2IP*

After three rounds of screening, two positive BAC clones (298A17 and 419H3) were confirmed using Southern blot analysis probed with a full-length sequence of DIP1/2 cDNA. Both BAC clones seem to have the same hybridization band (that is, 23 kb and 7.6 kb; Fig. 2A). Using the exon 1b probe, we also detected the similar 7.6-kb band in the 298A17 clone (Fig. 2B).

Using the BLASTN program (NCBI, http://www.ncbi.nlm.nih.gov/BLAST), we mapped clone 298 A17 (acc. no. AL365274) to chromosome 9 (172,027 bp in size). However, the sequence of clone 419H3 is still unavailable. To identify clone 419H3, we sequenced it using SP6 and T7 primers. Sequence data showed that the 3′ end of the clone 419H3 sequence aligned with the middle portion of AL365274. The 5′ end sequence aligned with AL136097 (located at the 5′ upstream of AL365274). These data indicate that both clones overlap and that the span of the entire *DAB2IP* gene is estimated at ~ 96 kb (Fig. 2C). Analyzing with the Locus Link program (http://www.ncbi.nlm.nih.gov/LocusLink), we determined the chromosomal location of *DAB2IP* to be 9q33.1–q33.3 (BAB21834 and AAK50336).

We deduced the exon–intron junction of *DAB2IP* by aligning its cDNA sequence with clone 298A17. Furthermore, PCR amplification and DNA sequencing confirmed all predicted exon–intron boundaries. A total of 15 exons and 14 introns are shown in Fig. 2C (summarized in Tables 1 and 2). Most splicing

Copyright © 2002 Elsevier Science (USA). All rights reserved.

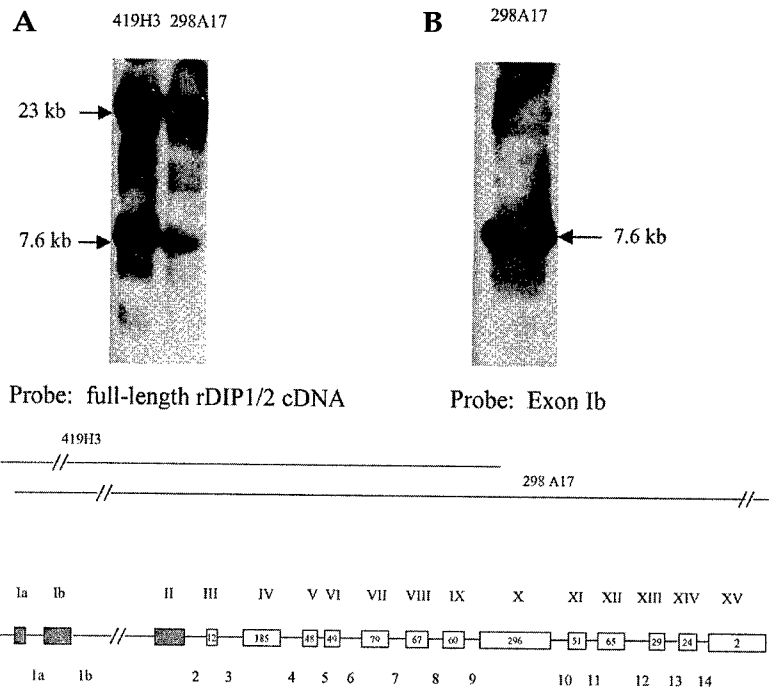

FIG. 2. Genomic organization of *DAB2IP*. BAC clones 419 H3 and 298 A17 were digested with *Eco*RI and analyzed by Southern blot analysis probed with a full-length cDNA sequence of DIP1/2 (A) or exon 1b of *DAB2IP* (B). The 5′- and 3′-noncoding regions (black box), the coding regions (open box), with indicated number of amino acids in each exon, and the relative position of each BAC clone are displayed (C).

junctions coincide with the GT...AG rule. Noticeably, exon 1 was separated from exon 2 by a large intron (~ 56 kb). The translation initiation site (ATG) is mapped at the 63 bp from the 5′ end of exon 3, and the protein termination site (TAG) is located at exon 15 and followed by a large, untranslated sequence.

TABLE 1: Different splicing variants of human *DAB2IP*

Exon	*DAB2IP* mRNA a (5192 bp)	*DAB2IP* mRNA b (5608 bp)	amino acid (967 aa)
Ia	1-88 (88)		
Ib		1-504 (504)	
II	89-242 (154)	505-658 (154)	
III	243-341(99) ***ATG (306-308)**	659-757 (99) ***ATG (722-724)**	1-12 (12)
IV	342-896 (555)	758-1312 (555)	13-197 (185)
V	897-1041(145)	1313-1457 (145)	198-245 (48)
VI	1042-1186 (145)	1458-1602 (145)	246-294 (49)
VII	1187-1423 (237)	1603-1839 (237)	295-373 (79)
VIII	1424-1625 (202)	1840-2041 (202)	374-440 (67)
IX	1626-1804 (179)	2042-2219 (179)	441-500 (60)
X	1805-2694 (889)	2220-3119 (889)	501-796 (296)
XI	2695-2846 (153)	3120-3262 (153)	797-845 (51)
XII	2847-3040 (194)	3263-3456 (194)	846-912 (65)
XIII	3041-3128 (88)	3457-3544 (88)	913-941 (29)
XIV	3129-3199 (71)	3545-3615 (71)	942-965 (24)
XV	3200-5192 (1993) ***TAG (3206-3208)**	3616-5608 (1993) ***TAG (3623-3625)**	966-967 (2)

Determination of the Transcription Starting Site of *DAB2IP*

We identified the transcription starting site (TSS) of *DAB2IP* using 5′ RACE and total cellular RNA prepared from human brain cells, PrEC cells, and PZ-HPV-7 cells. We chose three *DAB2IP*-specific primers (Sp1, Sp2, Sp3) to combine with outer and inner adapter primers for nested PCR (Fig. 3A).

We detected a single PCR transcript (230 bp) from the human brain using both the Sp1 and Sp2 primers (Fig. 3B). Using the same primers, we detected three bands (250, 290, and 600 bp) in either PrEC or PZ-HPV-7 cells. DNA sequencing data revealed that the 230-, 250- and 290-bp PCR transcripts were derived from the predicted exon 1 sequence (that is, exon 1a) with slightly different 5′ starting sites. In contrast, the 600-bp PCR transcript was derived from a new exon within intron 1. We named this exon "exon 1b."

Using the Sp2 and Sp3 primers (Fig. 3A), we detected two bands (320 bp and 670 bp) of PCR transcripts from PZ-HPV-7 and PrEC cells. DNA sequencing data revealed that the sequence of 320 bp and 670 bp was identical to the 250 bp and 600 bp sequence, respectively. These data suggest that *DAB2IP* mRNA has multiple TSSs. That variable sizes of *DAB2IP* mRNA were detected in different cells may be due to the lack of canonical TATA sequences within this region. It is characteristic that a gene containing a TATA-less promoter [6] has imprecise TSS.

Copyright © 2002 Elsevier Science (USA). All rights reserved.

doi:10.1006/geno.2002.6739, available online at http://www.idealibrary.com on IDEAL

On the other hand, we used an RNase protection assay to confirm the results obtained from 5′-RACE. We noticed low abundance of *DAB2IP* mRNA in prostate tissue because at least 100 μg total cellular RNA was needed for signal detection. Using an exon 1a (300 bp) antisense probe, we only observed that the presence of a 251-bp band corresponds to the 250-bp PCR transcript using the Sp1 and Sp2 primer set (Figs. 3B and 3C). These data confirm that the -14 site from the predicted TSS (Fig. 4) seems to be the major TSS in *DAB2IP*.

TABLE 2: Exon boundaries of *DAB2IP*

Exon	Size (bp)	3′ intron/5′ exon boundary	3′ exon/5′ intron boundary	Intron	Size (kb)
Ia	88		TGAGAG/**gt**gagccg	1a	1.4
Ib	504		GCTTGT/**gt**acgtaccc	1b	56
II	154	cacccc**ag**/GTCCCA	TTCGAG/**gt**gggtccc	2	1.7
III	99	ccccac**ag**/GTGACG	AACAAG/**gt**aagcctgc	3	0.9
IV	555	cacatac**ag**/GACAA	GTGAAG/**gt**gcgtgcag	4	3.3
V	145	cctcccc**ag**/GACTTC	CCCTAG/**gt**agggagtg	5	0.1
VI	145	tgtccat**ag**/GTGAGT	CTACTG/**gt**cagtggcgg	6	2.6
VII	237	ctcacac**ag**/TGCTTC	TGCCAA/**gt**gagtgcct	7	1.7
VIII	202	tctctcc**ag**/ATTTGG	GAGCAG/**gt**gcctgttg	8	1.9
IX	179	cctttac**ag**/AGCATA	TTCCGG/**gt**aagagctg	9	1.9
X	889	tccctgc**ag**/TCTGAT	AAGCAG/**gt**cagtgctg	10	0.8
XI	153	gtaaca**ag**/GGCCCT	GAAAG/**gt**aaaactgg	11	1.8
XII	194	cctggt**ag**/GACCTG	CAGCAG/**gt**ggggccca	12	5.0
XIII	88	tggctac**ag**/GTTGAT	GCCCAG/**gt**gggggctc	13	0.8
XIV	71	gtccac**ag**/GAGAAG	AGGGAG/**ga**agctaccc	14	1.0
XV	1993	cttttcac**ag**/CTGCAT			

Analysis of the 5′-Upstream Sequence of *DAB2IP*

To analyze the promoter region of *DAB2IP*, a 7.6-kb *Eco*RI fragment (Fig. 2A) from clone 298A17 was isolated and subcloned into pBluescriptSK (-) vector. This 7.6-kb fragment contained the 5′-upstream region of *DAB2IP* (5.5 kb), exon 1a, exon 1b, and partial intron 1. Results of DNA sequencing indicated that the 5′-upstream region from exon 1a is rich in CpG, which is indicative of the 5′-regulatory sequence in *DAB2IP*. A 1.6-kb fragment from position -598 to +981 (predicted transcription initial site as +1 analyzed by MacVector) was analyzed to predict the putative promoter (Fig. 4). Two promoters were predicted using the TSSW program (human Pol II recognition using the TRANSFAC database; http://genomic.sanger.ac.uk/gf/gf.html): one at -249, the other at +177. Furthermore, using both the Core Promoter program and TSS Human Core-promoter Finder for predicting core promoter position, neither the TATA box nor the CAAT box was found in the 1.6-kb region of *DAB2IP*. This suggests that *DAB2IP* is a typical gene containing a TATA-less promoter [6,7].

Differential Promoter Activity of *DAB2IP* between Normal Prostate and Prostate Cancer Cells

We used semi-quantitative RT-PCR to analyze the steady-state levels of *DAB2IP* mRNA in cell lines derived from either three normal epithelia (immortalized or primary culture) or six cancer cell lines. We observed significant difference in the *DAB2IP* mRNA levels among these cells (Fig. 5). In general, higher levels of *DAB2IP* mRNA were detected in normal epithelia (such as PrEC, SWNPC2, and PZ-HPV-7) than in cancer cell lines tested. We also detected the *DAB2IP* transcripts in human brain tissue.

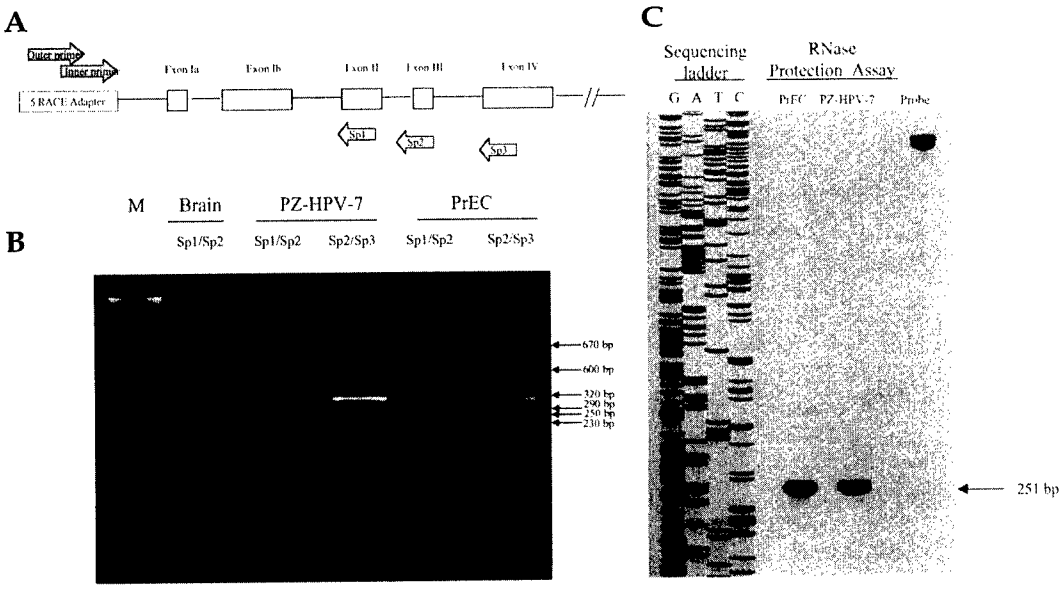

FIG. 3. Determination of the TSS in *DAB2IP*. (A) Schematic representation of relative position of each primer used in the 5′-RACE procedure. (B) Multiple starting sites of *DAB2IP* mRNA detected in human brain, PZ-HPV-7, and PrEC using 5′-RACE. M, 1 kb plus marker. (C) Detection of the major TSS in *DAB2IP* using RNase protection assay.

Copyright © 2002 Elsevier Science (USA). All rights reserved.

FIG. 4. 5′-Upstream regulatory sequence of *DAB2IP*. TSS as +1 predicted MacVector is displayed. Four experimental TSSs were determined by 5′-RACE at nt −52, −15, −12, and +13 relative to the TSS of *DAB2IP*. Putative *cis*-acting elements and restriction enzyme sites are also highlighted.

To unveil the mechanism responsible for the decreased expression of *DAB2IP* in various prostate cancer cells, we analyzed the promoter activity of *DAB2IP* using a luciferase reporter gene construct (pGL3). We constructed a variety of vectors based on the location of two putative promoters of *DAB2IP* (Fig. 6A). Using pGL3-1.6S (−598 and +981), we detected higher luciferase activity in the PZ-HPV-7 cell line than in the LNCaP, Du 145, PC-3, or TSU-Pr1 lines (Fig. 6B), and the relative luciferase activity in each cell line correlated with its own mRNA levels (Fig. 5). We detected highest promoter activity overall in PZ-HPV-7 cells; LNCaP and Du 145 had an intermediate level, and PC-3 and TSU-Pr1 had the lowest level. Furthermore, pGL3.1-1.6A did not show any luciferase activity in these cells (Fig. 6B). These data indicated that this 1.6-kb fragment contained the promoter of *DAB2IP*. Therefore, the differential expression of *DAB2IP* mRNA in prostate cancer cells may be due to transcriptional regulation.

To further map the location of the promoter of *DAB2IP*, we tested a series of deletion constructs of the *DAB2IP* promoter in the three prostate cell lines (PZ-HPV-7, LNCaP, and PC-3) with different *DAB2IP* mRNA levels. We observed two regions (P1, + 229 to +981, and P2, −359 to −141) within *DAB2IP* that possess promoter activities in PZ-HPV-7 cells (Fig. 6C). In general, the P1 promoter is active in PZ-HPV-7 cells, which seems to be a basal level promoter for *DAB2IP*. Nevertheless, the P1 is not active in prostate cancer cells, including LNCaP and PC-3 cells (Fig. 6C). On the other hand, we noticed the presence of a putative *cis*-acting element between +44 and +229 that may suppress the promoter activity of the P2 site.

In LNCaP cells, the overall activity of *DAB2IP* promoter is lower than that in PZ-HPV-7 cells (Fig. 6C), suggesting that the P1 is not very active in this cell line. However, the activity of P2 promoter in LNCaP cells could be active, as observed in PZ-HPV-7 cells, when the region between +44 and +229 was removed. These data suggest that the downregulation of *DAB2IP* in LNCaP cells may be due to the transcription inactivation.

Nevertheless, all the reporter gene constructs in PC-3 cells exhibited very low activity compared with either PZ-HPV-7 or LNCaP cells (Fig. 6C). We demonstrated that the P2 promoter became active in both PZ-HPV-7 and LNCaP cells when the region between +44 and +229 was removed (Fig. 6C). However, in PC-3 cells, the P2 activity was still not active. These data suggest that certain *trans*-acting factors responsible for *DAB2IP* expression may be absent from PC-3 cells.

Discussion

The structure and size of the DAB2IP (or DIP1/2) cDNA is remarkably conserved between rat and human, with 94.2% sequence homology. According to its sequence alignment, *DAB2IP* seems to be a new member of the RasGAP family. The alignment of the RasGAP domain of DAB2IP (or DIP1/2) with

Copyright © 2002 Elsevier Science (USA). All rights reserved.

doi:10.1006/geno.2002.6739, available online at http://www.idealibrary.com on IDEAL

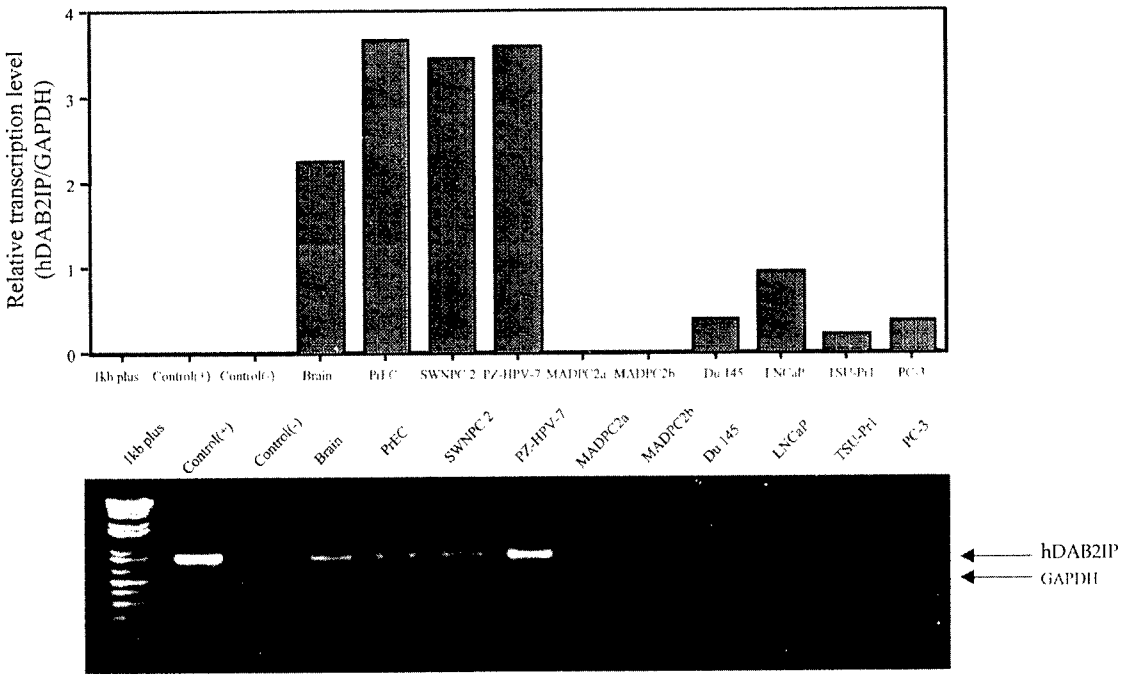

FIG. 5. Semi-quantitative RT-PCR analysis of *DAB2IP* mRNA levels in different prostate cell lines. Lane 1, 1 kb Plus marker; lane 2, 0.5 μg DAB2IP cDNA; lane 3, d_2H_2O (negative control); lane 4, 2 μg total cellular RNA from human brain; lanes 5–8, 2 μg total cellular RNA from each prostate cell line. Relative expression levels were determined by Bio Image Intelligent Quantifier software and calculated the ratio between *DAB2IP* and *GAPDH*.

other RasGAPs, such as GAP120, *Homo sapiens* neurofibrin (NF1) [8,9], synaptic Ras GAP (SynGAP) [10], *Rattus norvegicus* RasGAP (GAP) [11], and a novel human RasGAP (nGAP) [12], shows a high degree of amino acid homology (40% ~ 90%). All GAPs contain a common structural region called the GAP related domain (GRD). The GRD is the catalytic unit of this protein, which stimulates the GTPase activity of Ras protein. We demonstrated that DIP1/2 exhibited the RasGAP activity *in vivo* and *in vitro* (Z.W. *et al.*, *J. Biol. Chem.*, in press).

We also showed that DAB2IP levels were present in immortalized normal prostatic epithelial cells but absent from several prostate cancer cell lines, and that increased expression of DIP1/2 can inhibit their growth. Friedman *et al.* demonstrated mutations in the C-terminal SH2 region of RasGAP in a subset of basal cell carcinomas [13,14]. But these are presumably active mutations and therefore confer a direct oncogenic potential to RasGAP. Other researchers have documented an inverse correlation between RasGAP gene expression and the invasive/malignant potential in human tumors [15,16]. Thus, *DAB2IP* likely has a potential role in prostate carcinogenesis.

In this study, we delineated the structure of *DAB2IP* and its regulation. *DAB2IP*, located at 9q33.1–q33.3, is about 96 kb in length and contains 15 exons and 14 introns. This protein seems to express in the human brain. Nagase *et al.* reported the partial sequence of this protein as an unidentified human gene by sequencing brain cDNA clones [17]. After searching the GenBank database, von Bergh *et al.* (GenBank acc. no. AY032952) suggested that a novel RasGAP gene fused to a myeloid/lymphoid leukemia gene in acute myeloid leukemia with chromosomal translocation [t(9;11)(q34; q23)]. *DAB2IP* seems to be the candidate gene. It is likely that the chromosomal location of another potential tumor suppressor gene, *TSC1* (tuberous sclerosis) [18], is proximal to this DAB2IP locus. Noticeably, the second candidate for tuberous sclerosis (that is, TSC2) functions as a GAP [19]. Therefore, DAB2IP may be involved in the process of many diseases.

We found no canonical TATA boxes within the 5′-upstream sequence of *DAB2IP*. Therefore, the actual TSS of transcription may be heterogeneous, as evidenced by 5′-RACE results (Fig. 3B) obtained from PZ-HPV-7 and PrEC cells. Thus, *DAB2IP* is a typical gene with a TATA-less promoter [6,7]. However, using RNase protection assay (Fig. 3C), we confirmed that the major TSS in *DAB2IP* located at −14 from the predicted TSS (Fig. 4).

To understand the regulation of DAB2IP in prostatic epithelia, we studied its promoter activity (Fig. 6) by comparing PZ-HPV-7 (high DAB2IP expressing cell) with four prostate cancer cell lines (PC-3, Du 145, LNCaP, and TSU-Pr1), ranging from moderate to low levels of DAB2IP expression. We observed highest levels of relative luciferase activity (RLA) in the PZ-HPV-7 cell line. We observed decreased RLA levels in both LNCaP and Du 145 cell lines and lowest RLA levels in PC-3 and TSU-Pr1 cell lines. These results correlate with the steady-state levels of *DAB2IP* mRNA determined using semi-quantitative RT-PCR (Fig. 5), indicating that altered *de novo* synthesis of the *DAB2IP* mRNA may be responsible for the expression of *DAB2IP* in prostate cancer cells.

Copyright © 2002 Elsevier Science (USA). All rights reserved.

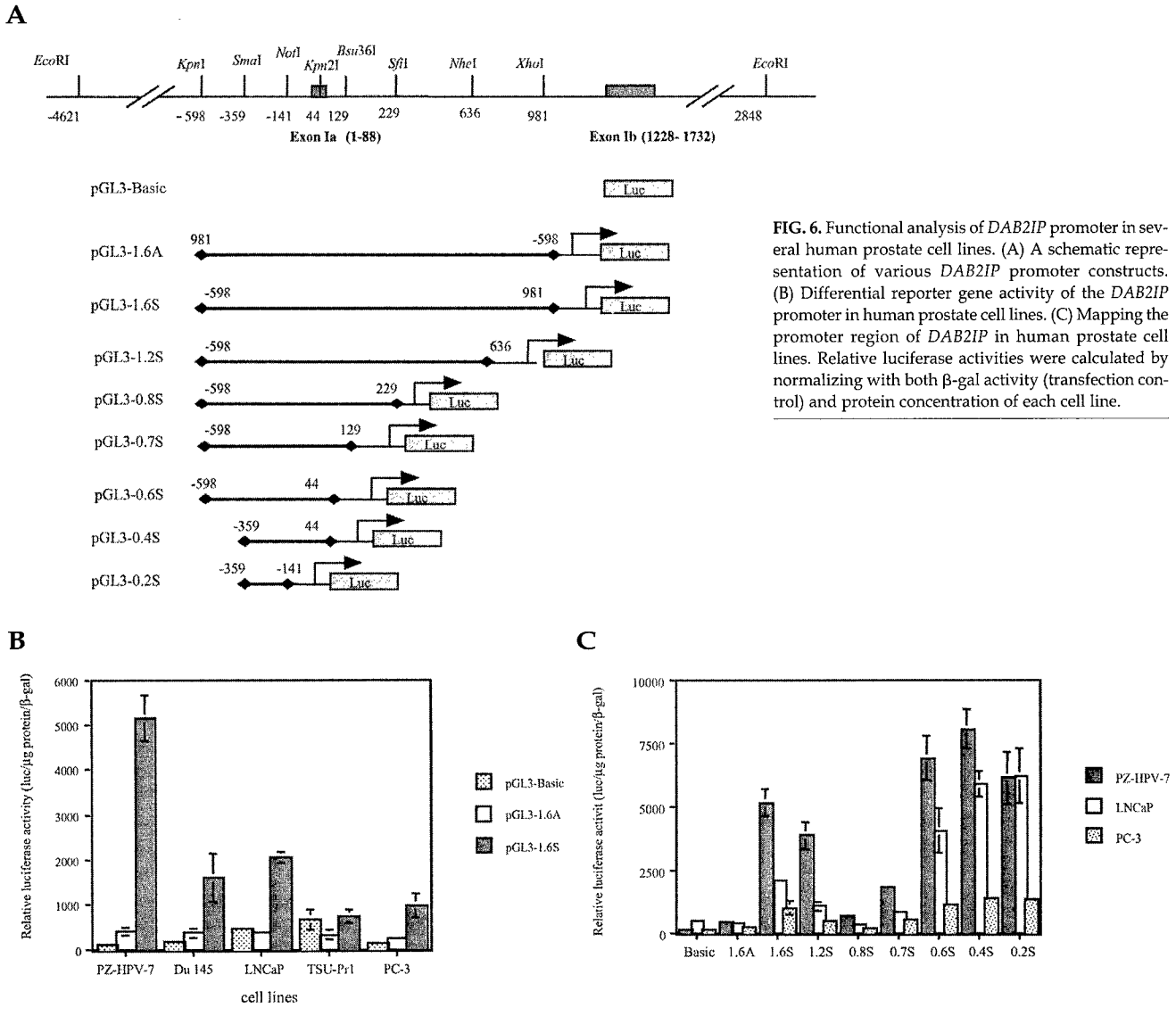

FIG. 6. Functional analysis of *DAB2IP* promoter in several human prostate cell lines. (A) A schematic representation of various *DAB2IP* promoter constructs. (B) Differential reporter gene activity of the *DAB2IP* promoter in human prostate cell lines. (C) Mapping the promoter region of *DAB2IP* in human prostate cell lines. Relative luciferase activities were calculated by normalizing with both β-gal activity (transfection control) and protein concentration of each cell line.

To further analyze the *DAB2IP* promoter (Fig. 6C), we delineated two promoters in *DAB2IP*: P1 locates within the first intron (+229 to +981); and P2 locates 5′-upstream of exon 1a (-359 and -141). In normal prostatic epithelia, P1 is active, but P2 activity may be modulated by the adjacent region binding with a negative *trans*-acting factor. Using both MatInspector/TRANSFAC and MacVector program, we identified several potential recognition sites for *trans*-acting factors including Sp1, AP-2, AP-3, ISRE, CTF-NFI, E4TF1, and Mal I box (Fig. 4). Further characterization of these *cis*-acting elements adjacent to the *DAB2IP* promoter will certainly provide useful information to understand the regulation of *DAB2IP* promoter activity. Nevertheless, in prostate cancer cells, we found that the P1 activity of *DAB2IP* promoter does not function in LNCaP or PC-3 cells. In addition, P2 activity is not active in PC-3 cells, even when a negative *cis*-acting element was deleted, which suggests that the factor binding to P2 regions is also absent from the PC-3 cell line.

Noticeably, the 5′-upstream sequence of *DAB2IP* is also very GC-rich, and we identified many CpG islands using CpG-win.xis software [20]. Therefore, it is possible that DNA methylation in the P2 region of *DAB2IP* may underlie the downregulation of this gene in PC-3 cells. Thus, more detailed analysis is warranted.

Materials and Methods

Tissue culture and RNA isolation. We maintained three human prostate cancer cell lines (LNCaP, TSU-Pr1, and PC-3) in T-medium supplemented with 5% fetal bovine serum. We maintained two human prostate cancer cell lines (MDAPCa 2a and MDAPCa 2b) [21] in BRFF-HPC1 medium (Biological Research Faculty and Facility, Inc.) supplemented with 20% fetal bovine serum.

Copyright © 2002 Elsevier Science (USA). All rights reserved.

doi:10.1006/geno.2002.6739, available online at http://www.idealibrary.com on IDEAL

Another human prostate cancer cell line (Du 145) was maintained in RPMI medium supplemented with 10% fetal bovine serum. We maintained three normal human prostate cell lines in a chemical-defined medium (PrEGM) purchased from Clonetics including PrEC (a primary epithelial cell derived from a 17-year-old juvenile prostate (Clonetics)), PZ-HPV-7 (an immortalized cell line derived from the peripheral zone of a normal prostate) [22,23], and SWNPC2 (a primary epithelial cell derived from a 40-year-old prostate). We isolated total cellular RNA using the RNAzol B method (TEL-TEST, Inc) according to the manufacturer's instructions. It was dissolved in water and quantified spectrophotometrically at 260 nm.

Isolation of DAB2IP cDNA by RT-PCR and determination of relative DAB2IP mRNA levels by semi-quantitative PCR. To isolate the entire coding region for human *DAB2IP*, we designed four sets of primers based on the full-length DIP1/2 cDNA sequence: set1, sense: 5′-GCGGGATAAGTGGATGGAGAACCTC-3′, antisense: 5′-GGATGGTGATGGTTTGGTAG-3′; set2, sense: 5′-TGGACGATGTGCTCTATGCC-3′, antisense: 5′-GGTCCCAGTTTGGATACTATG-3′; set3, sense: 5′-TGGCAGCAAGGAGGAATAC-3′, antisense: 5′-TACACAGGGTTCTGGAAGG-3′; set4, sense: 5′-GCATAGTATCCAAACTGGGAC-3′, antisense: 5′-CTGTGTTCCAGCAAGCGAGC-3′. With these primers, we then performed RT-PCR and RACE using RNA prepared from PrEC cells. We analyzed the expected PCR product by DNA gel electrophoresis, then cloned it into the TA cloning vector pCR 2.1-TOPO (Invitrogen) and sequenced it.

To measure *DAB2IP* mRNA levels, we reverse transcribed 2 μg of total cellular RNA from each cell line into first-strand cDNA using Superscript II reverse transcriptase (Life Technologies, Inc.). One-tenth of the cDNA was subjected to a 50 μl PCR (32 cycles of 94°C for 30 seconds, 50°C for 45 seconds, and 72°C for 2 minutes) using both sets of DAB2IP primer (5′-TCGTGGAAGGACTCATGACC-3′ and 5′-TCCACCACCCTGTTGCTGTA-3′, 2 ng/μl) and GAPDH primer sets (0.6 ng/μl). We electrophoresed the final PCR products (10 μl) in a 2% NuSieve agarose gel (3:1, FMC Bioproducts) and analyzed it using Bio-Image Intelligent Quantifier software (Bio Image). The relative level of DAB2IP mRNA from each sample was normalized to a *GAPDH* transcript from the same reaction.

Isolation of DAB2IP and Southern blot analysis. Because of the high homology of cDNA sequence between DAB2IP and DIP1/2, we screened the RPCI-11 Human BAC Library (Research Genetics, Inc.) with the full-length sequence of DIP1/2 cDNA probe. Two clones (298A17 and 419H3) were identified in three rounds of screening. We prepared BAC DNA according to the manufacturer's protocol (Qiagen). Briefly, BAC DNA was extracted from an overnight culture in 500 ml LB containing 12.5 μg/ml chloramphenicol. The bacteria was harvested and resuspended in 10 ml P1 buffer (50 mM Tris-Cl, pH 8.0, 10 mM EDTA, 100 μg/ml RNase A), then 10 ml P2 buffer (200 mM NaOH, 1% SDS) was added for 5 minutes at room temperature. We added 10 ml of P3 buffer (3 M potassium acetate, pH 5.5) to the mixture and placed it on ice for 5 minutes. After centrifugation (12,000*g*, 20 minutes) at 4°C, the supernatant was applied to the Qiagen-tip-100 and washed twice with 30 ml buffer QC. We eluted DNA using 15 ml preheated (65°C) buffer QF, then precipitated it with 0.7 volumes of isopropanol. Then we washed the DNA pellet with 5 ml of 70% ethanol, left it to air-dry, and re-dissolved it in TE buffer.

For Southern analysis, we digested DNA with *Eco*RI, separated on the 0.8% agarose gel electrophoresis, and then transferred it onto a nitrocellulose membrane. We labeled all the DNA probes with [α-^{32}P]dCTP using the random prime labeling kit (Pharmacia Biotech). We performed prehybridization and hybridization with a 1×10^6 cpm/ml probe using Rapid-hyd buffer (Amersham) at 65°C. Wash conditions were performed using 2× SSC/0.1% SDS for 15 minutes at room temperature (twice), and 0.1× SSC/0.1% SDS for 15 minutes at 60°C (twice). We exposed membranes to X-ray film overnight at −80°C with an intensifying screen.

Identification of TSS by both 5′-RACE and RNase protection assay. We subjected total cellular RNA (10 μg) from the human brain, PZ-HPV-7, and PrEC to 5′-RACE using the FirstChoice RLM-RACE Kit (Ambion). RLM-RACE represents a major improvement from the classic RACE technique [24,25]. It is designed to amplify cDNA only from full-length, capped mRNA. Briefly, we first treated RNA with calf intestinal phosphatase to digest any degraded RNAs or rRNA, tRNA, and contaminating genomic DNA. After it was purified with phenol-chloroform, we treated the remaining intact mRNA with Tobacco Acid Pyrophosphatase to remove the 5′-cap. We followed this with T4 RNA ligase treatment in the presence of a synthetic RNA adapter (5′-GGGUUCGGGCUUAGGCUCCAGUGCCUGUUCGGUCGCGGCGCUGAUGGCGAUGAAUGAACACUGCGGCAAGCCGCUUAUGACACUCGUUUGCUGGCUUUGAUGGGCGAGCUGGAAGGCCGUAUCUCCGGCAGCAUUCAUUACGACAAA-3′). A random-primed reverse transcription reaction and nested PCR were carried out to amplify the 5′ end of the *DAB2IP* mRNA transcript. We used two nested primers (outer RNA adapter primer, 5′-GCTGATGGCGATGAATGAACACTG-3′; and inner RNA adapter primer, 5′-CGCGGATCCGACACTCGTTTGCTGGCTTTGAT-3′) corresponding to the adapter sequence. In addition, three nested antisense primers (DAB2IP Sp1, 5′-GCTTGATGACCACCTCTTCCTCC-3′; DAB2IP Sp2, 5′-GTTCTCCATCCACTTATCCCGC-3′; and DAB2IP Sp3, 5′-ATTGTCCACAGGAGAAGCG-3′) were combined with two nested primers for the PCR reaction (94°C for 30 seconds, 55°C for 30 seconds, 72°C for 30 seconds, 35 cycles). We analyzed the PCR product and then cloned it into the TA cloning vector pCR2.1-TOPO (Invitrogen) for sequencing identification.

For RNase protection assay, we prepared an antisense riboprobe from a 300-bp fragment containing exon 1a (88 bp) and 5′-flanking sequence (212 bp) of *DAB2IP* using T7 RNA polymerase from MAXIscript *in vitro* transcription kit (Ambion). An RNase protection assay was carried out with the PRA III Ribonuclease Protection Assay Kit (Ambion). Briefly, we incubated about 4×10^5 cpm per transcript plus 100 μg total RNA isolated from PrEC or PZ-HPV-7 cells at 42°C overnight. After hybridization, we treated the mixtures with ribonucleaseA/T1 to degrade unhybridized probe. We analyzed the samples on a 6% denaturing polyacrylamide/urea gel. In the same gel, we used DNA fragments derived from DNA sequencing of the probe as a size marker to determine the TSS.

Construction of luciferase reporter plasmid containing the 5′ regulatory sequence of DAB2IP. We subcloned a 7.6-kb *Eco*RI fragment of the clone 298A17, containing the predicted first exon and further 5′ upstream sequence, into the *Eco*RI site of pBluescript SK (-) (Stratagene). This clone (pBS-7.6) was sequenced and aligned with the GenBank database (acc. no. AL365274).

To analyze the 5′ upstream sequence of human DAB2IP, a series of deletion constructs were subcloned into pGL3 basic vector (Promega). The pGL3-1.6S contains a 1.6-kb *Kpn*I-*Xho*I (from −598 to +981) fragment from pBS-7.6. The pGL3-1.6A contains the same insert as pGL3-1.6S in an antisense orientation. The pGL3-1.2S contains a 1.2-kb insert (from −598 to +636) from the *Kpn*I-*Nhe*I fragment of pGL3-1.6S (cut with *Nhe*I-*Xho*I and re-ligate the vector). The pGL3-0.8S contains a 0.8-kb insert (from −598 to +229) from the *Kpn*I-*Sfi*I fragment of pGL3-1.6S by removing the *Sfi*I-*Xho*I fragment from the vector. The pGL3-0.7S contains a 0.7-kb insert (from −598 to +129) from the *Kpn*I-*Bsu*36I fragment of pGL3-1.6S by removing the *Bsu*36I-*Xho*I fragment from the vector. The pGL3-0.6S contains a 0.6-kb insert (from −598 to +44) from the *Kpn*I-*Kpn*2I fragment of pGL3-1.6S by removing the *Kpn*2I-*Xho*I fragment from the vector. The pGL3-0.4S contains a 412-bp insert (from −359 to +44) from the *Sma*I-*Kpn*2I fragment of pGL3-0.6S by removing the *Kpn*I-*Sma*I fragment from the vector. The pGL3-0.2S contains a 208-bp insert (from −359 to −141) from the *Sma*I-*Not*I fragment of pGL3-0.4S by removing the *Not*I-*Hind*III fragment from the vector.

Determination of DAB2IP promoter activity. We plated cells at a density of 1.8×10^5 cells per well in a 6-well plate. After 24 hours, we transfected PZ-HPV-7, PC-3, Du 145, and TSU-Pr1 cell lines with both 0.8 μg of reporter vectors and 0.2 μg β-galactosidase vector (pCH110) using FuGene 6 (Roche Molecular Biochemicals). The LNCaP cell line was transfected with the same amount of DNA with Lipofectamine Plus transfection reagent (Life Technologies Inc.). Forty-eight hours after transfection, we washed the cells twice with cold phosphate-buffered saline (PBS) and harvested them in Lysis buffer (Promega). We determined luciferase and β-galactosidase (β-gal) assays as described [5]. We determined total protein concentrations of cell extracts using Bio-Rad Protein Assay (Bio-Rad), and repeated all experiments at least three times in triplicate.

Acknowledgments

We thank Nora Navone (MD Anderson Cancer Center) for providing MDAPCa 2a and MDAPCa 2b cell lines, Andrew Webb (UT Southwestern Medical Center) for editorial assistance, and Kenneth S. Koeneman (UT Southwestern Medical Center) for reading this manuscript. This work is supported in part by NIH DK 47657 and United States Army Grant PC 970259.

RECEIVED FOR PUBLICATION OCTOBER 5, 2001;
ACCEPTED JANUARY 25, 2002.

Copyright © 2002 Elsevier Science (USA). All rights reserved.

References

1. Tseng, C.-P, Brent, D. E., Li, Y.-M., Pong, R.-C., and Hsieh, J. T. (1998). Regulation of rat DOC-2 gene during castration-induced rat ventral prostate degeneration and its growth inhibitory function in human prostatic carcinoma cells. *Endocrinology* **139:** 3542–3553.
2. Schwahn, D. J., and Medina, D. (1998). P96, a MAPK-related protein, is consistently downregulated during mouse mammary carcinogenesis. *Oncogene* **17:** 1173–1178.
3. Fulop, V., *et al.* (1998). DOC-2/hDab2, a candidate tumor suppressor gene involved in the development of gestational trophoblastic diseases. *Oncogene* **17:** 419–424.
4. Fuzili, Z., Sun, W., Mittellstaedt, S., Cohen, C., and Xu, X. X. (1999). Disabled-2 inactivation is an early step in ovarian tumorigenicity. *Oncogene* **18:** 3104–3113.
5. Tseng, C.-P., *et al.* (1999). The role of DOC-2/DAB2 protein phosphorylation in the inhibition of AP-1 activity. *J. Biol. Chem.* **274:** 31981–31986.
6. Smale, S. T. (1994). *Transcription: Mechanisms and Regulation* (Conaway and Conaway, Eds.), pp. 63–81. Raven Press, New York.
7. Javahery, R., Khachi, A., Lo, K., Zenzie-Gregory. B., and Smale, S. T. (1994). DNA sequence requirements for transcriptional initiator activity in mammalian cells. *Mol. Cell. Biol.* **14:** 116–127.
8. Bernards, A., *et al.* (1992). Complete human NF1 cDNA sequence: two alternatively spliced mRNAs and absence of expression in a meuroblastoma line. *DNA Cell Biol.* **11:** 727–734.
9. Wallace, M. R., *et al.* (1990). Type1 neurofibromatosis gene: identification of a large transcript disrupted in three NF1 patients. *Science* **249:** 181–186.
10. Kim, J. H., Liao, D., Lau, L. F., and Huganir, R. L. (1998). SynGAP: a synaptic RasGAP that associates with the PSD-95/SAP90 protein family. *Neuron* **20:** 683–691.
11. Davis, M. M., Catino, J. J., Satch, T., Kaziro, Y., and Perkins, L. M. (1993). Sequence of the cDNA encoding Ras GTPase-activating protein from rat. *Gene* **134:** 305–306.
12. Noto, S., *et al.* (1998). A novel human RasGAP-like gene that maps within the prostate cancer susceptibility locus at chromosome 1q25. *FEBS Lett.* **441:** 127–131.
13. Friedman, E. (1995). The Role of ras GTPase activiating protein in human tumorigenesis. *Pathobiology* **63:** 348–350.
14. Friedman, E., Gejman P. V., Martin, G. A., and McCormick, F. (1993) Nonsense mutation in the C terminal SH2 region of the GTPase activating protein (GAP) gene in human tumors. *Nat. Genet.* **5:** 242–247.
15. DeClue, J. E., Zhang, K., Redford, P., Vass, W. C., and Lowy, D. R. (1991). Suppression of src transformation by overexpression of full length GTPase-activating protein (GAP) or of the GAP C-terminus. *Mol. Cell. Biol.* **11:** 2819–2825.
16. Stalhe-Backdhal, M., *et al.* (1995). Decreased expression of *ras*GTPase activating protein (*ras*GAP) in human trophoblastic tumors. *Am. J. Pathol.* **146:** 1073–1078.
17. Nagase, T., *et al.* (2000). Prediction of the coding sequences of unidentified human genes, xix. The complete sequences of 100 new cDNA clones from brain which code for large proteins in vitro. *DNA Res.* **7:** 347–355.
18. van Slegtenhorst, M., *et al.* (1997). Identification of the tuberous sclerosis gene TSC1 on chromosome 9q34. *Science* **277:** 805–808.
19. The European chromosome 16 tuberous sclerosis consortium (1993). Identification and characterization of the tuberous sclerosis gene on chromosome 16. *Cell* **75:** 1305–1315.
20. Anbazhagan, R., Herman, J. G., Enika, K., and Gabrielson, E. (2001). Spreadsheet-based program for the analysis of DNA methylation. *Biotechniques* **30:** 110–114.
21. Navone, N. M., *et al.* (1997). Establishment of two human prostate cancer cell lines derived from a single bone metastasis. *Clin. Cancer Res.* **3:** 2493–2500.
22. Weijerman P. C., *et al.* (1998). Expression of prostatic factors measured by reverse transcription polymerase chain reaction in human papillomavirus type 18 deoxyribonucleic acid immortalized prostate cell lines. *Urology* **51:** 657–662.
23. Weijerman, P. C., *et al.* (1997). Specific cytogenetic aberrations in two novel human prostatic cell lines immortalized by human papillomavirus type 18 DNA. *Cancer Genet. Cytogenet.* **99:** 108–115.
24. Maruyama, K., and Sugano, S. (1994). Oligo-capping: a simple method to replace the cap structure of eukaryotic mRNAs with oligoribomucleotides. *Gene* **138:** 171–174.
25. Shaefer, B. (1995). Revolution in rapid amplification of cDNA ends: new strategies for polymerase chain reaction cloning of full-length cDNA ends. *Analytical Biochem.* **227:** 255–273.

Sequence data from this article have been deposited with the DDBJ/EMBL/GenBank Data Libraries under accession number AF367051.

Copyright © 2002 Elsevier Science (USA). All rights reserved.

Cancer and Metastasis Reviews **20:** 351–362, 2001.
Appendix 4
© 2002 *Kluwer Academic Publishers. Printed in the Netherlands.*

Signal transduction targets in androgen-independent prostate cancer

Jian Zhou, Jessica Scholes and Jer-Tsong Hsieh
Department of Urology, University of Texas Southwestern Medical Center at Dallas, Dallas, TX, USA

Key words: prostate cancer, androgen-independent prostate cancer, signal transduction, growth factor, tumor suppressor

Abstract

Prostate cancer (PCa) first manifests as an androgen-dependent disease. Thus, androgen-deprivation therapy is a standard regimen for patients with metastatic PCa. Despite the initial success of androgen-deprivation therapy, PCa inevitably progresses from being androgen dependent (AD) to androgen independent (AI), and this marks the poor prognosis of this disease. Relapse of AIPCa becomes life threatening and accounts for the majority of mortality of PCa patients. Currently, no effective therapy is available for controlling AIPCa. Therefore, the challenge in providing a new intervention is to understand the fundamental changes that occur in AIPCa. Increasing evidence indicates that, under androgen-deprived milieu, several signal networks elicited by peptide growth factors dictate the AI phenotype of PCa. This review covers the latest studies investigating the potential involvement of autocrine growth factors in cell proliferation, survival, metastasis, and the reciprocal interaction with the androgen receptor pathway. In addition, loss of the negative feedback mechanism of the signal cascade further amplifies the effect of growth factors, and thus contributes significantly to the onset of AIPCa. The understanding of the signal target(s) in AIPCa should provide the new markers for prognosis and a new strategy for prevention and therapy.

Progression of androgen-independent prostate cancer

Clinical observations [1–3] indicate that eunuchs and prepubertal castrates do not develop prostate cancer (PCa). This suggests that all the steps of PCa carcinogenesis are prevented by prostatic atrophy associated with early castration or androgen deprivation. Animal models, first developed by Noble [4] and Pollard and Luckert [5] in which chronic administration of androgen and/or estrogen to certain strains of intact male rats caused PCa, further support these observations. Current effective therapeutic modalities, first developed by Huggins and Hodges in 1941 [6], interrupt the positive effect of growth stimulation by androgen. Androgen thus appears to be a 'pure' mitogen for the growth of PCa cells. Conversely, the morphogenic effect of androgen on normal prostatic epithelium must be impaired during the malignant process.

Despite the initial responsiveness of PCa toward androgen ablation, tumor cells invariably relapse to an androgen-refractory state that ultimately leads to mortality. Studies from the Shionogi mouse model [7] support the observation that androgen deprivation leads to a 90% regression of tumor mass (mainly androgen-dependent cells). But, recurrent tumors have a 500-fold increase in the number of androgen-independent (AI) cells over the fraction measured in the parent tumor. Using proliferation-associated antigens (Ki-67, PCNA, MIB 1) as markers, Bonkhoff and Remberger [8] estimated that approximately 70% of the proliferative activity is confined to basal cells in both normal and hyperplastic prostatic epithelia.

AIPCa cells thus appear resistant to a majority of chemotherapeutic agents that target rapidly cycling cells. These data indicate that the androgen eliciting differentiating pathway is often impaired in AIPCa, which may derive from the malignant transformation of 'stem cells' in the normal gland. Based on these findings, we believe that an effective therapy for AIPCa should focus on restoring the differentiation pathway that is operative in normal prostatic epithelia, but is often impaired in AIPCa cells.

Although the stem cells in the prostate are not well characterized, it is believed that certain basal cells may possess stem cell properties. Shortly after androgen deprivation, luminal epithelial cells in the prostate undergo apoptosis; the remaining epithelial cells are the AI basal cell population. Androgen administration can restore the normal acini/ductal structure and function in an involuted prostate by promoting the growth and differentiation of the remaining basal cell population [8,9]. Even after repeated administration of androgen to castrated animals, the prostate always re-grows to a previously programed organ size. This suggests that a limited number of stem cells from the basal cell population determine the ultimate growth potential of the gland [8–11].

The molecular signal(s) involved in this process are likely important in maintaining the homeostasis of the prostate gland. Imbalance in the homeostatic control of the signaling cascade in the stem cell may underlie the malignant phenotype of AIPCa cells. To better understand the biologic properties of AIPCa cells, we will elucidate: (a) the role of several key peptide growth factors that can stimulate cell growth, survival, and metastasis, (b) the intracellular pathways responsible for these processes, and (c) the cross-talk between these pathways and the steroid hormone-elicited pathway. In addition, we will discuss the potential impact of the loss of the negative feedback mechanism associated with these pathways on recurrent AIPCa.

Mitogenic signal pathways in AIPCa

Altered production of growth factors and/or aberrant expression of their receptors are usually associated with PCa cells. Increasing the production of autocrine growth factors is an important step for the appearance of AIPCa after androgen deprivation. For example, epidermal growth factor (EGF) is a mitogen required for normal prostate epithelial cells in both human and rat [12,13], and it is present, in a large amount, in human prostatic fluid [14]. Blocking EGF receptor (EGFR)-elicited signaling can inhibit the proliferation of both DU145 and LNCaP cells, which indicates the important involvement of the EGFR signal axis in the growth of PCa [15].

In the normal gland, the transforming growth factor-α (TGF-α), a ligand for EGFR, predominantly expresses in stromal cells [16]. However, the EGFR expresses in human prostatic epithelial cells with a higher expression in basal cells than luminal epithelia [17]. This suggests that TGF-α and EGFR have a paracrine interaction. In contrast, the autocrine interaction of EGF/TGF-α and its receptor has been shown to play an important role in the progression of PCa [18–20]. Particularly, increased autocrine production of EGF and/or TGF-α was found in several AIPCa cell lines including DU145. This caused the activation of EGFR as demonstrated by high levels of autophosphorylation of EGFR [19,21]. Furthermore, the addition of anti-EGFR antibody to DU145 cells can reduce EGFR autophosphorylation and subsequently inhibit cell proliferation [22].

In other cases, changing the receptor affinity in PCa allows cancer cells to utilize their own autocrine growth factor. In the Dunning tumor model, AT3 tumor cells expressed a different subclass of fibroblast growth factor receptor (FGFR) protein by switching exon IIIb (high affinity to keratinocyte growth factor [KGF]) to exon IIIc (high affinity to acidic FGF [aFGF] and basic FGF [bFGF]) as they acquire a more aggressive phenotype [23]. Similar exon switching has also been found in DU145 and its xenograft [24]. It is also found in PCa specimens, although incidence is low [25].

Autocrine production of FGF has been associated with the proliferation of AIPCa [23,26,27]. Moreover, AI tumors from Shionogi mice produce a bFGF-like protein [28]. In the Dunning tumor model, in concert with the switching of the receptor subtype in AT3 tumors, the increased steady-state levels of FGF-2, FGF-3, and FGF-5 mRNA were also found in these tumor cells [23].

Nerve growth factor (NGF) also appears to be a mitogen for AIPCa. For example, human prostate cell lines (TSU-Pr1, DU145, PC3, and LNCaP) are sensitive to NGF for proliferation [29,30]. Nevertheless, LNCaP does not produce NGF [31]. Since normal prostate stromal cells produce several active forms of NGF [32,33], this suggests that paracrine NGF could be a potent factor necessary for the growth of primary PCa. However, other AIPCa cell lines such as DU145, PC3, and TSU-Pr1 produce NGF in an autocrine manner [31], which indicates that paracrine and/or autocrine production of NGF contributes to the growth of AIPCa.

Immediately after autocrine growth factors bind to their specific receptor (protein receptor tyrosine kinase, PRTK), dimerization and autophosphorylation of the receptor promote interactions with cytoplasmic proteins. These interactions initiate a cascade of phosphorylation events through a variety of adapter proteins and kinases, which transduce the mitogenic signal by increasing gene expression in the nucleus (Figure 1).

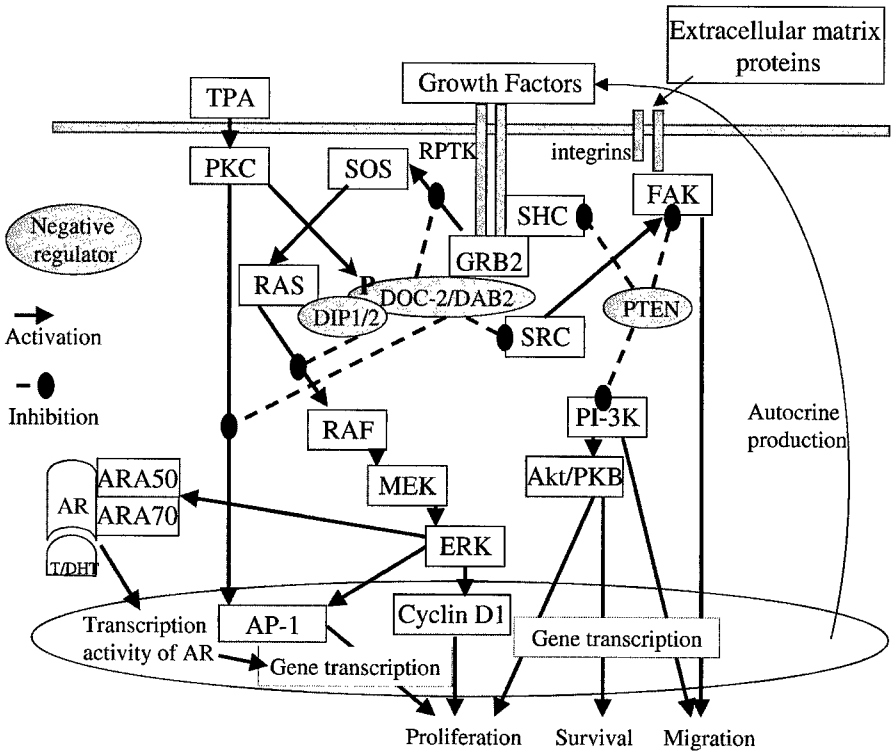

Figure 1. The homeostatic control of signal pathways in prostatic epithelium. The exogenous stimuli (such as hormones, growth factors, and extracellular matrix proteins) can elicit different specific signal cascades that activate gene transcription in the nucleus resulting in cell proliferation, survival, and migration. These signal networks are mainly modulated by protein–protein interaction and protein phosphorylation. Very often, the cross interaction between these pathways becomes more apparent in PCa cells, which underlies the autonomous growth of these cells. The presence of negative regulators prevents the constitutive activation of positive signals, which can maintain a delicate balance in normal cell. Conversely, loss of negative feedback regulators (such as DOC-2/DAB2 and PTEN) in PCa cells intensifies their malignant phenotype. T: testosterone, DHT: dihydrotestosterone.

The interaction between adapter proteins and their activated receptor can further initiate the translocation of a group of proteins, called guanine nucleotide exchange factors (GEFs such as SOS), which modulate the GTPase activity of G-protein such as RAS. Eventually, the GTP-binding RAS can activate a series of mitogen activated protein kinase (MAPK) reactions by Ser/Thr kinases (such as RAF [MAP kinase kinase kinase], ERK [MAP kinase]) and dual kinase (such as MEK [MAP kinase kinase]). MAP kinases can phosphorylate many transcriptional factors (e.g. EF-2) and cyclin (e.g. cyclin D1) is known to be involved in cell cycle regulation [34–36].

The *Ras* superfamily comprises nearly 50 currently known *Ras*-related genes, which encode GTP-binding proteins (i.e. G-protein), and RAS proteins are membrane-bound GTPase [34–36]. Furthermore, RAS proteins help control cell growth and differentiation, but any one of many single amino acid mutations can produce highly oncogenic proteins. In animals, tumors induced by chemicals (e.g. nitrosomethylurea, dimethylbenzanthracene, or N-methyl-N-nitro-N-nitrosoguanidine) or physical manipulation (e.g. X-ray treatment) show about a 70% frequency of *Ras* mutation. This mutation is commonly associated with a point mutation at codon 12 or 61 [37–39]. Activating mutations in *Ras* oncogene occur in a variety of human tumors, such as in pancreatic (90%), colon (50%), thyroid (50%), and lung (30%) cancers [40].

In PCa, enhanced expression of RAS protein correlates with increased tumor grade [41]. Expression of RAS protein has also been assessed in primary and metastatic tumors. Reports [39–44] indicate that most metastatic tumors expressed RAS protein, while only a fifth of primary tumor do. Noticeably, in an androgen-deprived environment, the expression of oncogenic

Ras (V12ras) enhances ERK activation, cyclin D1 induction, and proliferation in LNCaP cells [45,46]. Moreover, suppressing RAS function by inhibiting its protein farnesylation using a peptidomimetic inhibitor (L-744,832) leads to a significant delay in the development of PCa in a xenograft model [47]. These data indicate that RAS protein plays a critical role in the progression of PCa. Nevertheless, *Ras* gene mutation is rare in PCa [42–44,48–50]. This implies that some other factor(s) may be involved in increasing RAS protein levels in PCa.

It also appears that RAF plays a functional role in PCa cells. Suppression of *Raf* gene expression by an anti-sense oligonucleotide induces apoptosis in PC3 and reduces tumor formation in nude mice [51,52]. Surprisingly, prolonged activation of RAF and MAPK are also able to induce cell cycle arrest in LNCaP cells through induction of $p21^{WAF1/CIP1}$ [53] or apoptosis [54]. These data suggest that perturbing a delicate balance of each component of the mitogenic signal cascade could adversely effect cell growth.

Overwhelming data demonstrate the critical role of the MAPK pathway in cell growth and malignant transformation [55–60]. In several PCa cell lines such as LNCaP and DU145 cells, inactivation of MAPK (e.g. ERK) by interrupting EGF binding to EGFR using a flavonoid antioxidant (Silibinin), decreases DNA synthesis and cell growth [61]. Using anti-phosphorylated ERK antibody, heightened activation of MAPK is often detected in high-grade PCa and AIPCa [59]. In AIPCa cell line such as DU145 cells, the constitutive phosphorylation of ERK2, a hallmark of MAPK activation is also observed [15]. However, this ERK2 activation can be blocked by several EGFR inhibitors such as Tyrphostin AG1748 and MAb-EGFR-528, indicating that the EGFR-elicited signal axis is critical for activating the MAPK pathway in AIPCa [15]. Therefore, it is likely that the increased activation of MAPK in high grade PCa and AIPCa is due to the stimulation of autocrine growth factors, which provides a growth advantage for the progression of these cancer cells.

Activation of cyclin D1, a key downstream effector protein in both MAPK and the protein kinase C (PKC)-elicited signal pathway, prompts cells entering S phase during cell cycle. For example, in LNCaP cells, both EGF and TPA (a PKC activator) can induce cyclin D1 in LNCaP cells [62]. Overexpression of cyclin D1 in LNCaP cells results in accelerated cell growth and increased *in vivo* tumorigenicity [63]. However, unlike breast cancer, cyclin D1 gene amplification is relatively rare in PCa cell lines [64]. Using quantitative RT-PCR and Western analyses, Gumbiner et al. [65] demonstrate that no apparent increased cyclin D1 transcript and protein levels were observed in four prostate tumor cell lines and their xenografts tumors. However, an increased cyclin D1 transcript level was found in a small subset (4 out of 96) of clinical specimens derived from either stage C and D [65]. In another study using immunohistochemistry, cyclin D1 positive tumor (defined as identification of positive immunoreactivity in the nuclei of >20% of tumor cells) is 11% (10 of 86) of the primary cases compared with 68% for AI bone metastatic lesion prostate [66]. These data indicate that cyclin D1 may be involved in the onset of AIPCa.

Cell survival signals in AIPCa

Most mitogenic signals have a dual function involved not only in cell proliferation but also cell survival. For example, inhibition of MAPK activity by either Tyrphostin AG1748 (EGFR inhibitor) or PD98059 (MAPK inhibitor) enhances the G2/M cell cycle arrest and radiation-induced cell killing [67]. In addition, PTEN and the phosphatidylinositol triphosphate kinase (PI3-K) pathway have been implicated in the regulation of G1 growth arrest [68] and the regulation of cell survival. PTEN, a dual phosphatase for both phosphatidylinositol 3,4,5-triphosphate (PIP3) and tyrosine phosphoprotein, is frequently lost or mutated in AIPCa [69–72]. Loss of PTEN expression, mostly due to down-regulation of the gene by DNA hypermethylation, is found in PCa [72]. In the absence of PTEN, PIP3 phosphorylated by PI3-K accumulates in cells and it is an activator for Akt/PKB kinase, which promotes cell survival [73–75].

Recent data indicate that dephosphorylation of phosphoinositol-triphophate (PI3P) and focal adhesion kinase (FAK) by PTEN promotes apoptosis through inactivating the PI3-K/Akt cell survival pathway [74,75]. Also, activation of Akt can prevent TRAIL-induced apoptosis in LNCaP cells [76]. On the other hand, in LNCaP cells, the constitutive activation of PI3-K pathway due to PTEN mutation contributes to cell survival since inhibition of this pathway can cause cell apoptosis [77]. However, some data indicate that the PI3-K inhibitor-induced apoptosis in LNCaP cells can be reversed by activating EGFR and/or the androgen receptor (AR) [78], which suggests that the some pathway(s) parallel with the Akt/PKB pathway in PCa also contributes to cell survival.

Signal pathways involved in the metastasis of PCa

PCa cells have a high propensity to metastasize to bone, at which point AIPCa can arise and becomes a life-threatening disease. Metastasis requires not only cell mobility, but also the interaction between tumor cells and their surrounding environment. Several studies demonstrate that a growth factor and its receptor may be involved in this process. For example, overexpression of EGFR can increase the *in vivo* metastasis potential of DU145 cells [79]. Overexpression of Her-2/neu, a member of EGFR family, can facilitate the metastasis of a nontumorigenic rat prostate NbE cells to skeletal muscle in the rib [80]. Conversely, using EGFR-specific kinase inhibitor (PD153035) can reduce invasiveness of PCa using a transgenic adenocarcinoma mouse prostate (TRAMP) model [81]. These data indicate that the involvement of EGFR signaling in the metastasis of PCa.

The possible underlying mechanism for growth factor(s)-elicited PCa metastasis is due to the induction of cell migration. Rajan et al. [82] report that an EGF-like protein identified from several bone and leukemia cell lines acts as a potent chemoattractant, which increases cell migration of a PCa cell line (TSU-Pr1). This study suggests that the EGF-like molecule attracts PCa to invade or metastasize the peripheral lymph nodes and medullary bone. Concurrently, activation of the MAPK pathway is often associated with metastatic PCa [83,84]. It has been shown that the MAPK inhibitor can suppress the expression of the $\alpha 6$ integrin gene, a critical receptor for the interaction with matrix protein by the metastatic PCa, in both PC3 and LNCaP cells [85].

In LNCaP cells, increasing survival can also increase metastatic potential [86]. Conversely, PTEN can inhibit the PI-3K/Akt pathway by dephosphorylating PIP3, which leads to reduced cell motility [87,88]. Furthermore, PTEN can also inhibit cell migration by directly dephosphorylating FAK [89,90] and SRC homolog and collagen protein (SHC) [91] (Figure 1). The steady-state levels of FAK in three PCa cells (LNCaP, PC3, DU145) correlate with the cell migration capability [92]. Moreover, presence of the dominant negative FAK and inhibitor of SRC (oncogenic protein of Rous Sarcoma virus) protein can significantly inhibit migration of PCa [92], indicating that the involvement of integrin/matrix via SRC/FAK signaling is a key determinant for PCa metastasis. Similarly, overexpression of dominant negative SHC can inhibit cell migration in a PTEN-negative giloblastoma cell-U-87MG [93].

Cross-talk between steroid hormone and growth factor-elicited signal pathways

Androgen is known as a key mitogen for primary PCa. In an androgen deprived milieu, it is possible that the AR in AIPCa can function through a ligand-independent fashion. Some data indicate that the ligand independent activation of AR could be achieved by mutation occurring in the ligand binding domain of AR and/or by associating with the growth factor-mediated signaling pathway. In AIPCa, AR mutation and amplification have been found in 20–40% of cases [94–96]. Also, increasing evidence indicate that there is interaction between AR and the peptide growth factor receptor signaling pathway. Activation of MAPK and protein kinase A (PKA) pathways can lead to the phosphorylation of AR, which increases its interaction with cofactors such as ARA50 or ARA70 and consequently enhance the transcription activity of AR [97,98]. This is consistent with data showing that the transcription activity of AR in LNCaP cells can be activated by several growth factors (insulin-like growth factor-1 [IGF-1], KGF, and EGF) [99] capable of initiating the MAPK pathway. Also, overexpression of Her-2/neu can induce AR activation through activation of the MAPK phosphorylation cascade [100,101]. Moreover, Sehgal et al. [102] indicate that androgen can induce amphiregulin, a ligand for EGFR, which could activate EGFR-mediated signal transduction. These data clearly indicate that reciprocal interaction between the AR and MAPK-mediated pathways may underlie the AI growth of PCa.

Loss of homeostatic control of the signal pathway in AIPCa

Despite the prevalence of positive signal(s) involved in the relapse of AIPCa, loss of negative feedback control in the signal network also significantly impact the onset of AIPCa. Loss of the tumor suppressor PTEN (Figure 1) has been implicated in proliferation, cell survival, and metastasis of PCa cells. The dual phosphatase activity of PTEN can dephosphorylate PIP3 which is required for activating the PI3-Kinsae/Akt pathway implicated in promoting proliferation and cell survival in PCa [77,78]. PTEN can also suppress cell

proliferation, survival, and migration of prostate cells by dephosphorylating tyrosine phosphoprotein such as FAK and SHC [89–91].

Based on animal models and clinical observation, we believe AIPCa possesses similar stem cell properties as the normal prostate gland. To unveil the fundamental changes that occur in AIPCa, we hypothesized that altered homeostatic control machinery, operative in normal prostatic basal cells, underlie the malignant phenotype of AIPCa. Our laboratory has screened cDNAs from the enriched basal cell population of the degenerated prostate gland. A candidate gene has recently been identified as DOC-2/DAB2 (differential-expressed in ovarian cancer-2/disabled 2), which was cloned from differential display as a potential tumor suppressor in ovarian cancer [103]. It encodes an 82 kDa phosphoprotein with a highly conserved sequence between human and rodent, which implies its important biological function. The N-terminal of DOC-2/DAB2 contains a homology domain (i.e. DAB domain) with the *disabled* (SRC-binding protein) gene involved in the differentiation of the neuron [104]. The C-terminal of DOC-2/DAB2 contains three proline-rich domains that can bind to SH3-containing protein [105]. Therefore, DOC-2/DAB2 appears to be a typical molecule involved in the signal network.

In the normal prostate, DOC-2/DAB2 is predominantly associated with basal epithelia cells when the prostate undergoes androgen-deprived degeneration [103]. Decreased expression of DOC-2/DAB2 has been found in several tumors including ovarian, choriocarcinoma, breast, and prostate. We also observed the absence of DOC-2/DAB2 in several PCa cell lines derived from AIPCa patients [103]. Increased expression of DOC-2/DAB2 can suppress cell growth and increase G1/Go growth arrest in a tumorigenic LNCaP subline (C4-20 cell). Similar results were observed in other cancer types [106–108]. In ovarian cancer, reintroducing DOC-2/DAB2 into cancer cells can reduce cell growth, tumorigenicity and suppress the serum induced *c-fos* gene expression [106–109]. These data indicate that DOC-2/DAB2 is a potent tumor suppressor.

The mechanism responsible for the loss of DOC-2/DAB2 in PCa is not fully understood. However, some evidence indicate that the expression of DOC-2/DAB2 is suppressed by the RAS-mediated pathway because DOC-2/DAB2 is down regulated at least 100-fold in RAS-transformed cells and such suppression can be reverted in the presence of MAPK inhibitor PD98059 [110]. Also, the gene transcription of DOC-2/DAB2 can be modulated by either GATA-6 or retinoic acid during embryonic differentiation [111,112]. Noticeably, retinoic acid treatment can cause apoptosis in PCa cells [113,114]. However, the relationship of DOC-2/DAB2 and retinoic acid-induced apoptosis in PCa remains undetermined. Moreover, our data also demonstrate that DOC-2/DAB2 is induced during TPA-induced megakarocyte differentiation of K562 cells [115]. Based on these findings, we believe that the regulation DOC-2/DAB2 gene is associated with cell differentiation in several cell types including prostatic epithelia.

To examine the role of DOC-2/DAB2 in modulating signal transduction which may impact the phenotype of AIPCa cells, we first demonstrated that the presence of DOC-2/DAB2 is able to inhibit TPA-induced gene expression [116]. Moreover, DOC-2/DAB2 (Figure 1) can be rapidly phosphorylated by treatment of growth factor and TPA [116]. Therefore, we examined the impact of DOC-2/DAB2 phosphorylation on the effect of TPA in PCa cell lines such as LNCaP cells. It appears that the serine 24 in the N-terminal of DOC-2/DAB2 is the key phosphoamino acid residue in modulating PKC-elicited signal pathway, since the alteration of this residue abolishes the activity of AP-1 induced by TPA [115].

Recently, we identified a novel RAS-GTPase-activating protein (RAS-GAP) as a DOC-2/DAB2 interactive protein (DIP1/2) [117]. The human DIP1/2 gene locates at 9q33.1–33.3 [118] proximal to a potential tumor suppressor gene, TSC1 (Tuberous Sclerosis) [119]. It has also been reported [120] that a novel RAS-GAP gene fused to a myeloid/lymphoid leukemia gene in acute myeloid leukemia with chromosomal translocation [t(9;11)(q34; q23)]; DIP1/2 may be that candidate gene.

Using detailed biochemical analyses, we demonstrated that DIP1/2 is a typical RAS-GAP that hydrolyzes RAS-GTP (active RAS) to become RAS-GDP (inactive RAS). We further demonstrated that the interaction between DOC-2/DAB2 and DIP1/2 enhance the GAP activity in PCa cells (Figure 1), and, decreased expression of DIP1/2 is associated with several PCa cell lines derived from AIPCa patients. Apparently, one of the mechanisms of action of DOC-2/DAB2/DIP1/2 is to modulate RAS activity in AIPCa. In addition, the DAB domain of DOC-2/DAB2 directly associates with Smad and mad-related protein 2 and 3 (Smad2 and Smad3), which restores the transforming growth factor-β (TGF-β) signaling pathway in TGF-β mutant cells [121]. Thus, DOC-2/DAB2

appears to have multiple mechanisms of action that modulate the growth/differentiation of mammalian cells.

As shown previously, DOC-2/DAB2 interacts with GRB2 in mouse macrophage treated with colony stimulating factor-1 [105]. We further analyzed the functional role of the C-terminal of DOC-2/DAB2, particularly the proline rich domain, in growth factor-elicited signal transduction. In PCa, the expression of DOC-2/DAB2 prevents the SOS from binding GRB2 (Figure 1), which leads to the suppression of MAPK activation initiated by EGF [122]. Similar action of DOC-2/DAB2 is also observed in PC12 cells stimulated with neurotropin NT3 [122], suggesting that DOC-2/DAB2 is involved in the growth/differentiation of neuronal cells. Moreover, our preliminary data indicated that some other SH3-containing proteins such as SRC and NCK can interact with the DOC-2/DAB2 (Figure 1). The biologic implication of this interaction warrants further investigation. Nevertheless, the DOC-2/DAB2 complex represents a unique negative feedback machinery for balancing the signaling cascade elicited by exogenous stimuli. Altered expression of this complex underlies the onset of AIPCa.

Concluding remarks

Relapse of AIPCa signifies that PCa has become autonomous after androgen deprivation; the presence of peptide growth factors or cytokines becomes a prevalent mitogen for AIPCa. However, it is clear that these exogenous stimuli elicit various signal networks critical for cell proliferation, survival, and metastasis. Among these pathways, increased MAPK activation appears to predominate in the AIPCa cells. This is evidenced by several molecular markers such as RAS, ERK, and cyclin D1. Overwhelming *in vitro* and *in vivo* data demonstrate this relationship. Moreover, recent data also indicate the MAPK and AR pathways have a reciprocal interaction, which underlies the mechanism for the AI progression. Nevertheless, unlike other cancer types, the mutation rate of these key effectors (such as *Ras* and *cyclin D1*) is relatively low in PCa. Therefore, it is likely that other regulatory pathways such as the negative feedback mechanism are impaired in the PCa cells.

Several molecules were identified as a part of a negative regulatory network. PTEN is an excellent example of such a molecule because, (a) decreased or frequent loss of PTEN expression is found in PCa, and (b) loss of PTEN is known to increase the cell survival of PCa through the PI-3K/Akt pathway or through cell migration/metastasis through the SRC or FAK pathway. In addition, our laboratory identified a unique complex (DOC-2/DAB2/DIP1/2) that modulates the RAS and TGF-β mediated pathway. Since this complex can associate with many other effectors, it is possible to predict the potential impact of this complex on the progression of AIPCa.

The ultimate goal in studying the signal network in AIPCa is to identify marker(s) for early prognosis of AI disease and to develop specific agent(s) for disease intervention. Recent clinical approval of the c-ABL tyrosine kinase inhibitor (STI-571, Gleevec) marks the beginning of target-specific cancer therapy. In addition to the completion of the human genome project, in the foreseeable future, cancer therapy could be customized based upon an individual patient's genetic profile. Therefore, profiling signal transduction targets in AIPCa has tremendous clinical application.

Key unanswered questions

1. It appears that AIPCa contains a heterogeneous cell population. What are the critical signal networks operative in AIPCa cells?
2. AIPCa has a high propensity to grow in bone. What are the critical signal networks responsible for the interaction between these cells?
3. There is a significant overlapping in the signal cascade-elicited by many biologic responses. Are there key merging points in AIPCa?
4. What is the impact of different nerve growth factors on the progression of AIPCa?
5. It appears that a close interaction exists between AR and MAPK pathways. Can DOC-2/DAB2 complex modulate the AR-mediated signal transduction?
6. The presence of negative regulator is to prevent the constitutive activation of positive signal cascade elicited by stimuli. Therefore, what is the mechanism resulting in the association between these proteins immediately after the initial activation?
7. Loss of DOC-2/DAB2 expression is often found in AIPCa. What is the underlying mechanism(s) leading to the loss of DOC-2/DAB2 expression?
8. The underlying mechanism of negative feedback pathways is somewhat similar. Can these negative feedback pathways complement each other in AIPCa?

Acknowledgements

This work is supported by a grant from the National Institute of Health (DK 4765707). We also thank Andrew Webb for editing the manuscript.

References

1. Lipsett B: Interaction of drugs, hormones and nutrition in the causes of cancer. Cancer 43: 1967–1981, 1979
2. Wagenseil F: Chinesische eunuchen. Zeitschrift für Morphologie und Anthropologie 32: 416–468, 1933
3. Hamilton JB, Mestler GE: Mortality and survival: Comparison of eunuchs with intact men and women in a mentally retarded population. J Gerontol 24: 395–411, 1969
4. Noble RL: The development of prostatic adenocarcinoma in NB rats following prolonged sex hormone administration. Cancer Res 37: 1929–1933, 1977
5. Pollard M, Luckert PH: Production of autochtoneous prostate cancer in Lobound-Wistar rats by treatment with N-nitroso-N-methylurea and testosterone. JNCI 77: 583–587, 1986
6. Huggins C, Hodges CV: Studies on prostatic cancer I. The effect of castration of estrogen and of androgen injection on serum phosphatase in metastatic carcinoma of the prostate. Cancer Res 1: 293–297, 1941
7. Bruchovsky N, Rennie PS, Coldman AJ, Goldenberg SL, To M, Lawson D: The effects of androgen withdrawal on the stem cell composition of Shionogi carcinoma. Cancer Res 50: 2275–2282, 1990
8. Bonkohoff H, Remberger K: Differentiation pathways and histogenetic aspects of normal and abnormal prostatic growth: A stem cell model. Prostate 28: 98–106, 1996
9. Issacs JT, Coffey DS: Etiology and disease process of benign prostatic hyperplasia. Prostate, 2(Suppl): 33–50, 1989
10. Coffey DS, Walsh PC: Clinical and experimental studies of benign prostatic hyperplasia. Urol Clin North Am 17: 461–475, 1990
11. English HF, Santen RJ, Isaacs JT: Response of glandular versus basal rat ventral prostate. Prostate 11: 229–242, 1987
12. Mckeehan WL, Adams PS, Rosser MP: Direct mitogenic effects of insulin, epidermal growth factor and possibly prolactin, but not androgen, on normal rat prostate epithelial cells in serum-free primary cell culture. Cancer Res 44: 1998–2010, 1984
13. Peehl DM, Wong S, Bazinet M, Stamey TA: *In vitro* studies of human prostate epithelial cells. Growth Factors 1: 237–250, 1989
14. Gregory J, Willshire IR, Kavanagh JP, Blacklock NJ, Chowdury S, Richards RC: Urogastrone-epidermal growth factor concentration in prostatic fluid of normal individuals and patients with benign prostatic hypertrophy. Clin Sci 70: 359–363, 1986
15. Putz T, Cuilig Z, Eder IE, Nassler-Menardi C, Bartsch G, Grunicke H, Uberall F, Klocker H: Epidermal growth factor (EGF) receptor blockade inhibits the action of EGF, insulin-like growth factor I, and a protein kinase A activator on the mitogen-activated protein kinase pathway in prostate cancer cell lines. Cancer Res 59: 227–233, 1999
16. Cohen DW, Simak R, Fair WR, Melded J, Scher HI, Cordon-Cardo C: Expression of transforming growth factor-α and the epidermal growth factor receptor in human prostate tissue. J Urol 152: 2120–2124, 1994
17. Maygarden SJ, Novotny DB, Moul JW, Bae VL, Ware JL: Evaluation of cathepsin D and epidermal growth factor receptor in prostate carcinoma. Mod Pathol 7: 930–936, 1994
18. Scher HI, Sarkis A, Reuter V, Cohen D, Netto G, Petrylak D, Lianes P, Fuks Z, Mendelsohn J, Cordon-Cardo C: Changing pattern of expression of the epidermal growth factor receptor and transforming growth factor–α in the progression of prostatic neoplasms. Clin Cancer Res 1: 545–550, 1995
19. Connolly JM, Rose DP: Production of epidermal growth factor and transforming growth factor-α by the androgen-responsive LNCaP human prostate cancer cell line. Prostate 16: 209–218, 1990
20. Fong CJ, Sherwood ER, Mendelsohn J, Lee C, Kozlowski JM: Epidermal growth factor receptor monoclonal antibody inhibits constitutive receptor phosphorylation, reduces autonomous growth, and sensitizes androgen-independent prostatic carcinoma cells to tumor necrosis factor α. Cancer Res 52: 5887–5892, 1992
21. Connolly JM, Rose DP: Secretion of epidermal growth factor and related polypeptides by the Du145 human prostate cell line. Prostate 15: 177–186, 1989
22. MacDonald A, Habib FK: Divergent responses to epidermal growth factor in hormone sensitive and insensitive human prostate cancer cell lines. Br J Cancer 65: 177–182, 1992
23. Yan G, Fukabori Y, Mcbride G, Nikolaropolous S, McKeehan WL: Exon switching and activation of stromal and embryonic fibroblast growth factor (FGF)-FGF receptor genes in prostate epithelial cells accompany stromal independence and malignancy. Mol Cell Biol 13: 4513–4522, 1993
24. Carstens RP, Eaton JV, Krigman HR, Walther PJ, Garcia-Blanco MA: Alternative splicing of fibroblast growth factor receptor 2 (FGF-R2) in human prostate cancer. Oncogene 15: 3059–3065, 1997
25. Kwabi-Addo B, Ropiquet F, Giri D, Ittmann M: Alternative splicing of fibroblast growth factor receptors in human prostate cancer. Prostate 46: 163–172, 2001
26. Gleave M, Hsieh JT, Gao CA, von Eschenbach AC, Chung LW: Acceleration of human prostate cancer growth *in vivo* by factors produced by prostate and bone fibroblasts. Cancer Res 51: 3753–3761, 1991
27. Nakamoto T, Chang CS, Li AK, Chodak GW: Basic fibroblast growth factor in human prostate cancer cells. Cancer Res 52:571–577, 1992
28. Sato N, Watabe Y, Suzuki H, Shimazaki J: Progression of androgen-sensitive mouse tumor

(Shionogi cancinoma 115) to androgen-insensitive tumor after long-term removal of testosterone. Jpn J Cancer Res 84: 1300–1308, 1993
29. Pflug B, Djakiew D: Expression of p75NTR in a human prostate epithelial tumor cell line reduces nerve growth factor-induced cell growth by activation of programmed cell death. Mol Carcinog 23: 106–114, 1998
30. Angelsen A, Sandvik AK, Syversen U, Stridsberg M, Waldum HL: NGF-β, NE-cells and prostatic cancer cell lines. A study of neuroendocrine expression in the human prostatic cancer cell lines DU-145, PC-3, LNCaP, and TSU-pr1 following stimulation of the nerve growth factor-β. Scand J Urol Nephrol 32: 7–13, 1998
31. Dalal R, Djakiew D: Molecular characterization of neurotrophin expression and the corresponding tropomyosin receptor kinases (trks) in epithelial and stromal cells of the human prostate. Mol Cell Endocrinol 134: 15–22, 1997
32. Delsite R, Djakiew D: Characterization of nerve growth factor precursor protein expression by human prostate stromal cells: A role in selective neurotrophin stimulation of prostate epithelial cell growth. Prostate 41: 39–48, 1999
33. Djakiew D, Delsite R, Pflug B, Wrathall J, Lynch JH, Onoda M: Regulation of growth by a nerve growth factor-like protein which modulates paracrine interactions between a neoplastic epithelial cell line and stromal cells of the human prostate. Cancer Res 51: 3304–3310, 1991
34. Schlessinger J: SH2/SH3 signaling proteins. Curr Opin Genet Dev 4: 25–30, 1994
35. Seger R, Kreb EG: The MAPK siganling cascade. FASEB J 9: 726–735, 1995
36. Post GR, Brown JH: G protein-coupled receptors and signaling pathways regulating growth responses. FASEB J 10: 741–749, 1996
37. Bredel M, Pollack IF: The p21-Ras signal trnasduction pathway and growth regulation in human high-grade glioma. Brain Res Brain Res Rev 29: 232–249, 1999
38. Barbacid M: Ras genes. Annu Rev Biochem 56: 779–827, 1987
39. Nakazawa H, Aguelon AM, Yamasaki H: Identification and quantification of a carcinogen-induced molecular initiation event in cell transformation. Oncogene 7: 2295–2301, 1992
40. Bos JL: Ras oncogenes in human cancer: Review. Cancer Res 49: 4682–4689, 1989
41. Viola MV, Fromowitz F, Oravez S, Deb S, Finkel G, Lundy J, Hand P, Thor A, Schlom J: Expression of ras oncogene p21 in prostate cancer. N Engl J Med 314: 133–137, 1986
42. Sumiya H, Masai M, Akimoto S, Yatani R, Shimazaki J: Histochemical examination of expression of ras p21 protein and R 1881-binding protein in human prostatic cancers. Eur J Cancer 26: 786–789, 1990
43. Carter BS, Epstein JI, Isaacs WB: Ras gene mutation in human prostate cancer. Cancer Res 50: 6830–6832, 1990
44. Pergolizzi RG, Kreis W, Rottach C, Susin M, Broome JD: Mutational status of codons 12 and 13 of the N- and K-ras genes in tissue and cell lines derived from primary and metastatic prostate carcinomas. Cancer Invest 11: 25–32, 1993
45. Voeller HJ, Wilding G, Gelmann EP: v-rasH expression confers hormone-independent *in vitro* growth to LNCaP prostate carcinoma cells. Mol Endocrinol 5: 209–216, 1991
46. Fribourg AF, Knudsen KE, Strobeck MW, Lindhorst CM, Knudsen ES: Differential requirements for ras and the retinoblastoma tumor suppressor protein in the androgen dependence of prostatic adenocarcinoma cells. Cell Growth Differ 11: 361–372, 2000
47. Sirotnak FM, Sepp-Lorenzino L, Kohl NE, Rosen N, Scher HI: A peptidomimetic inhibitor of ras functionality markedly suppresses growth of human prostate tumor xenografts in mice. Prospects for long-term clinical utility. Cancer Chemother Pharmacol 46: 79–83, 2000
48. Gumerlock PH, Poonamallee UR, Meyers FJ, deVere White RW: Activated ras alleles in human carcinoma of the prostate are rare. Cancer Res 51: 1632–1637, 1991
49. Moul JW, Friedrichs PA, Lance RS, Theune SM, Chang EH: Infrequent RAS oncogene mutations in human prostate cancer. Prostate 20: 327–338, 1992
50. Ozen M, Pathak S: Genetic alterations in human prostate cancer: A review of current literature. Anticancer Res 20: 1905–1912, 2000
51. Lau QC, Brusselbach S, Muller R: Abrogation of c-Raf expression induces apoptosis in tumor cells. Oncogene 16: 1899–1902, 1998
52. Geiger T, Muller M, Monia BP, Fabbro D: Antitumor activity of a C-raf antisense oligonucleotide in combination with standard chemotherapeutic agents against various human tumors transplanted subcutaneously into nude mice. Clin Cancer Res 3: 1179–1185, 1997
53. Ravi RK, McMahon M, Yangang Z, Williams JR, Dillehay LE, Nelkin BD, Mabry M: Raf-1-induced cell cycle arrest in LNCaP human prostate cancer cells. J Cell Biochem 72: 458–469, 1999
54. Gschwend JE, Fair WR, Powell CT: Bryostatin 1 induces prolonged activation of extracellular regulated protein kinases in and apoptosis of LNCaP human prostate cancer cells overexpressing protein kinase c-α. Mol Pharmacol 57: 1224–1234, 2000
55. Cowley S, Paterson H, Kemp P, Marshall CJ: Activation of MAP kinase kinase is necessary and sufficient for PC12 differentiation and for transformation of NIH 3T3 cells. Cell 77: 841–852, 1994
56. Mansour SJ, Matten WT, Hermann AS, Candia JM, Rong S, Fukasawa K, Vande Woude GF, Ahn NG: Transformation of mammalian cells by constitutively active MAP kinase kinase. Science 265: 966–970, 1994
57. Magi-Galluzzi C, Mishra R, Fiorentino M, Montironi R, Yao H, Capodieci P, Wishnow K, Kaplan I, Stork PJ, Loda M: Mitogen-activated protein kinase phosphatase 1 is overexpressed in prostate cancers and is inversely related to apoptosis. Lab Invest 76: 37–51, 1997
58. Oka H, Chatani, Hoshino R, Ogawa O, Kakehi Y, Terachi T, Okada Y, Kawaichi M, Kohno M, Yoshida O: Constitutive activation of mitogen-activated protein (MAP) kinases in human renal cell carcinoma. Cancer Res 55: 4182–4187, 1995
59. Gioeli D, Mandell JW, Petroni GR, Frierson HF Jr, Weber MJ: Activation of mitogen-activated protein kinase

associated with prostate cancer progression. Cancer Res 59: 279–284, 1999
60. Sebolt-Leopold JS: Development of anticancer drugs targeting the MAP kinase pathway. Oncogene 19: 6594–6599, 2000
61. Sharma Y, Agarwal C, Singh AK, Agarwal R: Inhibitory effect of silibinin on ligand binding to erbB1 and associated mitogenic signaling, growth, and DNA synthesis in advanced human prostate carcinoma cells. Mol Carcinog 30: 224–236, 2001
62. Perry JE, Grossmann ME, Tindall DJ: Epidermal growth factor induces cyclin D1 in a human prostate cancer cell line. Prostate 35: 117–124, 1998
63. Chen Y, Martinez LA, LaCava M, Coghlan L, Conti CJ: Increased cell growth and tumorigenicity in human prostate LNCaP cells by overexpression to cyclin D1. Oncogene 16: 1913–1920, 1998
64. Han EK, Lim JT, Arber N, Rubin MA, Xing WQ, Weinstein IB: Cyclin D1 expression in human prostate carcinoma cell lines and primary tumors. Prostate 35: 95–101, 1998
65. Gumbiner LM, Gumerlock PH, Mack PC, Chi SG, deVere White RW, Mohler JL, Pretlow TG, Tricoli JV: Overexpression of cyclin D1 is rare in human prostate carcinoma. Prostate 38: 40–45, 1999
66. Drobnjak M, Osman I, Scher HI, Fazzari M, Cordon-Cardo C: Overexpression of cyclin D1 is associated with metastatic prostate cancer to bone. Clin Cancer Res 6: 1891–1895, 2000
67. Hagan M, Wang L, Hanley JR, Park JS, Dent P: Ionizing radiation-induced mitogen-activated protein (MAP) kinase activation in DU145 prostate carcinoma cells: MAP kinase inhibition enhances radiation-induced cell killing and G2/M-phase arrest. Radiat Res 153: 371–383, 2000
68. Ramaswamy S, Nakamura N, Vazquez F, Batt DB, Perera S, Roberts TM, Sellers WR: Regulation of G1 progression by the PTEN tumor suppressor protein is linked to inhibition of the phosphatidylinositol 3-kinase/Akt pathway. Proc Natl Acad Sci USA 96: 2110–2115, 1999
69. Li J, Yen C, Liaw D, Podsypanina K, Bose S, Wang SI, Puc J, Miliaresis C, Rodgers L, McCombie R, Bigner SH, Giovanella BC, Ittmann M, Tycko B, Hibshoosh H, Wigler MH, Parsons R: PTEN, a putative protein tyrosine phosphatase gene mutated in human brain, breast, and prostate cancer. Science 275: 1943–1947, 1997
70. Steck PA, Lin H, Langford LA, Jasser SA, Koul D, Yung WK, Pershouse MA: Functional and molecular analyses of 10q deletions in human gliomas. Genes Chromosomes Cancer 24: 135–143, 1999
71. Vlietstra RJ, van Alewijk DC, Hermans KG, van Steenbrugge GJ, Trapman J: Frequent inactivation of PTEN in prostate cancer cell lines and xenografts. Cancer Res 58: 2720–2723, 1998
72. Whang YE, Wu X, Suzuki H, Reiter RE, Tran C, Vessella RL, Said JW, Isaacs WB, Sawyers CL: Inactivation of the tumor suppressor PTEN/MMAC1 in advanced human prostate cancer through loss of expression. Proc Natl Acad Sci USA 95: 5246–5250, 1998
73. Stambolic V, Suzuki A, de la Pompa JL, Brothers GM, Mirtsos C, Sasaki T, Ruland J, Penninger JM, Siderovski DP, Mak TW: Negative regulation of PKB/Akt-dependent cell survival by the tumor suppressor PTEN. Cell 95: 29–39, 1998
74. Wu X, Senechal K, Neshat MS, Whang YE, Sawyers CL: The PTEN/MMAC1 tumor suppressor phosphatase functions as a negative regulator of the phosphoinositide 3-kinase/Akt pathway. Proc Natl Acad Sci USA 95: 15587–15591, 1998
75. Tamura M, Gu J, Danen EH, Takino T, Miyamoto S, Yamada KM: PTEN interactions with focal adhesion kinase and suppression of the extracellular matrix-dependent phosphatidylinositol 3-kinase/Akt cell survival pathway. J Biol Chem 274: 20693–20703, 1999
76. Nesterov A, Lu X, Johnson M, Miller GJ, Ivashchenko Y, Kraft AS: Elevated AKT activity protects the prostate cancer cell line LNCaP from TRAIL-induced apoptosis. J Biol Chem 276: 10767–10774, 2001
77. Lin J, Adam RM, Santiestevan E, Freeman MR: The phosphatidylinositol 3′-kinase pathway is a dominant growth factor-activated cell survival pathway in LNCaP human prostate carcinoma cells. Cancer Res 59: 2891–2897, 1999
78. Carson JP, Kulik G, Weber MJ: Antiapoptotic signaling in LNCaP prostate cancer cells: A survival signaling pathway independent of phosphatidylinositol 3′-kinase and Akt/protein kinase B. Cancer Res 59: 1449–1453, 1999
79. Turner T, Chen P, Goodly LJ, Wells A: EGF receptor signaling enhances *in vivo* invasiveness of DU-145 human prostate carcinoma cells. Clin Exp Metastasis 14: 409–418, 1996
80. Marengo SR, Sikes RA, Anezinis P, Chang SM, Chung LW: Metastasis induced by overexpression of p185neu-T after orthotopic injection into a prostatic epithelial cell line (NbE). Mol Carcinog 19: 165–175, 1997
81. Kassis J, Moellinger J, Lo H, Greenberg NM, Kim HG, Wells A: A role for phospholipase C-γ-mediated signaling in tumor cell invasion. Clin Cancer Res 5: 2251–2260, 1999
82. Rajan R, Vanderslice R, Kapur S, Lynch J, Thompson R, Djakiew D: Epidermal growth factor (EGF) promotes chemomigration of a human prostate tumor cell line, and EGF immunoreactive proteins are present at sites of metastasis in the stroma of lymph nodes and medullary bone. Prostate 28: 1–9, 1996
83. Krueger JS, Keshamouni VG, Atanaskova N, Reddy KB: Temporal and quantitative regulation of mitogen-activated protein kinase (MAPK) modulates cell motility and invasion. Oncogene 20: 4209–4218, 2001
84. Turner CE: Paxillin interactions. J Cell Sci 23: 4139–4140, 2000
85. Onishi T, Yamakawa K, Franco OE, Kawamura J, Watanabe M, Shiraishi T, Kitazawa S: Mitogen-activated protein kinase pathway is involved in α6 integrin gene expression in androgen-independent prostate cancer cells: role of proximal Sp1 consensus sequence. Biochim Biophy Acta 1538: 218–227, 2001
86. McConkey DJ, Greene G, Pettaway CA: Apoptosis resistance increases with metastatic potential in cells of the

human LNCaP prostate carcinoma line. Cancer Res 56: 5594–5599, 1996
87. Maehama T, Dixon JE: The tumor suppressor, PTEN/MMAC1, dephosphorylates the lipid second messenger, phosphatidylinositol 3,4,5-trisphosphate. J Biol Chem 273: 13375–13378, 1998
88. Morimoto AM, Tomlinson MG, Nakatani K, Bolen JB, Roth RA, Herbst R: The MMAC1 tumor suppressor phosphatase inhibits phospholipase C and integrin-linked kinase activity. Oncogene 19: 200–209, 2000
89. Tamura M, Gu J, Matsumoto K, Aota S, Parsons R, Yamada KM: Inhibition of cell migration, spreading, and focal adhesions by tumor suppressor PTEN. Science 280: 1614–1617, 1998
90. Tamura M, Gu J, Takino T, Yamada KM: Tumor suppressor PTEN inhibition of cell invasion, migration, and growth: Differential involvement of focal adhesion kinase and p130Cas. Cancer Res 59: 442–449, 1999
91. Gu J, Tamura M, Pankov R, Danen EH, Takino T, Matsumoto K, Yamada KM: Shc and FAK differentially regulate cell motility and directionality modulated by PTEN. J Cell Biol 146: 389–403, 1999
92. Slack JK, Adams RB, Rovin JD, Bissonette EA, Stoker CE, Parsons JT: Alterations in the focal adhesion kinase/Src signal transduction pathway correlate with increased migratory capacity of prostate carcinoma cells. Oncogene 20: 1152–1163, 2001
93. Gu J, Tamura M, Yamada KM: Tumor suppressor PTEN inhibits integrin- and growth factor-mediated mitogen-activated protein (MAP) kinase signaling pathways. J Cell Biol 143: 1375–1383, 1998
94. Gaddipati JP, McLeod DG, Heidenberg HB, Sesterhenn IA, Finger MJ, Moul JW, Srivastava S: Frequent detection of codon 877 mutation in the androgen receptor gene in advanced prostate cancers. Cancer Res 54: 2861–2864, 1994
95. Taplin ME, Bubley GJ, Shuster TD, Frantz ME, Spooner AE, Ogata GK, Keer HN, Balk SP: Mutation of the androgen-receptor gene in metastatic androgen-independent prostate cancer. N Engl J Med 332: 1393–1398, 1995
96. Visakorpi T, Hyytinen E, Koivisto P, Tanner M, Keinanen R, Palmberg C, Palotie A, Tammela T, Isola J, Kallioniemi OP: *In vivo* amplification of the androgen receptor gene and progression of human prostate cancer. Nat Genet 9: 401–406, 1995
97. Abreu-Martin MT, Chari A, Palladino AA, Craft NA, Sawyers CL: Mitogen-activated protein kinase kinase kinase 1 activates androgen receptor-dependent transcription and apoptosis in prostate cancer. Mol Cell Biol 19: 5143–5154, 1999
98. Chen T, Cho RW, Stork PJ, Weber MJ: Elevation of cyclic adenosine 3′,5′-monophosphate potentiates activation of mitogen-activated protein kinase by growth factors in LNCaP prostate cancer cells. Cancer Res 59: 213–218, 1999
99. Culig Z, Hobisch A, Cronauer MV, Radmayr C, Trapman J, Hittmair A, Bartsch G, Klocker H: Androgen receptor activation in prostatic tumor cell lines by insulin-like growth factor-I, keratinocyte growth factor, and epidermal growth factor. Cancer Res 54: 5474–5478, 1994
100. Craft N, Shostak Y, Carey M, Sawyers CL: A mechanism for hormone-independent prostate cancer through modulation of androgen receptor signaling by the HER-2/neu tyrosine kinase. Nat Med 5: 280–285, 1999
101. Yeh S, Lin HK, Kang HY, Thin TH, Lin MF, Chang C: From HER2/Neu signal cascade to androgen receptor and its coactivators: A novel pathway by induction of androgen target genes through MAP kinase in prostate cancer cells. Proc Natl Acad Sci USA 96: 5458–5463, 1999
102. Sehgal I, Bailey J, Hitzemann K, Pittelkow MR, Maihle NJ: Epidermal growth factor receptor-dependent stimulation of amphiregulin expression in androgen-stimulated human prostate cancer cells. Mol Biol Cell 5: 339–347, 1994
103. Tseng CP, Ely BD, Li Y, Pong RC, Hsieh JT: Regulation of rat DOC-2 gene during castration-induced rat ventral prostate degeneration and its growth inhibitory function in human prostatic carcinoma cells. Endocrinology 139: 3542–3553, 1998
104. Howell BW, Gertler FB, Cooper JA: Mouse disabled (mDab1): A Src binding protein implicated in neuronal development. EMBO J 16: 121–132, 1997
105. Xu XX, Yi T, Tang B, Lambeth JD: Disabled-2 (Dab2) is an SH3 domain-binding partner of Grb2. Oncogene 16: 1561–1569, 1998
106. Mok SC, Chan WY, Wong KK, Cheung KK, Lau CC, Ng SW, Baldini A, Colitti CV, Rock CO, Berkowitz RS: DOC-2, a candidate tumor suppressor gene in human epithelial ovarian cancer. Oncogene 16: 2381–2387, 1998
107. Fulop V, Colitti CV, Genest D, Berkowitz RS, Yiu GK, Ng SW, Szepesi J, Mok SC: DOC-2/hDab2, a candidate tumor suppressor gene involved in the development of gestational trophoblastic diseases. Oncogene 17: 419–424, 1998
108. Fazili Z, Sun W, Mittelstaedt S, Cohen C, Xu XX: Disabled-2 inactivation is an early step in ovarian tumorigenicity. Oncogene 18: 3104–3113, 1999
109. He J, Smith ER, Xu XX: Disabled-2 exerts its tumor suppressor activity by uncoupling c-Fos expression and MAP kinase activation. J Biol Chem 276: 26814–26818, 2001
110. Zuber J, Tchernitsa OI, Hinzmann B, Schmitz AC, Grips M, Hellriegel M, Sers C, Rosenthal A, Schafer R: A genome-wide survey of RAS transformation targets. Nat Genet 24: 144–1452, 2000
111. Morrisey EE, Musco S, Chen MY, Lu MM, Leiden JM, Parmacek MS: The gene encoding the mitogen-responsive phosphoprotein Dab2 is differentially regulated by GATA-6 and GATA-4 in the visceral endoderm. J Biol Chem 275: 19949–19954, 2000
112. Cho SY, Cho SY, Lee SH, Park SS: Differential expression of mouse Disabled 2 gene in retinoic acid-treated F9 embryonal carcinoma cells and early mouse embryos. Mol Cells 9: 179–184, 1999
113. Lu XP, Fanjul A, Picard N, Shroot B, Pfahl M: A selective retinoid with high activity against an androgen-resistant prostate cancer cell type. Int J Cancer 80: 272–278, 1999
114. Liang JY, Fontana JA, Rao JN, Ordonez JV, Dawson MI, Shroot B, Wilber JF, Feng P: Synthetic retinoid CD437

induces S-phase arrest and apoptosis in human prostate cancer cells LNCaP and PC-3. Prostate 38: 228–236, 1999
115. Tseng CP, Huang CH, Tseng CC, Lin MH, Hsieh JT, Tseng CH: Induction of disabled-2 gene during megakaryocyte differentiation of k562 cells. Biochem Biophys Res Commun 285: 129–135, 2001
116. Tseng CP, Ely BD, Pong RC, Wang Z, Zhou J, Hsieh JT: The role of DOC-2/DAB2 protein phosphorylation in the inhibition of AP-1 activity. An underlying mechanism of its tumor-suppressive function in prostate cancer. J Biol Chem 274: 31981–31986, 1999
117. Wang Z, Tseng CP, Pong RC, McConnell JD, Hsieh JT: A Novel RasGTPase activating protein that interacts with DOC-2/DAB2: A downstream effector leading to the suppression of prostate cancer. J Biol Chem (submitted), 2001
118. Chen H, Pong RC, Wang Z, Hsieh JT: Differential regulation of the human DIP1/2 gene in normal and malignant prostatic epithelia: Cloning and characterization of the DIP1/2 gene. Genomics (submittted), 2001
119. van Slegtenhorst M, de Hoogt R, Hermans C, Nellist M, Janssen B, Verhoef S, Lindhout D, van den Ouweland A, Halley D, Young J, Burley M, Jeremiah S, Woodward K, Nahmias J, Fox M, Ekong R, Osborne J, Wolfe J, Povey S, Snell RG, Cheadle JP, Jones AC, Tachataki M, Ravine D, Kwiatkowski DJ: Identification of the tuberous sclerosis gene TSC1 on chromosome 9q34. Science 277: 805–808, 1997
120. Genbank accession # AY032952.
121. Hocevar BA, Smine A, Xu XX, Howe PH: The adaptor molecule Disabled-2 links the transforming growth factor β receptors to the Smad pathway. EMBO J 20: 2789–2801, 2001
122. Zhou J, Hsieh JT: The inhibitory role of DOC-2/DAB2 in growth factor receptor-mediated signal cascade. DOC-2/DAB2-mediated inhibition of ERK phosphorylation via binding to Grb2. J Biol Chem 276: 27793–27798, 2001

Address for offprints: JT Hsieh, Department of Urology, University of Texas Southwestern Medical Center, 5323 Harry Hines Boulevard, Dallas, TX 75390-9110, USA; *Tel:* 214-648-3988; *Fax:* 214-648-8786; *e-mail:* jt.hsieh@utsouthwestern.edu